

RADIO ASTRONOMY

Journal of the Society of Amateur Radio Astronomers
Mar-Apr 2021



SARA Scope in a Box



Dennis Farr
SARA President

Richard A. Russel
Bogdan Vacaliuc
Editors

Steve Black
Whitham D. Reeve
Michael Stewart
Contributing Editors

Radio Astronomy is published bimonthly as the official journal of the Society of Amateur Radio Astronomers. Duplication of uncopyrighted material for educational purposes is permitted but credit shall be given to SARA and to the specific author. Copyrighted materials may not be copied without written permission from the copyright owner.

Radio Astronomy is available for download only by SARA members from the SARA web site and may not be posted anywhere else.

It is the mission of the Society of Amateur Radio Astronomers (SARA) to: Facilitate the flow of information pertinent to the field of Radio Astronomy among our members; Promote members to mentor newcomers to our hobby and share the excitement of radio astronomy with other interested persons and organizations; Promote individual and multi station observing programs; Encourage programs that enhance the technical abilities of our members to monitor cosmic radio signals, as well as to share and analyze such signals; Encourage educational programs within SARA and educational outreach initiatives. Founded in 1981, the Society of Amateur Radio Astronomers, Inc. is a membership supported, non-profit [501(c) (3)], educational and scientific corporation. Copyright © 2019 by the Society of Amateur Radio Astronomers, Inc. All rights reserved.

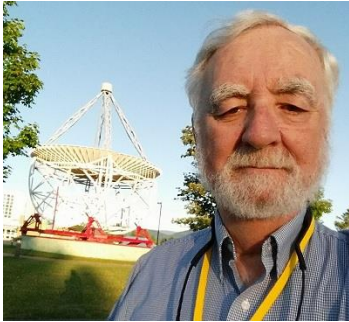
Cover photo: **Alberto Sagüés**

Contents

Radio Waves	3
President’s Page	3
Editor’s Notes	4
News	5
Technical Knowledge & Education:	9
Announcements ~ March-April 2021	11
For Your Radio Astronomy Bookshelf	13
BAA Radio Astronomy Section 2021 JANUARY	14
SuperSID	23
Feature Articles	26
New Specialty Amplifier with Small Parabolic Antenna Advances Hydrogen Line Observing	26
“Scope in a Box” First Experience and Some Enhancements.	30
Sample of HF Radio Reflections from Aurora Observed at Anchorage, Alaska USA	40
Getting the Best out of PRESTO ⁽¹⁾ - Part 2 The PRESTO Period/P-Dot Search Graphic ..	44
Mapping Extent of Neutral Hydrogen Clouds near Sagittarius A* at 1420 MHz.....	54
RF Choke for VLF and LF Applications	64
Superlatives in Science Journalism and other Science Junk compiled for April 1, 2021 .	73
Membership	75
New Members	75
Journal Archives & Other Promotions.....	76
SARA Online Discussion Group.....	76
What is Radio Astronomy?	77
Administrative	78
Officers, directors, and additional SARA contacts.....	78
Resources	79
Great Projects to Get Started in Radio Astronomy	79
Radio Astronomy Online Resources	81
For Sale, Trade and Wanted	83
SARA Advertisements.....	85
SARA Brochure	87

Radio Waves

President's Page



Just finished the Spring Conference. Great international attendance. As always, the presentations were top notch. If you did not attend, you are missing one of the greatest benefits of belonging to SARA.

We have once again decided to hold the Eastern conference as a virtual ZOOM conference. We are very hopeful that 2022 will be the year we return to Green Bank for an in-person conference. There will still be a virtual ZOOM conference. Dates will be July 31 and August 1.

The scope in a box program is fully implemented. All we need now are orders. Remember, the kit could be made available as a grant to worthy programs. If you know of a group that might qualify, please have them contact us at grants@radio-astronomy.org

Please take a moment to check out the new online SARA store. It should be much easier now to order anything we offer using one site for both PayPal and Credit card payments.

<https://www.radio-astronomy.org/store/>

The Drakes lounge monthly ZOOM meetings are extremely interesting and cover topics in an informal manner. Typically, we are getting about 20 people attend. Always room for more. You should be receiving an email each month with the schedule and link to the meeting. The meetings are held the 3rd Sunday of each month starting at 1400 ET.

We have redone the membership brochure that is used as a handout at meetings and conventions such as Hamvention. The new brochure can be seen at <https://www.radio-astronomy.org/pdf/brochure.pdf> or, click on the link on the membership page. If anyone has any of the old brochures, please throw them away. They had names and addresses on them that have changed.

Keep your antennas pointed up!

Dennis

Editor's Notes

We are always looking for basic radio astronomy articles, radio astronomy tutorials, theoretical articles, application and construction articles, news pertinent to radio astronomy, profiles and interviews with amateur and professional radio astronomers, book reviews, puzzles (including word challenges, riddles, and crossword puzzles), anecdotes, expository on "bad astronomy," articles on radio astronomy observations, suggestions for reprint of articles from past journals, book reviews and other publications, and announcements of radio astronomy star parties, meetings, and outreach activities.

If you would like to write an article for Radio Astronomy, please follow **the newly updated Author's Guide** on the SARA web site:

http://www.radio-astronomy.org/publicat/RA-JSARA_Author's_Guide.pdf.

Let us know if you have questions; we are glad to assist authors with their articles and papers and will not hesitate to work with you. You may contact your editors any time via email here: edit@radio-astronomy.org.

The editor(s) will acknowledge that they have received your submission within two days. If they do not reply, assume they did not receive it and please try again.

Please consider submitting your radio astronomy observations for publication: any object, any wavelength. Strip charts, spectrograms, magnetograms, meteor scatter records, space radar records, photographs; examples of radio frequency interference (RFI) are also welcome.

Guidelines for submitting observations may be found here: http://www.radio-astronomy.org/publicat/RA-JSARA_Observation_Submission_Guide.pdf

Tentative *Radio Astronomy* due dates and distribution schedule

Issue	Articles	Radio Waves	Review	Distribution
May – Jun	June 12	June 20	June 25	June 30
Jul – Aug	August 12	August 20	August 25	August 31
Sep – Oct	October 12	October 20	October 25	October 31
Nov – Dec	December 12	December 15	December 20	December 31

News

2021 SARA Annual Conference – Call for Nominations

As required by Section 3 of SARA By-Laws (see below), this is the official call for nominations for SARA officers and board members. If you are interested in running for office and would like to know more about the positions, please contact a board member or SARA President Dennis Farr. The requirement to be on the board is to attend the board meetings at the annual meeting and to actively participate in board-related activities, usually email or teleconference meetings. If you are unable to attend the annual meetings, then the director at large position may be for you. This position is a full board position except that attending the annual meeting is not required. The following positions will be up for election in Aug 2021: Secretary, Treasurer, two Directors at Large, and two regular Directors.

If you would like to run for one of the available SARA officer or board positions, please send a note to Secretary Bruce Randall, copying President Dennis Farr. The president and secretary will “nominate” qualified individuals who volunteer. If you nominate someone, you must get their permission prior to nomination.

Contact information:

Secretary: Bruce Randall, NT4RT, <https://www.radio-astronomy.org/contact/Secretary>
+1 803-327-3325

President: Dennis Farr, WB4RJK, <https://www.radio-astronomy.org/contact/President>
+1 248-425-6016

Text from the By-Laws: SECTION 3:

Elections of Directors and Officers will be accomplished by the President placing an initial call for nominations in "The Journal" no less than ninety (90) days prior to the regular scheduled meeting. Two (2) nominations from different members will be required to nominate a member for an office. No less than thirty (30) days prior to this meeting (in a newsletter issued prior to the meeting), the President will place a notice of the results of the nominations in "The Journal", along with a ballot for the members to use to vote for the nominee of their choice. This ballot will be forwarded to the Secretary for collection and counting at the regular meeting.

SARA Student & Teacher Grant Program

All, SARA has a grant program that is, sad to say very underutilized. We will provide kits or money to students and teachers including college students to help them with a radio telescope project. SARA can supply any of the following kits:

- SuperSID
- Scope in a Box
- IBT (Itty Bitty Telescope)
- Radio Jove kit
- Inspire
- Sky Scan

We can also provide up to five hundred dollars (\$500.00 USD) for an approved radio telescope project.

We have on occasion provided more money based on the merits of the project and the SARA Grant Committee approval.

More information on the grant program can be found at the URL below.

[SARA Student and Teacher Project Grants | Society of Amateur Radio Astronomers \(radio-astronomy.org\)](#)

All that is required is the SARA grant request form be filled out and sent in. If it needs more work for approval, we will work with the student to help insure their success.

Please pass the word that SARA will fund any legitimate radio telescope project anywhere in the world.

If you have a question, contact me at [crowleytj at hotmail](mailto:crowleytj@hotmail.com) dot com

Tom Crowley
SARA Grant Program Administrator

Drake's Lounge

Join the SARA community as we discuss the latest astronomy and radio astronomy news. The lounge also provides a forum to share and get advice on your radio astronomy projects from very experienced amateur radio astronomers.

Drake's Lounge is every month on the 3rd Sunday at 2 pm Eastern time. ZOOM email notifications will be sent to all members.

See you there!

2021 SARA Eastern Conference is Virtual Only Again (Hopefully for the last time!)

We are sorry that we will not be able to see each other at Green Bank this year but we are planning to restart the physical conferences next year at the VLA for the Western Conference and Green Bank for the Eastern Conference. The 2021 SARA Eastern virtual conference will be held on Saturday and Sunday to allow for peoples work. The new dates are **July 31 – August 1, 2021**. The schedule will include sessions all day Saturday and half of the day Sunday afternoon to accommodate peoples worship services in the morning.

Conference cost will be \$25 to cover expenses.

Register at: <https://www.radio-astronomy.org/node/318>

Contact Rich Russel (Conference Coordinator) if you would like to present a paper.

drrichrussel@netscape.net

SARA 2021 Eastern Conference Keynote Speaker

Dr. Sander Weinreb

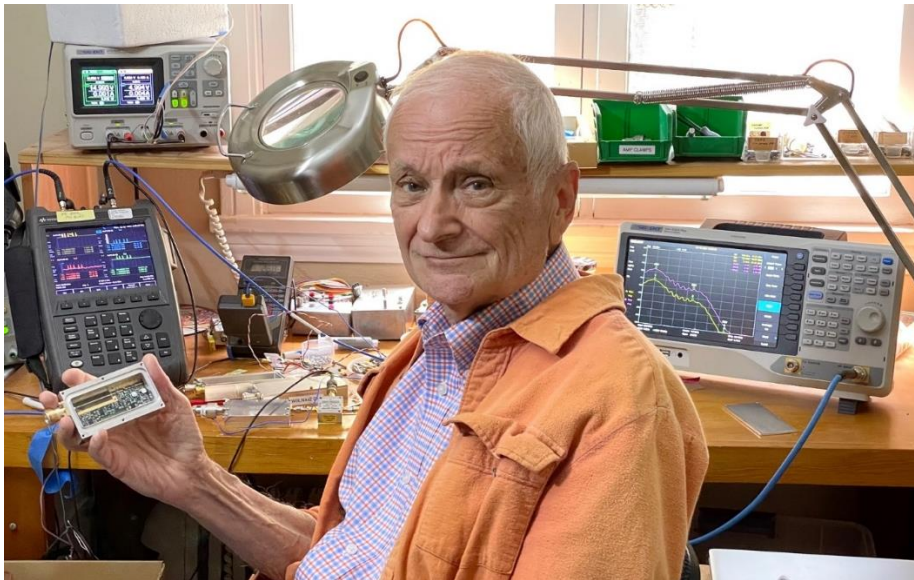
Dr. Weinreb was awarded the 2008 Grote Reber Medal for lifetime innovative contributions to radio astronomy. His pioneering developments of novel techniques and instrumentation over nearly half a century helped to define modern radio astronomy.

<http://www.weinreb.org/sandy/index.html>

Presentation

New Directions in Radio Astronomy

In the past we believed that astronomical sources other than planets only varied over times of millions of years. In the recent several years, a whole new world of sources with variations in the time scales of milliseconds to months have become exciting targets for new research. The most widely studied time-variable sources in radio astronomy are the Fast Radio Bursts, FRBs – a ms pulse of radiation in the low microwave range which sweeps in frequency and in most cases does not repeat. The search and characterization for these single-event objects are tantalizing objectives for amateur radio astronomers. This talk will begin with discussion of FRBs followed by descriptions of new radio astronomy arrays, and new LNAs with noise of the order of 10K without a need for costly cryogenic cooling.

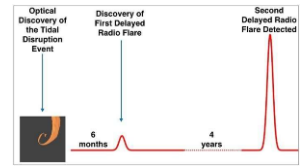


Phys.org ~ Video: A signal from beyond: <https://phys.org/news/2021-02-video.html>

Spaceweather.com ~ Ham Radio Signals from Mars:
<https://spaceweather.com/archive.php?view=1&day=17&month=02&year=2021>

Hey, Mac, of course it has, but what's up with the probing?: Phys.org ~ *Has Earth been visited by an alien spaceship? Harvard Professor Avi Loeb vs. everybody else:*
<https://phys.org/news/2021-02-earth-alien-spaceship-harvard-professor.html>

Phys.org ~ *Delayed radio flares from a tidal disruption event:*
<https://phys.org/news/2021-02-radio-flares-tidal-disruption-event.html>



The SETI Project ~ Observatories: <https://exoplanetschannel.wixsite.com/home/observatories-1>

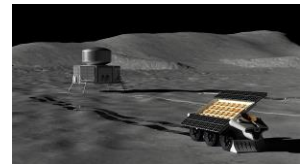
Universe Today ~ *One Type of Fast Radio Bursts... Solved?:*
<https://www.universetoday.com/150293/one-type-of-fast-radio-bursts-solved/>



American Geophysical Union (AGU) ~ *A 21st Century View of the March 1989 Magnetic Storm:* <https://agupubs.onlinelibrary.wiley.com/doi/full/10.1029/2019SW002278>

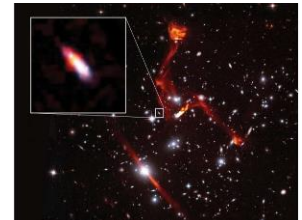
CU Boulder Today ~ *NASA-funded project to explore one-of-a-kind lunar observatory:*
<https://www.colorado.edu/today/2021/03/01/nasa-funded-project-explore-one-kind-lunar-observatory>

Universe Today ~ *NASA is Considering a Radio Telescope on the Far Side of the Moon:*
<https://www.universetoday.com/150417/nasa-is-considering-a-radio-telescope-on-the-far-side-of-the-moon/>



[Thomas Ashcraft Radio Fireball Observatory](https://apod.nasa.gov/apod/ap210315.html) ~ *Meteor Fireballs in Light and Sound:*
<https://apod.nasa.gov/apod/ap210315.html>

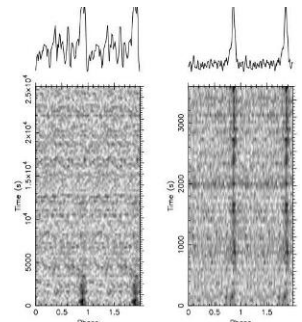
Phys.org ~ *Cosmic lens reveals faint radio galaxy:* <https://phys.org/news/2021-03-cosmic-lens-reveals-faint-radio.html>



National Science Foundation ~ *NSF begins planning for decommissioning of Arecibo Observatory's 305-meter telescope due to safety concerns:*
https://www.nsf.gov/news/news_summ.jsp?cntn_id=301674&org=NSF&from=news

Phys.org ~ *Eight new millisecond pulsars discovered by MeerKAT:*
<https://phys.org/news/2021-03-millisecond-pulsars-meerkat.html>

Universe Today ~ *There Could be Magnetic Monopoles Trapped in the Earth's Magnetosphere:* <https://www.universetoday.com/150603/there-could-be-magnetic-monopoles-trapped-in-the-earths-magnetosphere/>



Youtube Video ~ *The discovery of pulsars - a graduate student's tale* (Jocelyn Bell Burnell: "In this talk I will describe how pulsars were accidentally discovered, and reflect on several instances where they were 'nearly' discovered. I will highlight the implications for new telescopes with high data rates."): <https://www.youtube.com/watch?v=ot1Ggv6YZyQ>

ScienceNews ~ *A new black hole image reveals the behemoth's magnetic fields:*
<https://www.sciencenews.org/article/black-hole-picture-magnetic-fields-event-horizon-telescope>



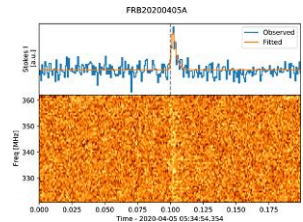
YouTube video ~ *Interview: Jack Burns and the Lunar FARSIDE (Radio) Telescope:*
https://www.youtube.com/watch?v=Ubdzspuf2_Q

ScienceNews ~ *The 'USS Jellyfish' emits strange radio waves from a distant galaxy cluster:*
<https://www.sciencenews.org/article/uss-jellyfish-galaxy-cluster-strange-radio-waves>



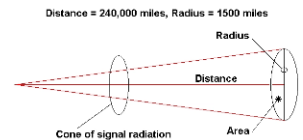
Phys.org ~ *Radio telescope reveals thousands of star-forming galaxies in early Universe:*
<https://phys.org/news/2021-04-radio-telescope-reveals-thousands-star-forming.html>

Research Notes of the AAS ~ *The First Fast Radio Burst Detected with VLITE-Fast:*
<https://iopscience.iop.org/article/10.3847/2515-5172/abea22>



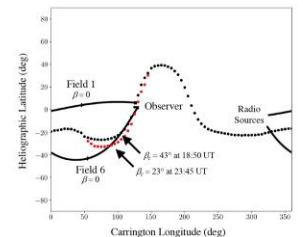
History of Geo- and Space Sciences ~ *The formation of ionospheric physics – confluence of traditions and threads of continuity:*
<https://hgss.copernicus.org/articles/12/57/2021/>

Electronic Design News ~ *The search for extraterrestrial radio signals:*
<https://www.edn.com/the-search-for-extraterrestrial-radio-signals/>



Technical Knowledge & Education:

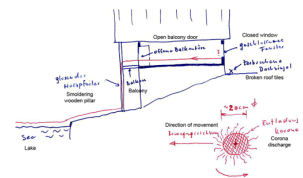
Community of European Solar Radio Astronomers (CESRA) ~ *VLA Measurements of Faraday Rotation through a Coronal Mass Ejection Using Multiple Lines of Sight:*
<http://www.astro.gla.ac.uk/users/eduard/cesra/?p=2793>



Cornell University ~ *Galactic Radio Explorer: an all-sky monitor for bright radio bursts:*
<https://arxiv.org/abs/2101.09905>

Online radio astronomy courses ~ audit for free or pay to receive certification:
The Radio Sky I: Science and Observations: <https://www.edx.org/course/radio-sky-1>
Plasma Physics: Introduction: <https://www.edx.org/course/plasma-physics-introduction>

History of Geo- and Space Sciences (HGGS) ~ *A brief history of ball lightning observations by scientists and trained professionals:*
<https://hgss.copernicus.org/articles/12/43/2021/>

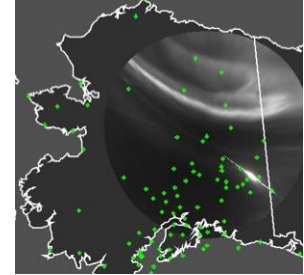


Hey, Mac, I want my Arecibo and I want it now: Cornell University ~ *The Future Of The Arecibo Observatory: The Next Generation Arecibo Telescope:*
<https://arxiv.org/abs/2103.01367>

Signal Hound ~ *Understanding the Noise Floor on a Real-Time Spectrum Analyzer:*
<https://signalhound.com/content/tech-briefs/understanding-the-noise-floor-on-a-real-time-spectrum-analyzer/>

US Naval Post Graduate School ~

- ⚙ *The Mitigation of Radio Noise from External Sources at Radio Receiving Sites:*
www.arrl.org/files/file/Technology/pdf/ExternalNoiseHandbook.pdf
- ⚙ *The Mitigation of Radio Noise and Interference from On-Site Sources at Radio Receiving Sites:*



www.arrl.org/files/file/Technology/RFI%20Main%20Page/Naval_RFI_Handbook.pdf

University of Alaska Fairbanks ~ *Space Weather Underground:* <https://sites.google.com/alaska.edu/swug/>

Rhode & Schwarz ~ *Making Better Oscilloscope Measurements:* https://www.rohde-schwarz.com/us/campaigns/rsa/icr/making-better-oscilloscope-measurements_253739.html

Community of European Solar Radio Astronomers (CESRA) ~ *On the occurrence of type IV solar radio bursts in the solar cycle 24 and their association with coronal mass ejections:*

<http://www.astro.gla.ac.uk/users/eduard/cesra/?p=2807>

$$\Gamma = \frac{Z-1}{Z+1} = \frac{(R+X)-1}{(R+X)+1} = \frac{(R-1)+jX}{(R+1)+jX} \cdot \frac{(R+1)-jX}{(R+1)-jX}$$

$$\Gamma = \frac{(R-1)(R+1)+jX(R+1)-jX(R-1)-j^2X^2}{(R+1)^2-j^2X^2}$$

$$\Gamma = \frac{[(R-1)(R+1)+X^2]+j[XR+X-XR+X]}{(R+1)^2+X^2}$$

$$\Gamma = \frac{[(R-1)(R+1)+X^2]+j2X}{(R+1)^2+X^2}$$

EDN ~ *The math behind the Smith chart:* <https://www.edn.com/the-math-behind-the-smith-chart/>

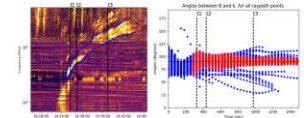
$$\Gamma = \frac{(R-1)(R+1)+X^2}{(R+1)^2+X^2} + j \frac{2X}{(R+1)^2+X^2}$$

Real part of gamma. Imaginary part of gamma.

Vice ~ *Why Channel 37 Doesn't Exist (And What It Has to Do With Aliens):*
<https://www.vice.com/en/article/dy8by7/why-channel-37-doesnt-exist-and-what-it-has-to-do-with-aliens>

Cornell University ~ *A modern reconstruction of Carrington's observations (1853-1861):*
<https://arxiv.org/abs/2103.05353>

CESRA ~ *Analyzing the propagation of EUV waves and their connection with type II radio bursts by combining numerical simulations and multi-instrument observations:*
<http://www.astro.gla.ac.uk/users/eduard/cesra/?p=2817>





SolFER Spring 2021 Meeting

<https://solfer.umd.edu/events/conference.html>

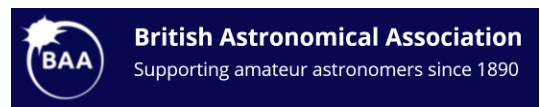
The SolFER DRIVE Science Center is announcing a web-based science meeting on Solar Flare Energy Release to take place on May 24-26, 2021. The meeting is open to all scientists working on the topic. The meeting will include invited talks, submitted oral talks as well as poster presentations and will provide substantial time for informal scientific discussion. We encourage paper submissions that are based on remote and in situ observational data as well as those based on theory and modeling. Extensive use will be made of Gather meeting software to facilitate interactive poster sessions as well as informal discussion between meeting participants. The meeting will be organized around the key scientific topics listed as follows:

- ✓ What mechanisms facilitate the fast release of magnetic energy in impulsive solar flares?
- ✓ What controls the onset of fast flare energy release?
- ✓ Why and how do flares transfer a large fraction of the released magnetic energy into energetic electrons?
- ✓ What mechanism drives the energization of ions and the measured abundance enhancements of some species during impulsive flares?
- ✓ What mechanisms control energetic particle transport in flares?
- ✓ How does reconnection heat plasma in flares and the small events (nanoflares) that may be responsible for heating the corona?

More information on these scientific topics can be found on the SolFER website (solfer.umd.edu). Information on abstract submission and more details on the daily timeline of the meeting are being developed for posting on the website.

The SolFER science team also encourages community participation in the ongoing science discussion related to flare energy release. A detailed calendar of working group meetings as well as the monthly webinar can be found on the SolFER website (solfer.umd.edu).

Radio Astronomy Group of the British Astronomical Association



The Radio Astronomy Group hosts bi-weekly Zoom Conferences that include presentations and posters on various aspects of radio astronomy. Scheduled conferences are listed below. The conferences are recorded and archived for viewing later and have the following format:

- ⚙ 18:15 UTC - Meeting room open for discussion
- ⚙ 18:30 UTC - Introductions/notices
- ⚙ 18:40 UTC - Main presentation
- ⚙ 19:30 UTC - Q & A
- ⚙ 19:50 UTC - Poster session, 10 min each. Brief presentation on current research and/or observations.
- ⚙ 20:30 UTC - Finish

If you are interested in attending a conference or presenting for a main session or a poster session please contact Paul Hearn at paul@hearn.org.uk. The Zoom link will be sent by email the day before the conference. A

current list of conferences can be found at <https://britastro.org/node/25793> and archives at <https://britastro.org/node/25798> . Conferences so far scheduled:

March 26th. RAGZoom2

Main Presentation: **Radio Meteor Detection collaboration Project** - John Berman

"A talk about what we are currently doing with data collected and where we may go in the future"

Poster sessions to be confirmed

April 9th. RAGZoom3

Main Presentation: **SIDs and TIDs - the ups and downs of the ionosphere** - Mark Edwards

Poster sessions to be confirmed

April 23rd. RAGZoom4

Main Presentation: **Geomagnetism ~ Earth's Magnetic Field and the Sun** - Whitham D. Reeve

Poster sessions to be confirmed

May 14th. RagZoom5

Main Presentation: **Hydrogen-Line Observations and Instrumentation** - Brian Coleman

Poster sessions to be confirmed

May 28th. RAGZoom6

Main Presentation: **Current Observations from Astropeiler Stockert** - Wolfgang Herrmann

Poster sessions to be confirmed

June 25th. RAGZoom7

Main Presentation: **On the tricky question of Pulsars** - Peter East OBE FREng

Poster sessions to be confirmed

July 23rd. RAGZoom8

Main Presentation: **e-Callisto a Radio eye for Solar Activity** - Christian Monstein

Poster sessions to be confirmed



For Your Radio Astronomy Bookshelf

(Prices in USD)

- ⚙ **Antenna Models for Electromagnetic Compatibility Analyses**, C.W. Wang, T. Keech, NTIA TM-13-489, October 2012, Free download:
https://www.ntia.doc.gov/files/ntia/publications/antenna_models_report_tm-13-489.pdf
- ⚙ **Fundamentals of Radio Astronomy Observational Methods**, Marr, J.M.; Snell, R.L.; Kurtz, S.E.; 2016, CRC Press, \$110.00 (hardcover)
- ⚙ **Galactic Radio Astronomy**, Sofue, Y., ISBN 978-981-10-3444-2, Springer, \$64.99 (hardcover)
- ⚙ **Geomagnetism, Aeronomy and Space Weather – A Journey from Earth’s Core to the Sun**, edited by M. Manda, M. Korte, A. Yau and E. Petrovsky, ISBN 978-1-1084-1848-5, 2020, 140 USD (hardback), Cambridge University Press
- ⚙ **Geomagnetic Disturbances Impacts on Power Systems: Risk Analysis and Mitigation Strategies**, O. Sokolova, N. Korovkin, M. Hayakawa, ISBN 978-03-676-8086-2, 170 USD (hardcover), 153 USD (eBook) , 2021, CRC Press
- ⚙ **Handbook of Pulsar Astronomy**, Lorimer, D.R.; Kramer, M.; ISBN 0-521-82823-6; 2005, Cambridge University Press; \$94.00, (hardcover)
- ⚙ **Pulsar Astronomy**, Lyne, A.G.; Graham-Smith, F. ISBN 0-521-32681-8, 1990, Cambridge University Press; \$47.95 (hardcover)
- ⚙ **Radio Astronomy**, 2nd Ed.; Kraus, J.D., ISBN 65-28593, 1986, McGraw-Hill, Inc. \$49.95 (spiral bound)
- ⚙ **The Cosmos: Astronomy in the New Millennium, 5th Ed.**, J. M. Pasachoff & A. Filippenko, ISBN: 978-1-1084-3138-5, 2019, \$80 (softcover), e-Book available, Cambridge University Press
- ⚙ **Tools of Radio Astronomy**, 6th Ed., Wilson, T.L.; Rohlfs, K.; Hüttemeister, S.; ISBN 3662517329, Springer, \$118.00 (hardcover)



Founded in 1890

The British Astronomical Association

A company limited by guarantee

Registered Charity No. 210769

Burlington House, Piccadilly, London, W1J 0DU

Telephone: 020 7734 4145

Fax No.: 020 7439 4629

Email: office@britastro.org

Website: www.britastro.org

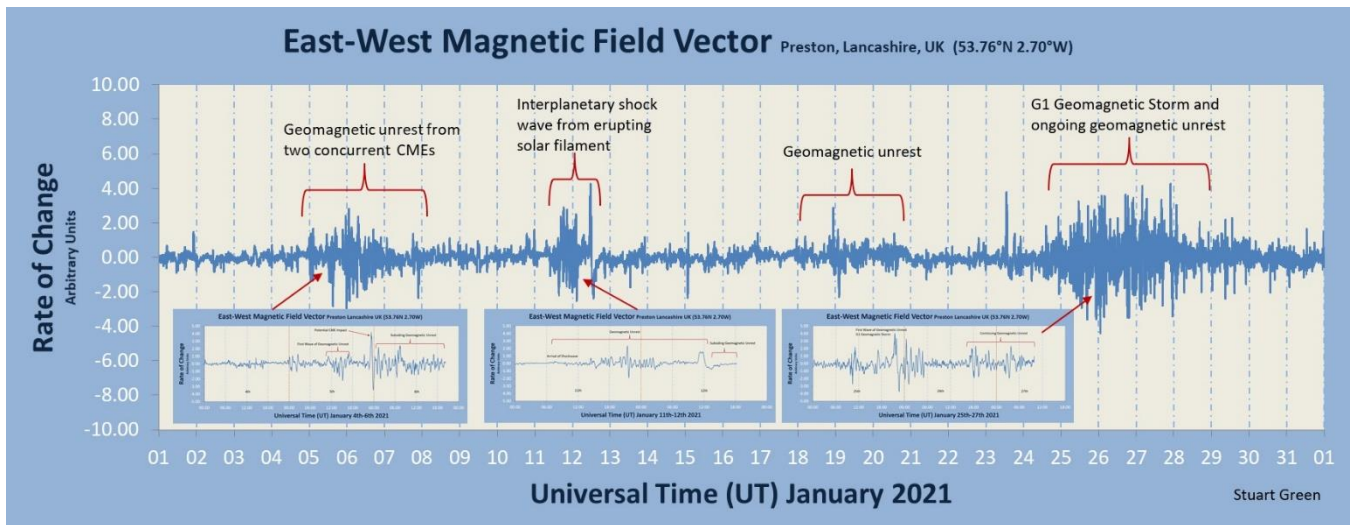


Please send all reports and observations to jacook@jacook.plus.com

BAA Radio Astronomy Section 2021 JANUARY

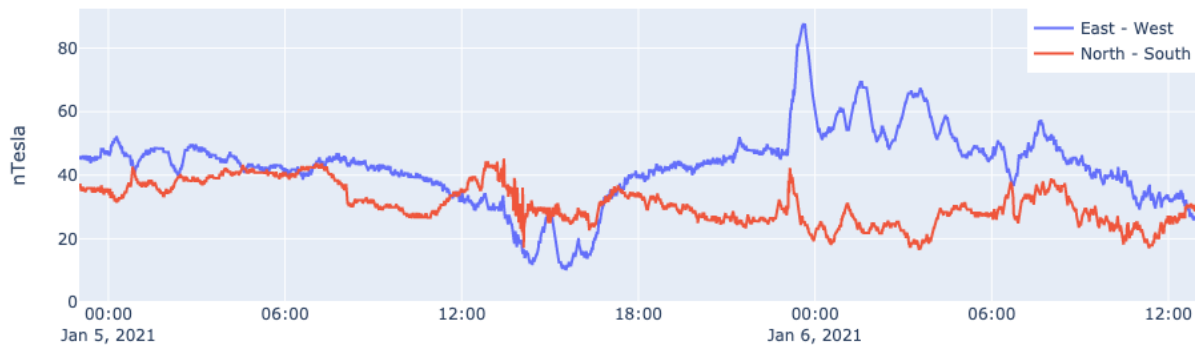
Solar activity through January was very low, with a short period mid-month of small B-class flares. The strongest flare listed in the space weather bulletins was C1.4 peaking at 12:53UT on the 20th. Although well timed for detection, it was not recorded on the very noisy signals typical at this time of year. The 23.4kHz signal has also shown some large and rapid changes in signal strength towards the end of the month that have not helped.

MAGNETIC OBSERVATIONS

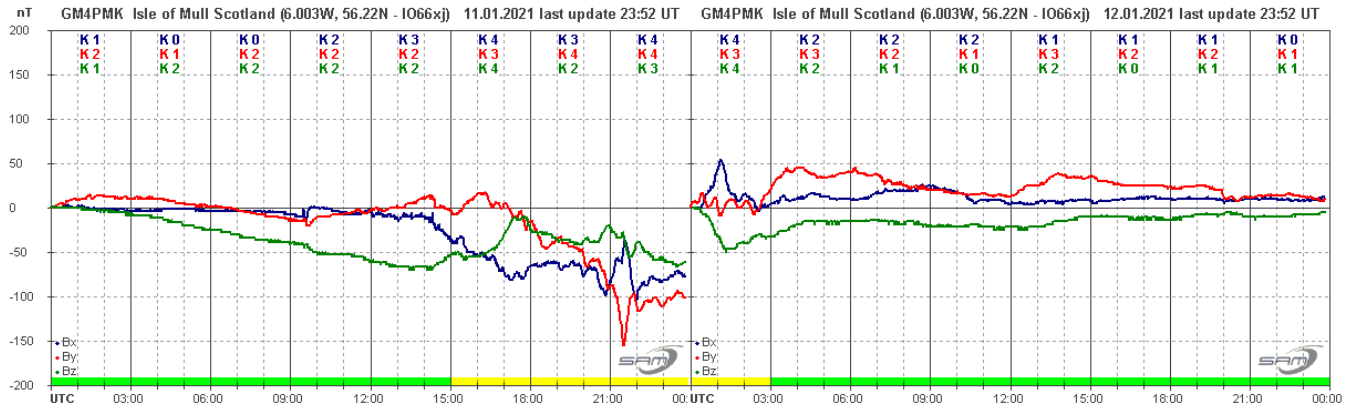


This chart shows the month's activity recorded by Stuart Green. Despite the lack of flare activity, there were some CMEs recorded in satellite images. These were from filament eruptions, and fairly mild. Combining with coronal hole high speed winds they did result in some magnetic disturbances in the first half of the month.

Steyning Magnetometer (50.8 North, 0.3 West)



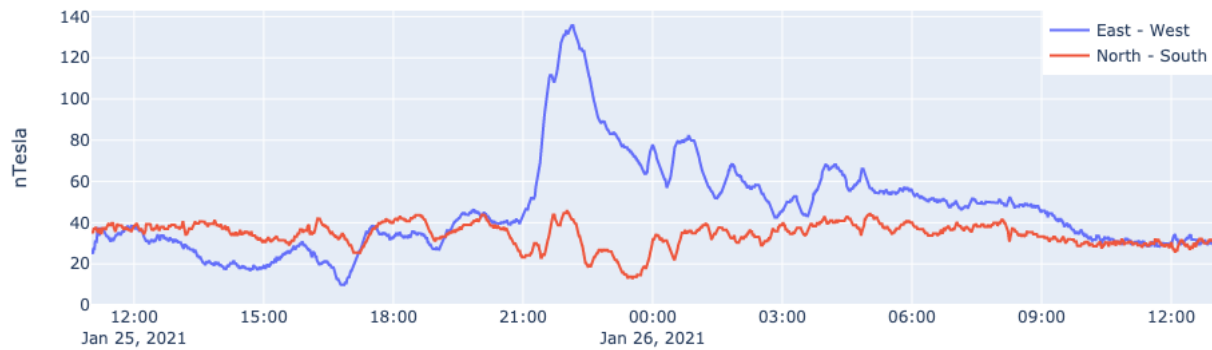
This recording by Nick Quinn shows the CME arrival just before midnight on the 5th, following a day of mild disturbance from the CHSS. Nick is using a fluxgate sensor buried 0.6m underground to reduce thermal effects. The disturbance faded out during the 6th. The second CME / CHSS combination arrived on the 11th, shown here by Roger Blackwell:



There was clearly quite a strong shift in the magnetic field in the evening of the 11th, although the turbulence produced was fairly mild. The sensor is reset at midnight, hence the apparent break in the trace.

The magnetic disturbance starting on the 25th was entirely due to coronal hole effects, shown in this recording by Nick Quinn:

Steying Magnetometer (50.8 North, 0.3 West)

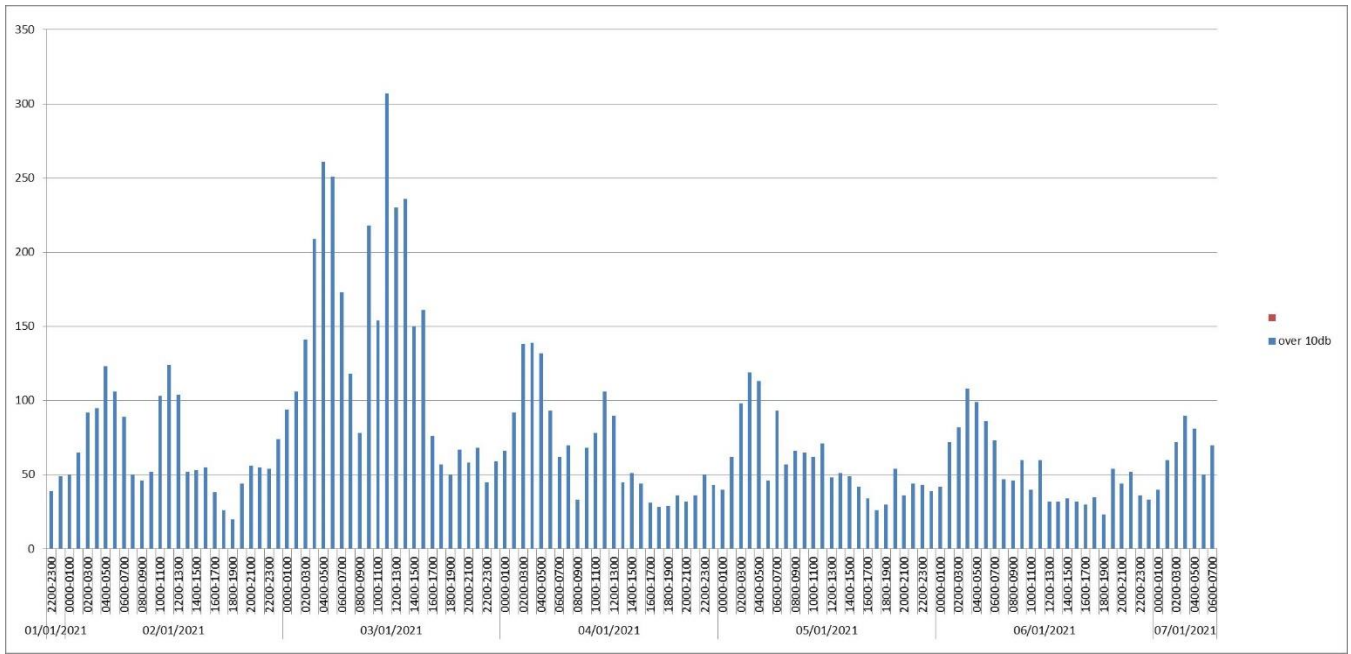


There was a very mild disturbance during the morning, increasing through the afternoon with a large shift in the east-west field just before midnight. The mild disturbance continued through the 26th, fading out in the morning of the 27th. There were no reports of any effects on the 37.5kHz signal from these magnetic disturbances as they were most active well after the winter sunset time.

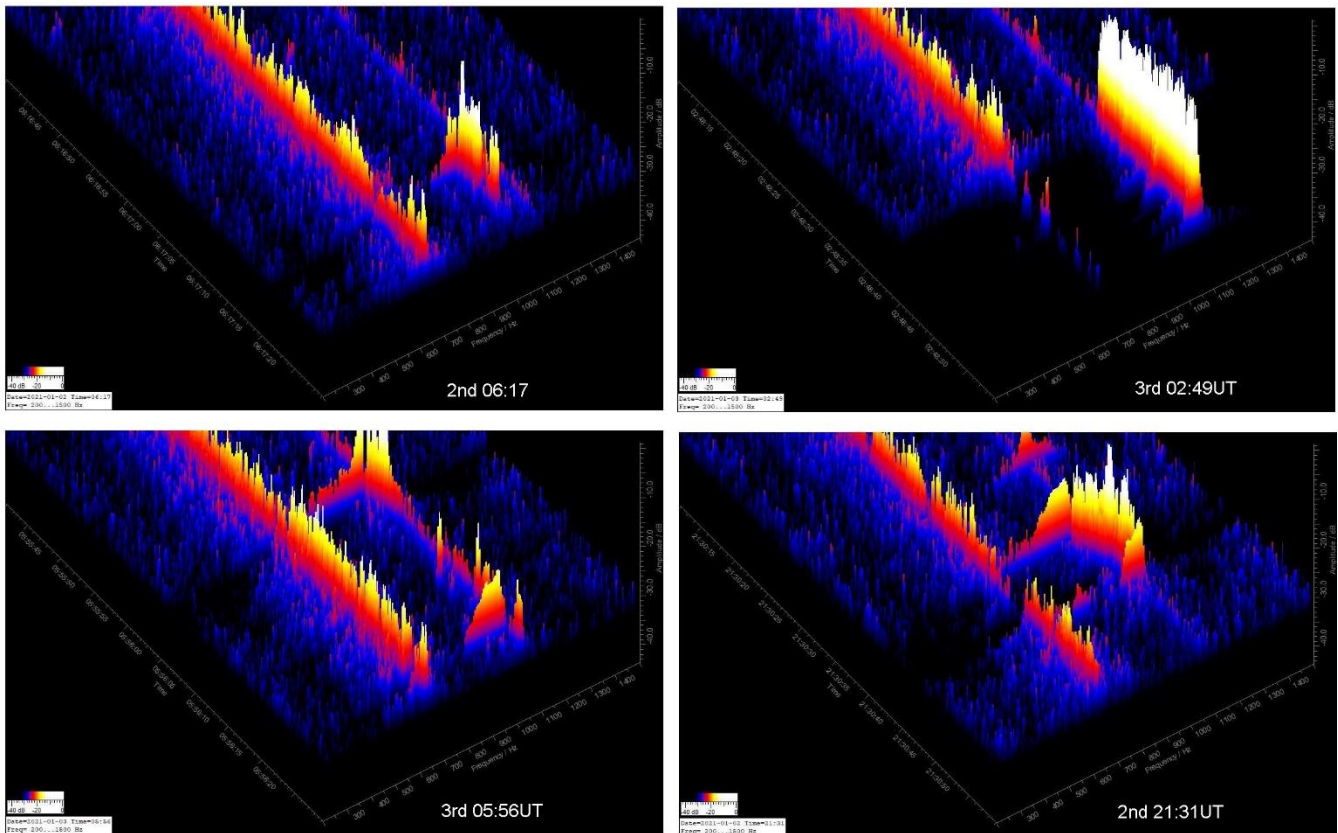
Magnetic observations received from Roger Blackwell, Chris Bailey, Colin Clements. Stuart Green, Paul Hearn, Andrew Thomas, Nick Quinn and John Cook.

QUADRANTID METEORS

Chris Bailey has continued his meteor recording with the GRAVES radar signal to catch the January Quadrantids. His echo counts are shown in the chart on the next page:

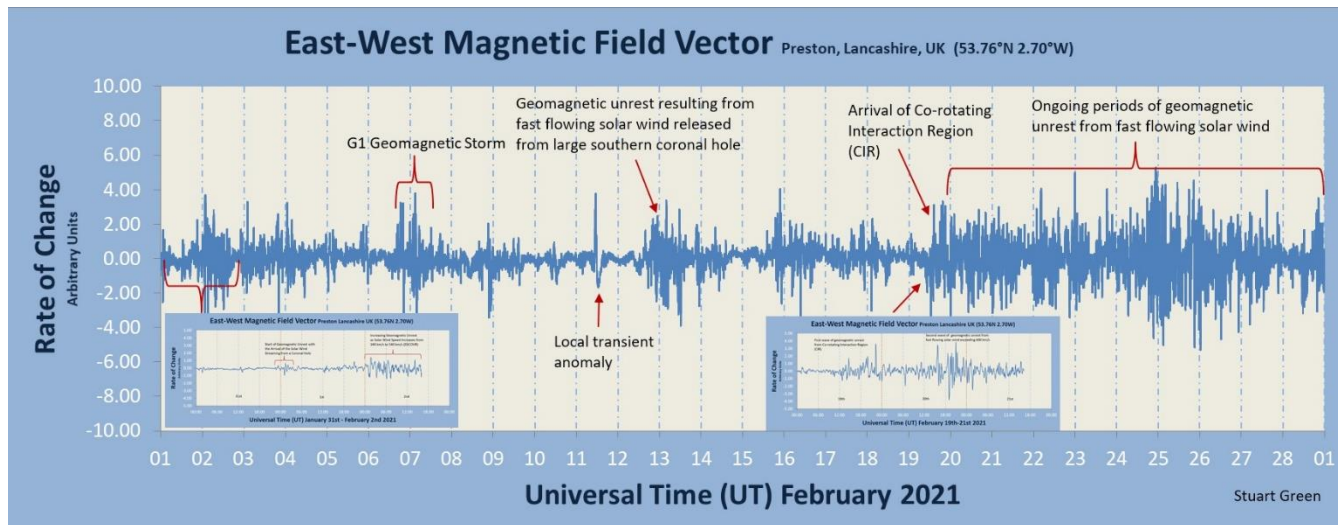


The peak in the morning of the 3rd is in good agreement with the details in the BAA handbook, with over 300 radar reflections being detected between 10 and 11UT. Good rates were also recorded over the entire six day period shown. Some of the recordings are shown below. Note that the bright line underneath each echo is due to interference.



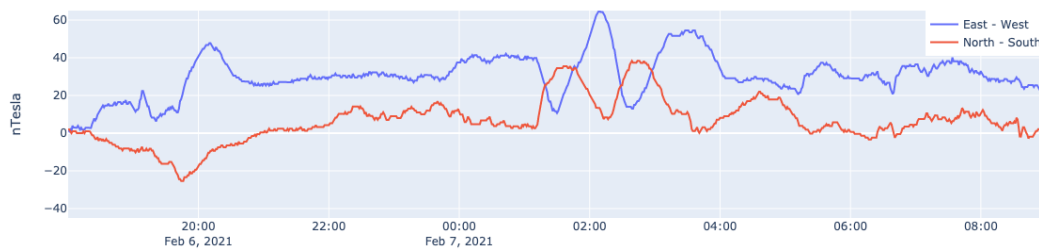
February started with a very inactive sun, mostly without any sunspots. AR12804 became active in the last week of the month, producing many small B-class flares. The strongest event of the month being a C3.9 flare at 06:46UT on the 28th. This was far too early in the morning for us to detect, and so we have another month without any recorded SIDs. Signals have been very noisy due to the low level of solar activity.

MAGNETIC OBSERVATIONS



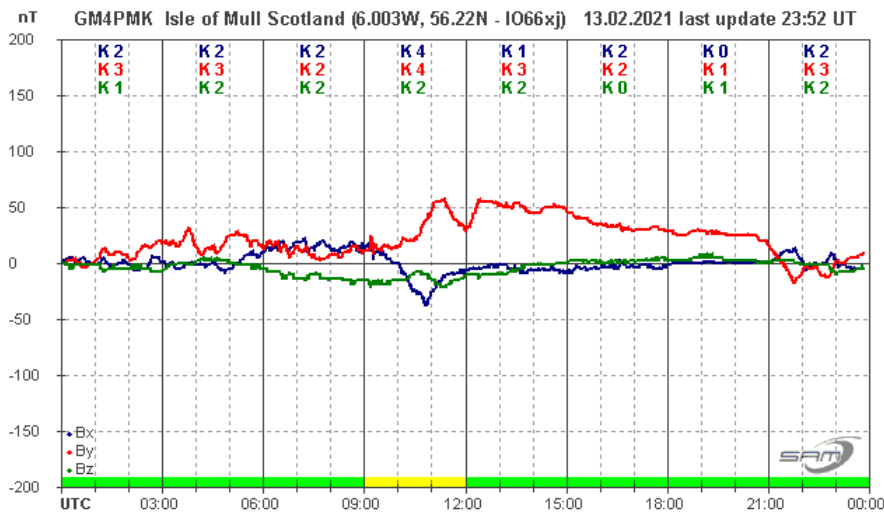
The monthly magnetic summary from Stuart Green shows that February was a very active month, with magnetic disturbances present on most days. The majority of the disturbance was due to the high speed wind from coronal holes.

Steying Magnetometer (50.8 North, 0.3 West)

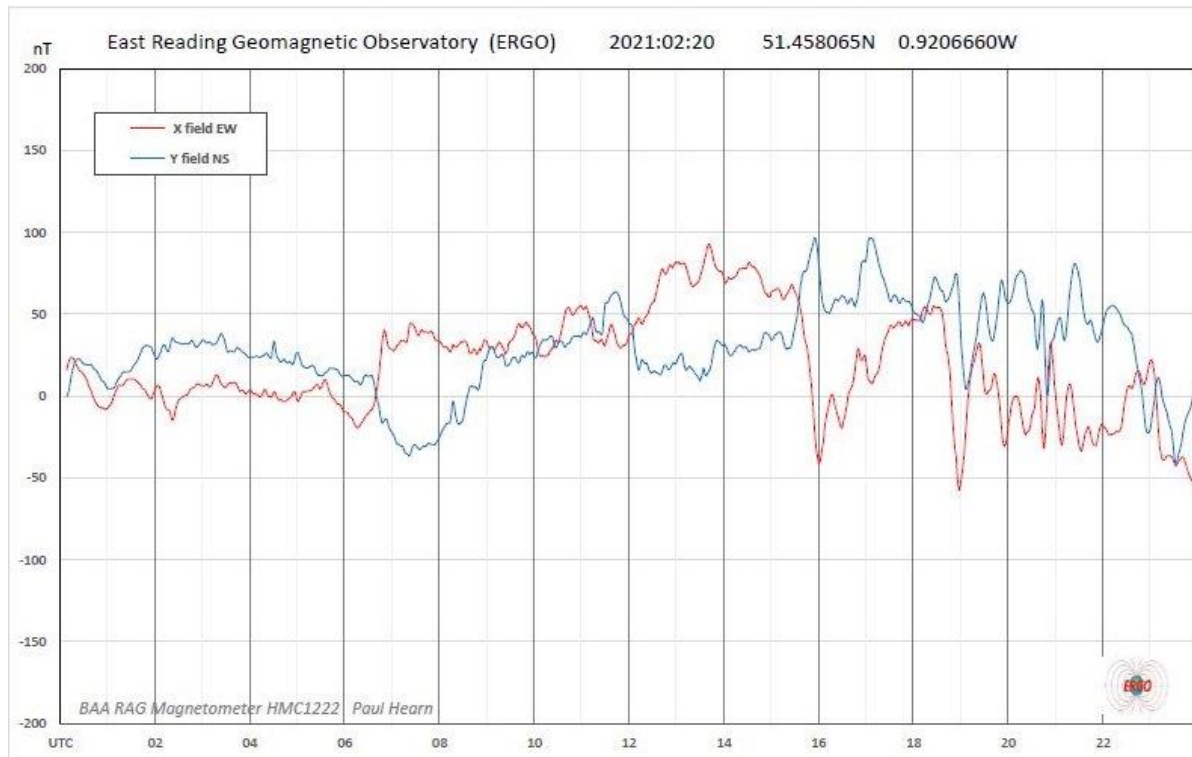


This recording by Nick Quinn shows quite a strong disturbance starting in the evening of the 6th and continuing into the 7th. This faded out later in the afternoon, but there was a further brief disturbance in the evening of the 8th.

Unusually, the disturbance on the 13th was at its strongest in the morning, fading out after midday. This is shown in the recording by Roger Blackwell:

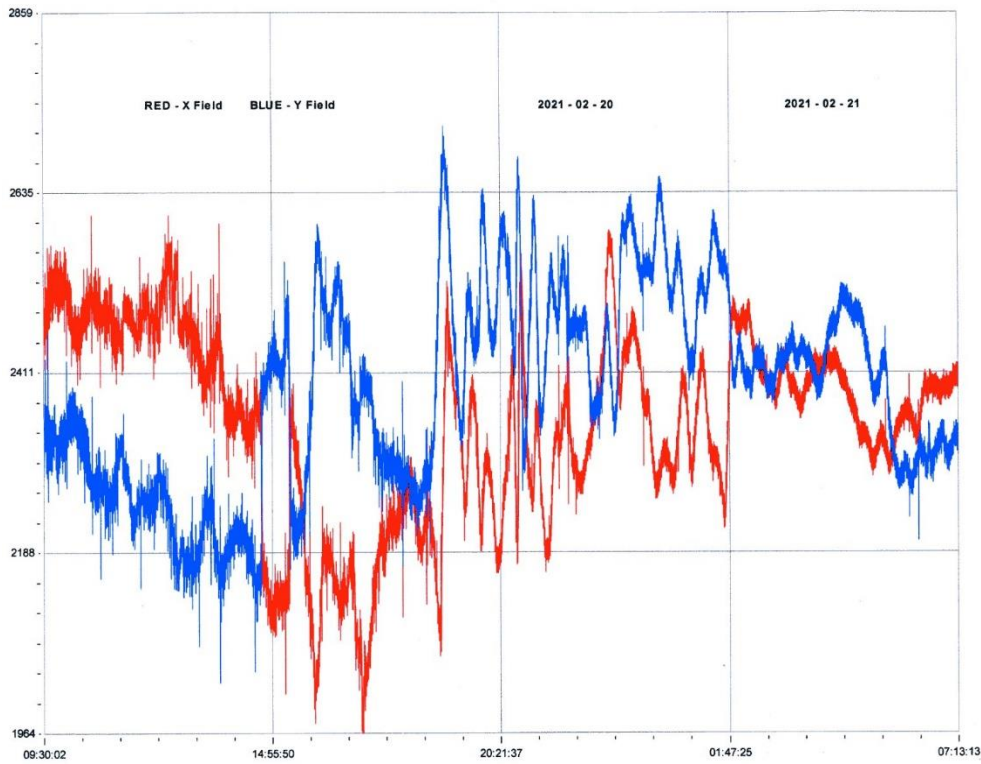


A combination of multiple coronal holes as well as a possible glancing blow from a small CME led to the magnetic disturbance starting on the 19th and running right through to the end of the month.

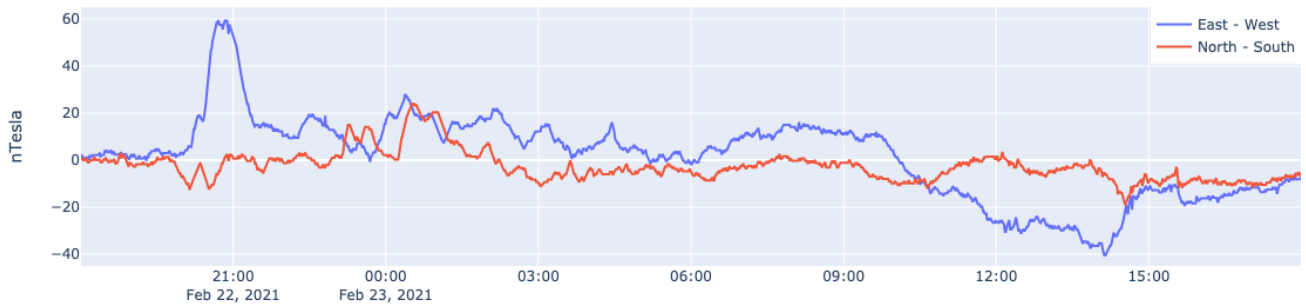


This recording by Paul Hearn shows a strong build-up of activity in the late afternoon of the 20th as the effects of the southern polar coronal hole and equatorial coronal hole combine. These coronal holes were over quite a large area, but were very patchy. The Earth-Sun geometry at this time of year allows easier access of the solar wind into the Earth's magnetosphere.

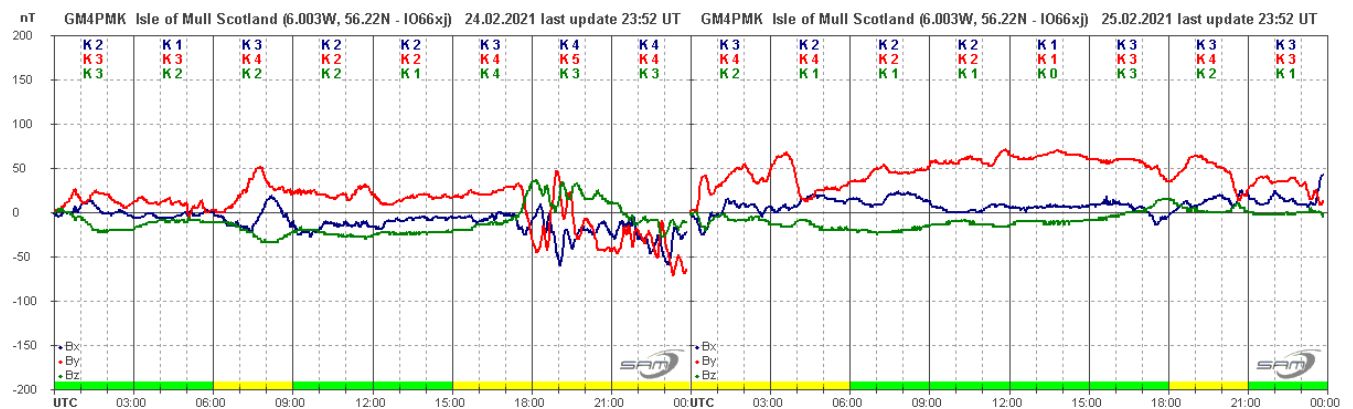
Activity reduced a little after 02UT on the 21st, shown in the following recording by Colin Clements:



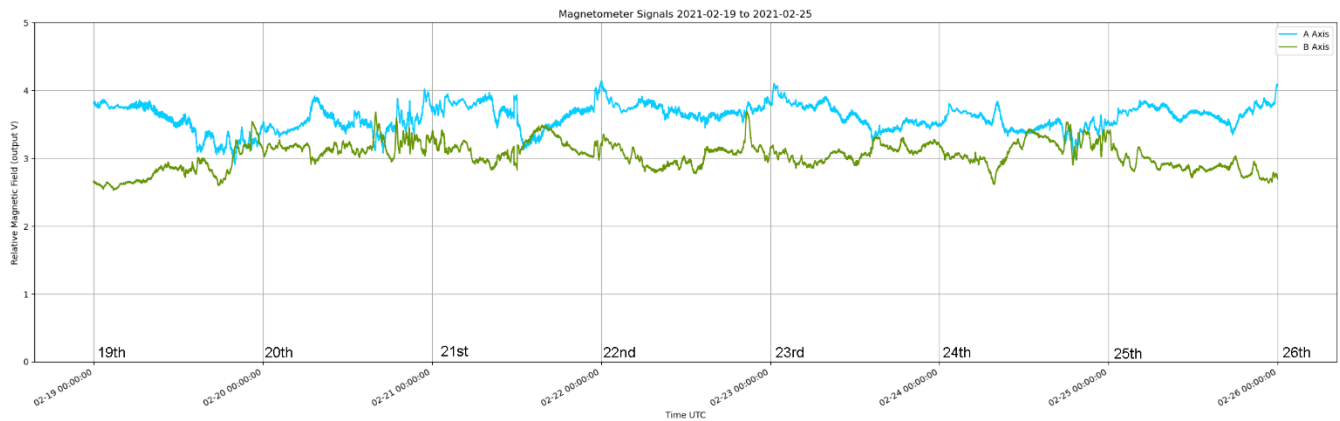
Steying Magnetometer (50.8 North, 0.3 West)



Nick Quinn's recording shows a brief pulse of activity around 21UT on the 22nd, followed by more gentle disturbances in the morning of the 23rd.



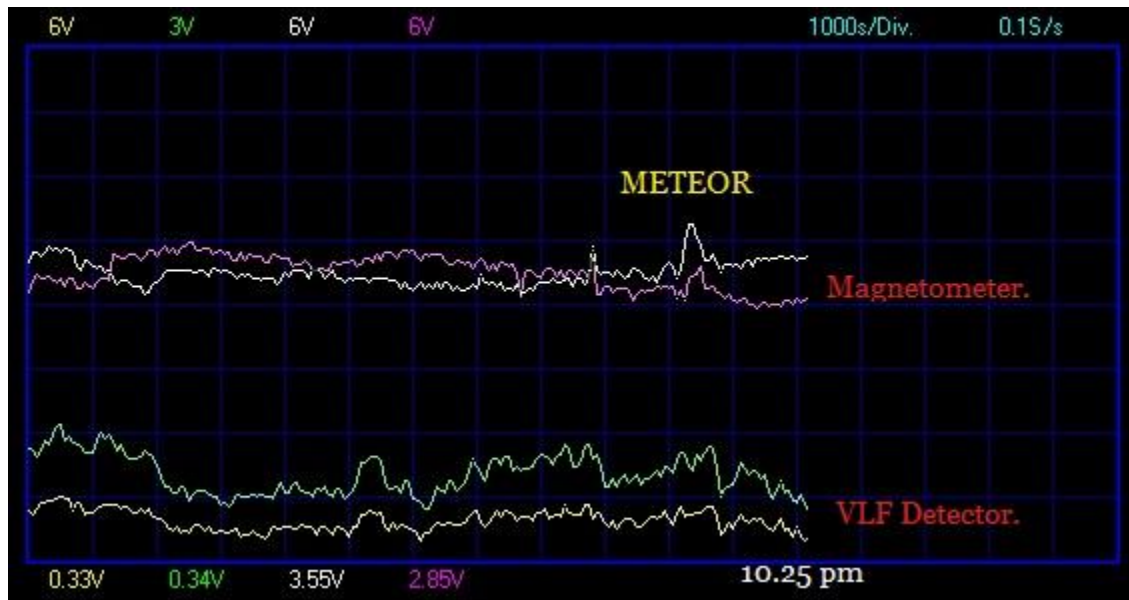
The recording by Roger Blackwell shows a further period of active disturbance in the evening of the 24th, with more gentle activity on the 25th. Mild disturbance continued through to the end of the month.



Andrew Thomas has combined the week’s magnetic activity into a single chart, shown above.

Magnetic observations received from Roger Blackwell, Colin Clements, Stuart Green, Paul Hearn, Nick Quinn, Andrew Thomas and John cook.

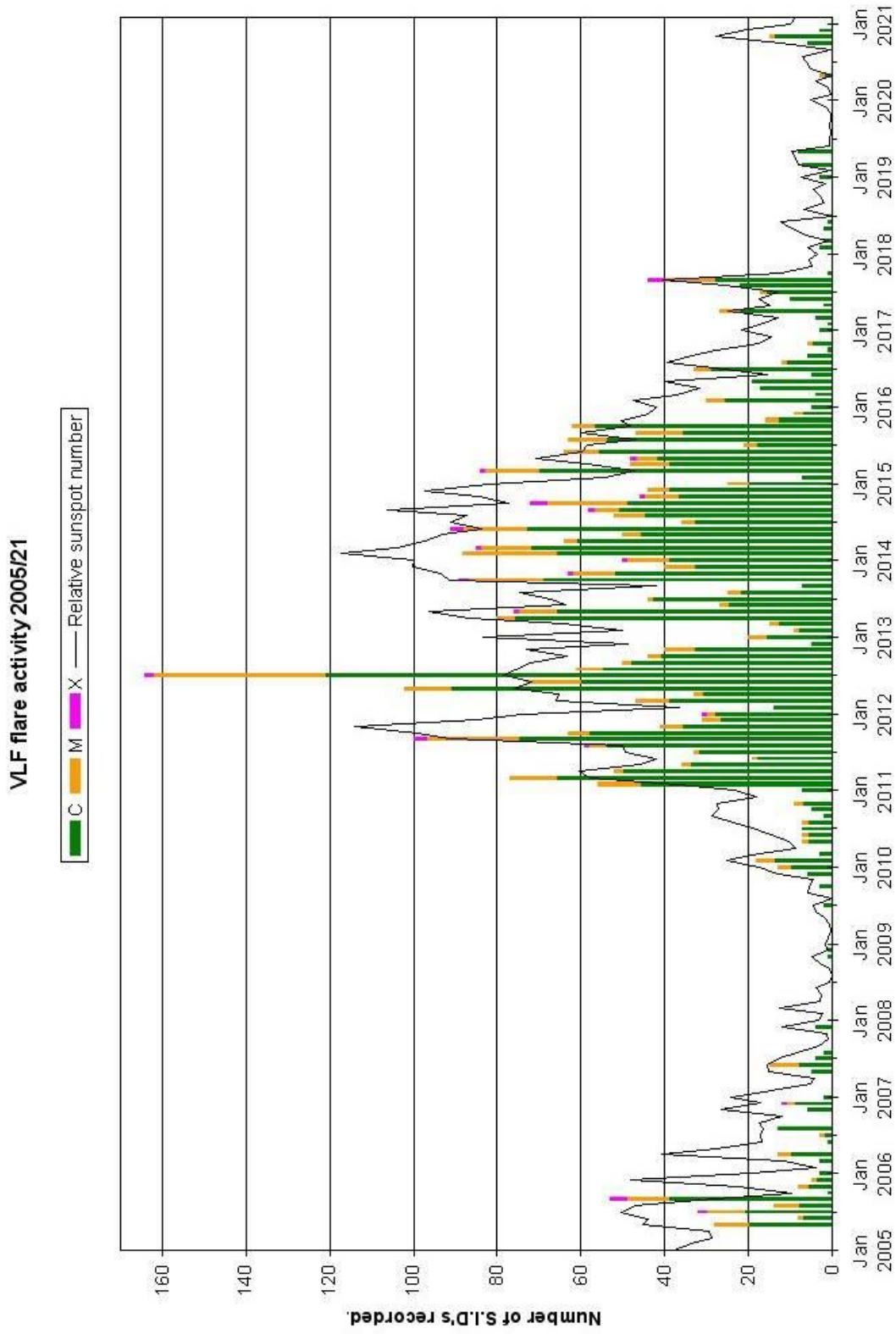
METEOR OBSERVATIONS



Gordon Holmes, a new member, has sent in this recording made at the time of the widely seen fireball on February 28th. Grid lines are at 16 minute intervals. The fireball images that I have seen were timed at 21:54UT, about 10 minutes before the magnetic pulse recorded here. I have received no other recordings around this time. I suspect that this might just be a coincidence, but include it here to invite any comments. Meteors have been well documented producing VLF effects, but usually at frequencies lower than those used for SID detection. After sunset the signals are far too random to show any connection.

Paul Hearn has started a series of zoom meetings for the radio astronomy section. The first of these proved to be very popular and has led to a number of suggestions for topics to be covered in future meetings. A full programme is available on our BAA website (URL on the heading of this summary), and is being updated as more

dates are confirmed. If you are interested and able to join in, then please do follow the links shown there. I do not have adequate equipment on this old XP PC, so I have had to take the back-seat for this. My thanks to Paul.



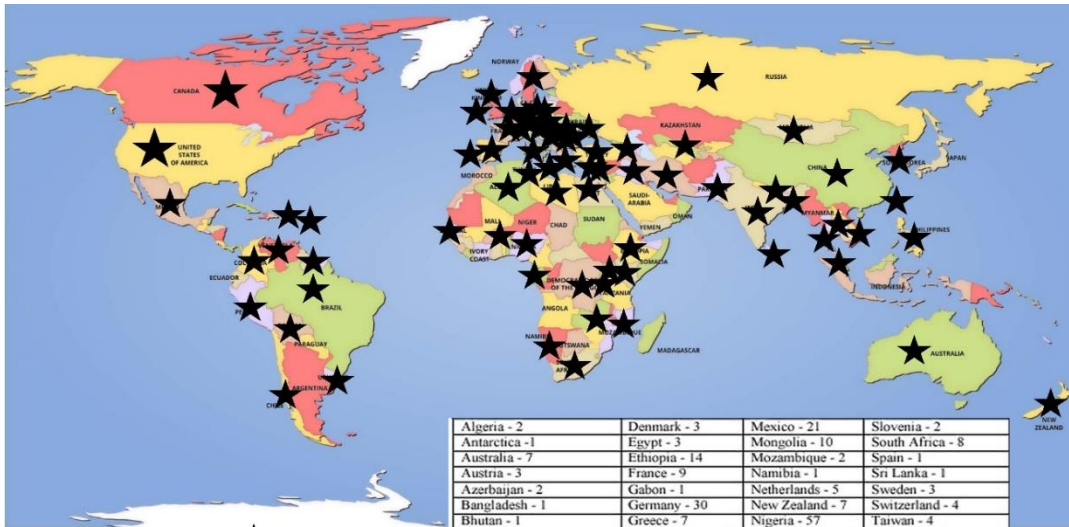
ROTATION	KEY:	DISTURBED.	ACTIVE	SFE	B, C, M, X = FLARE MAGNITUDE.	Synodic rotation start (carrington's)
2529	F	26	27 28 29 30 31	2019 January 1 2	3 4 5 6 7 8 9 10 11 12 13 14 15 16 17	2213 18 19 20 21
2530	F	22	23 24 25 26 CB	2019 February 1 2 3 4 5 6 7 8 9 10 11 12	2214 13 14 15 16 17	
2531	F	18 19 20 21 22 23 24 25 26	2019 March 1 2 3 4 5 6 7 8 9 10 11 12	2215 13 14 15 16		
2532	F	17 18 19 20 C	2019 April 1 2 3 4 5 6 7 8 9 10 11 12	2216 9 10 11 12 B		
2533	F	13 14 15 16 17 18 19 20 B	2019 May 1 2 3 4 5 6 7 8 9 10 11 12	2217 6 7 8 9 CCCC BCC		
2534	F	10 11 12 13 14 15 16 17 18 19 20 21 22 23 24 25 26 27 28 29 30 31	2019 June 1 2 3 4 5	2218 30 1 2		
2535	F	6 7 8 9 10 11 12 13 14 15 16 17 18 19 20 21 22 23 24 25 26 27 28 29	2019 July 1 2 3 4 5 6 7 8 9 10 11 12 13 14 15 16 17 18 19 20 21 22 23 24 25 26 27 28 29	2219 30 1 2		
2536	F	3 4 5 6 7 8 9 10 11 12 13 14 15 16 17 18 19 20 21 22 23 24 25 26	2220 27 28 29			
2537	F	2019 August 30 31 1 2 3 4 5 6 7 8 9 10 11 12 13 14 15 16 17 18 19 20 21 22	2221 23 24 25			
2538	F	2019 September 26 27 28 29 30 31 1 2 3 4 5 6 7 8 9 10 11 12 13 14 15 16 17 18	2222 19 20 21			
2539	F	22 23 24 25 26 27 28 29 30	2019 October 1 2 3 4 5 6 7 8 9 10 11 12 13 14 15 16	2223 17 18		
2540	F	19 20 21 22 23 24 25 26 27 28 29 30 31	2019 November 1 2 3 4 5 6 7 8 9 10 11 12	2224 13 14		
2541	F	15 16 17 18 19 20 21 22 23 24 25 26 27 28 29 30	2019 December 1 2 3 4 5 6 7 8 9 10 11	2225 10 11		
2542	F	12 13 14 15 16 17 18 19 20 21 22 23 24 25 26 27 28 29 30 31	2020 January 1 2 3 4 5 6 7	2226 4 5 6 7		
2543	F	8 9 10 11 12 13 14 15 16 17 18 19 20 21 22 23 24 25 26 27 28 29 30 31	2020 February 1 2 3	2227 1 2 3		
2544	F	4 5 6 7 8 9 10 11 12 13 14 15 16 17 18 19 20 21 22 23 24 25 26 27 28 29	2228 28 29 1			
2545	F	2020 March 2 3 4 5 6 7 8 9 10 11 12 13 14 15 16 17 18 19 20 21 22 23 24 25 26 27 28	2229 28 29			
2546	F	29 30 31	2020 April 1 2 3 4 5 6 7 8 9 10 11 12 13 14 15 16 17 18 19 20 21 22 23 24			
2547	F	2230 25 26 27 28 29 30	2020 May 1 2 3 4 5 6 7 8 9 10 11 12 13 14 15 16 17 18 19 20 21			
2548	F	2231 22 23 24 25 26 27 28 29 30 31 MCCB	2020 June 1 2 3 4 5 6 7 8 9 10 11 12 13 14 15 16 17			
2549	F	2032 18 19 20 21 22 23 24 25 26 27 28 29 30	2020 July 1 2 3 4 5 6 7 8 9 10 11 12 13 14			
2550	F	2033 15 16 17 18 19 20 21 22 23 24 25 26 27 28 29 30 31	2020 August 1 2 3 4 5 6 7 8 9 10			
2551	F	2234 11 12 13 14 15 16 17 18 19 20 21 22 23 24 25 26 27 28 29 30 31	2020 September 1 2 3 4 5 6			
2552	F	2235 7 8 9 10 11 12 13 14 15 16 17 18 19 20 21 22 23 24 25 26 27 28 29 30	2020 October 1 2 3			
2553	F	2236 4 5 6 7 8 9 10 11 12 13 14 15 16 17 18 19 20 21 22 23 24 25 26 27 28 29 30 CC BCCC				
2554	F	2237 2020 November 31 1 2 3 4 5 6 7 8 9 10 11 12 13 14 15 16 17 18 19 20 21 22 23 24 25 26 B CBCC CBC B CC				
2555	F	2238 27 28 29 30 C CM	2020 December 1 2 3 4 5 6 7 8 9 10 11 12 13 14 15 16 17 18 19 20 21 22 23 C C C			
2556	F	2239 24 25 26 27 28 29 30 31	2021 January 1 2 3 4 5 6 7 8 9 10 11 12 13 14 15 16 17 18 19			
2557	F	20 21 22 23 24 25 26 27 28 29 30 31	2021 February 1 2 3 4 5 6 7 8 9 10 11 12 13 14 15			
2558	F	2241 16 17 18 19 20 21 22 23 24 25 26 27 28	2021 March 1 2 3 4 5 6 7 8 9 10 11 12 13 14			



SuperSID
*Collaboration of Society
of Amateur Radio
Astronomers and
Stanford Solar Center*



- ✓ Stanford provides data hosting, database programming, and maintains the SuperSID website
- ✓ Society of Amateur Radio Astronomers (SARA) sells the SuperSID monitors for 48 USD to amateur radio astronomers and the funds are then used to support free distribution to students all over the world (image below as of Fall 2017)
- ✓ Jonathan Pettingale at SARA is responsible for building and shipping the SuperSID monitor kits: SuperSID@radio-astronomy.org
- ✓ SuperSID kits may be ordered through the SARA SuperSID webpage: <http://radio-astronomy.org/node/210>
- ✓ Questions about the SuperSID project may be directed to Steve Berl at Stanford: steveberl@gmail.com
- ✓ Jaap Akkerhuis at Stanford is responsible for the SuperSID software and SARA has provided financial support for his efforts
- ✓ SuperSID website hosted by Stanford: <http://solar-center.stanford.edu/SID/sidmonitor/>
- ✓ SuperSID database: <http://sid.stanford.edu/database-browser/>
- ✓ The data is searchable by time, station, date, and multiple plots may be placed on the same graph for comparison.



**SID Monitor
Distribution**
1078 instruments
82 countries
7 continents

Algeria - 2	Denmark - 3	Mexico - 21	Slovenia - 2
Antarctica - 1	Egypt - 3	Mongolia - 10	South Africa - 8
Australia - 7	Ethiopia - 14	Mozambique - 2	Spain - 1
Austria - 3	France - 9	Namibia - 1	Sri Lanka - 1
Azerbaijan - 2	Gabon - 1	Netherlands - 5	Sweden - 3
Bangladesh - 1	Germany - 30	New Zealand - 7	Switzerland - 4
Bhutan - 1	Greece - 7	Nigeria - 57	Taiwan - 4
Bolivia - 1	Guyana - 1	Pakistan - 4	Thailand - 5
Bosnia-Herzegovina - 2	Hungary - 1	Peru - 10	Tunisia - 9
Brazil - 11	India - 33	Philippines - 3	Turkey - 2
British Virgin Islands - 1	Indonesia - 2	Poland - 2	Uganda - 5
Bulgaria - 2	Iran - 4	Portugal - 3	UK - 32
Burkina Faso - 1	Iraq - 1	Rep of Congo - 3	Uruguay - 9
Canada - 33	Ireland - 9	Romania - 4	US Virgin Islands - 2
Chile - 1	Italy - 42	Russia - 3	USA - 491
China - 38	Kenya - 23	Rwanda - 1	Uzbekistan - 2
Columbia - 9	Korea (South) - 2	S Africa - 4	Venezuela - 2
Croatia - 7	Lebanon - 11	Senegal - 1	Vietnam - 1
Cyprus - 1	Libya - 1	Serbia - 1	Zambia - 2
Czech Republic - 1	Malaysia - 19	Singapore - 3	
D Rep of Congo - 4	Malta - 1	Slovak Repub - 2	

For official use only
 Monitor assigned: _____
 Site name: _____
 Country: _____

SuperSID Space Weather Monitor Request Form

<i>Your information here</i>				
Name of site/school (if an institution):				
Choose a site name: (3-6 characters) No Spaces				
Primary contact person:				
Email:				
Phone(s):				
Primary Address:	Name School or Business Street Street City State/Province Country Postal Code			
Shipping address, if different:	Name School or Business Street Street City State/Province Country Postal Code			
Shipping phone number:	<table border="1" style="width: 100%; border-collapse: collapse;"> <tr> <td style="width: 33%; height: 20px;"></td> <td style="width: 33%; height: 20px;"></td> <td style="width: 33%; height: 20px;"></td> </tr> </table>			
Latitude & longitude of site:	Latitude: _____ Longitude: _____			

I understand that neither Stanford nor the Society of Amateur Radio Astronomers is responsible for accidents or injuries related to monitor use. I will assure that a surge protector and other lightning protection devices are installed if necessary.

Signature: _____ **Date:** _____

I will need:

<i>What</i>	<i>Cost</i>	<i>How many?</i>
SuperSID distribution USB Power	\$48 (assembled)	
USB Sound card 96 kHz sample rate (or provide this yourself)	\$40 (optional)	
Antenna wire (120 meters) (or you can provide this yourself)	\$23 (optional) with connectors attached and tested	
RG 58 Coax Cable (9 meters) (or provide this yourself)	\$14 (optional) with connectors attached and tested	
Shipping	US \$12 Canada & Mexico \$40 all other \$60	
	TOTAL	\$

_____ I have included a \$ _____ check (payable to SARA)

_____ I will make payment thru www.paypal.com to treas@radio-astronomy.org

or

_____ If you are a Minority-serving institution, in a Developing or economically deprived nation, and/or you are using the monitor with students for educational purposes, you may qualify for obtaining a monitor at reduced or no cost. Check here if you wish to apply for this designation. Then tell us how you want to use the SuperSID monitor. Include type of site, number of students involved, whether public or private school, grade levels, etc. and describe your program. The goal of the SuperSID project is to provide as many students with systems as possible. If you are able to pay for a system, even if you qualify for a free one, please do so and help support our goal.

For more details on the Space Weather Monitor project, see: <http://sid.stanford.edu>

To set up a SuperSID monitor you will need:

1. Access to power and an antenna location that is relatively free of electric interference (could be indoors or out)
2. A **PC**** with the following minimal specifications:
 - A sound card that can record (sample) up to 96 kHz, or a USB port to connect such a sound card (for North and South America)
 - All other countries can use AC97 sound card with 48 kHz record (sample) rate. Most computers made after 1997 will have AC97.
 - Windows 2000 or more recent operating system
 - 1 GHz Processor with 128 mb RAM
 - Ethernet connection & internet browser (desirable, but not required)
 - Standard keyboard, mouse, monitor, etc.
3. An inexpensive antenna that you build yourself. You'll need about 120 meters (400 feet) of **insulated** wire. Solid wire is easier to wind than stranded. Magnet wire will work but be more fragile. You can use anything from #18 to #26 size wire. The antenna frame can be made of wood, PVC pipe, or similar materials. We'll provide instructions. You can purchase the wire from us or obtain your own.
4. RG58 coax cable with a BNC connector at one end to run from the antenna to the SuperSID receiver. 9 meters is recommended, but the length will depend on where you place the antenna. You can purchase the coax from us or obtain your own.
5. Surge protector and other protection against a lightning strike

Return this form to: SuperSID@radio-astronomy.org

or mail to: SARA
Brian O'Rourke, SARA Treasurer
337 Meadow Ridge Rd,
Troy, VA 22974-3256

New Specialty Amplifier with Small Parabolic Antenna Advances Hydrogen Line Observing

By Stephen Tzikas, MS Chemical Engineering

Introduction

Small radio telescopes are frequently constructed by university students for the observations of the 21 cm hydrogen line. Many skilled amateurs build such telescopes as do-it-yourself plans that have been available on the internet for years. However, no ready-made affordable kits for easy assembly have been available until now. Pablo Lewin of the Maury Lewin Astronomical Observatory in Glendora, California, and a member of the Society of Amateur Radio Astronomers (SARA) followed the instructions on the internet for the construction of one of these radio telescopes. The radio telescope was constructed for under \$300. Discussion with SARA on standardizing the supply of materials and the software requirements lead to the first ever “scope-in-a-box” for any individual to purchase a ready-made hydrogen line telescope. The “scope-in-a-box system is based on the article from rtl-sdr.com who developed the approach:

<https://www.rtl-sdr.com/cheap-and-easy-hydrogen-line-radio-astronomy-with-a-rtl-sdr-wifi-parabolic-grid-dish-1na-and-sdrsharp/>

Pablo’s insight to help create the “scope-in-a-box” will help bring radio astronomy to the masses, who otherwise might not have had the confidence to construct the telescope on their own. He implemented the instructions and even improved on them by adding a bigger antenna and another low noise amplifier (wideband) in line with the original one. A video of his set-up which is based on the same system noted at rtl-sdr.com can be seen at this link: https://www.youtube.com/watch?v=jgTAW_SvH48

As one of the beta-testers of the “scope-in-a-box,” I had the opportunity to assemble the instrument, install the software, follow the initial instructions, and finally evaluate the process and recommend improvements to the instructions. The radio telescope can now be ordered from SARA for under \$300 (SARA places the order on Amazon.com for the consumer electronics and hardware required). It is an excellent way to learn and observe in radio astronomy. The part I enjoyed the most was the hands-on experience I obtained through the scope’s easy assembly and software use. It is that interactive practical experience that I discuss in this article. While optical telescopes are fairly straight forward, radio telescopes require a little more familiarity with electronics. I hope this article helps your adventure into hydrogen line observing. The SARA kit is a radio telescope with some simple assembly and software installation. The scope-in-a-box allows one to learn about the working components of their radio telescope.

Background

In 1951, Harvard scientists Ewen & Purcell were the first to detect the 21cm line (at 1420 MHz). This allowed the measurement of the galactic rotation curve, as this radiation from hydrogen penetrates galactic dust clouds. By 1952 the first radio charts of the neutral hydrogen in the galaxy were plotted, and the spiral structure of the galaxy was revealed. This radiation is generated from a transition between two energy levels of the electron spin in the neutral hydrogen 1s ground state. This galactic emission was first predicted by H. van de Hulst in 1945. This built on earlier discoveries in the 1930s of radio emissions from the center of our galaxy, and that they could be associated with emission lines in the radio part of the electromagnetic spectrum. Hulst predicted this frequency

to be at 1420.4058 MHz. For those who attend the Eastern summer conference of SARA at the Greenbank Observatory, the original horn antenna used by Ewen and Purcell can be found on campus in front of the classic 1960s architecture of the Jansky Laboratory. For the artist, it makes a perfect scene for a sketch or oil painting.

The Scope-In-A-Box

For those who order the scope-in-a-box, they will receive the following main components:

Hardware

- Antenna with feedhorn and reflector
- Tripod and mount
- Rabbit Ears Antenna for testing

Electronics

- RTLSDR and connecting cable for laptop.
- SAWBird LNA, and the adapter between Feedhorn and SWABird LNA
- 50 Ohm Terminator
- A few miscellaneous parts (of larger packages) not required for the scope.

Software

- Software on the SARA thumb-drive

Hardware Assembly

The scope-in-a-box comes with a Premiartek Outdoor 2.4 GHz 24 DBI Directional High Gain N-Type Female Aluminum Die Cast Reflector Grid Parabolic Antenna (ANT-GRID-24DBI) valued at about \$85. It has a height of 23.6" and a width of 41.7". The Beamwidth/Horizontal is 14°, while the Beamwidth/Vertical is 10°. Those who have purchased other radio astronomy telescope kits in the past will notice this antenna is different. It is not the parabolic dish of an IBT, nor the loop antenna of a SuperSID, nor the dipole antenna of a Radio Jove kit. To help put this in perspective, antennas are classified by their physical structure and functionality. Some types of antennas include, but are not limited to:

- Wire Antennas: Dipole, Helix, Whip, and Loop for appliances, buildings and conveyances
- Reflector Antennas: Parabolic for microwave transmission, satellite tracking and radio astronomy
- Aperture Antennas: Horn antennas for aircraft and spacecraft
- Microstrip Antennas: Metallic patch/strip for conveyances and mobile phones
- Array Antennas: Yagi antennas for high gain applications with control of the radiation pattern
- Lens Antennas: Lens for very high frequency applications

Notice that the parabolic grid antenna of the scope-in-a-box also comes with a feedhorn. A feedhorn is a horn antenna. It receives the reflected waves from the parabolic grid. Some key functions of a feedhorn include supporting a specific frequency range; supporting a particular type of polarization based on its waveguide shape; providing a certain amount of gain; and offering flange compatibility to connect the feedhorn to a low noise band (or block) converter of frequencies, which can convert to another frequency for input to a receiver.

Finally for hardware, the tripod assembly consists of a Model SKY6016 tripod/base mount with level and compass, 3 feet tall, costing about \$43. The antenna, tripod, and mount are all metal.

Electronics Assembly

The electronics parts in the scope-in-a-box consists of:

- Nooelec SAWbird+ H1 – Premium Saw Filter & Cascaded Ultra-Low Noise Amplifier (LNA) Module for Hydrogen Line (21cm) Applications 1420MHz Center Frequency. Designed for Software Defined Radio (SDR), about \$45.
- RTL-SDR Blog V3 R820T2 RTL2832U 1PPM TCXO HF Bias Tee SMA Software Defined Radio with Dipole Antenna Kit (this is the dongle and rabbit ears antenna), about \$38.
- USB 3.0 Extension Cable 10FT Type A Male to female Extension Cord AINOPE High Data Transfer Compatible with USB Keyboard, Flash Drive, Hard Drive, about \$10.
- Maxmoral N Type Male to SMA Male convertor Wi-Fi Adaptor Connector, about \$7.
- DHT Electronics RF Coaxial Connector Adapter SMA Male Coaxial Termination Loads 1W DC – 3.0GHz 50 Ohm, about \$6.

The NooElec LNA and filter is specifically designed for amateur radio astronomers, and to be used with the RTL-SDR dongle for the reception of hydrogen line. This LNA has a high gain and a good RF filter for reducing interference. It comes with a power LED indicator.

The RTL-SDR dongle comes in a multipurpose antenna set. This smaller whip antenna is used for testing the dongle and software installation of the scope-in-a-box. Beside hydrogen line observing, the RTL-SDR dongle can be used for many other amateur ham radio applications associated with meteor scatter monitoring; satellite and weather balloon reception; public safety radio; and general radio scanning. It has a frequency range of 500 KHz to 1.7 GHz. It has up to 3.2 MHz of instantaneous bandwidth and is 2.4 MHz stable. It is safe for travel through airport scanners. X-rays don't create currents in the circuitry, especially if not powered. RTL is short for RTL2832U. It is a Realtek RTL2832U chipset that is popular and can be used for wideband Software Defined Radio (SDR) receivers. Such devices known as RTL-SDR dongles. It takes radio frequency signals and converts them to audio frequency. Hence the scope-in-a-box picks up many FM radio stations. The SDR software performs all of the digital signal processing,

In electronics, there are many types of connectors. The N type male to SMA male connector is used in radio frequency electronics. N connectors are named after Paul Neill of Bell Labs. It's a threaded, weatherproof connector for coaxial cables. SMA connectors stand for subminiature version A. They too are used to connect coaxial cables and have a screw-type coupling mechanism.

The 50 ohm terminator can be placed on unused coaxial ports to prevent the RF signal from reflecting. It is used in the calibration process for the scope-in-a-box.

SDRSharp Software Installation and Calibration

The scope-in-a-box uses an SDR receiver. As the name implies, it is digital based rather than analog based. This software must take the analog signals received from the sky and convert it to digital. It accomplishes this by converting the electrical signals to binary format. The continuous analog signal is sampled at regular intervals and assigned a discrete string of bits, that is, the binary digits. The actual creation is based on two voltage bands. One is near a reference value (ground or zero volts). The other near the supply voltage. These represent zero and one. For example, when a microcontroller is powered by 5 volts, it recognizes 0 volts as binary 0, and 5 volts as binary 1. The instrument that converts from analog to digital is called an Analog to Digital Converter (ADC). It takes an

analog voltage on a pin and converts it to a digital format. Since the conversion quantizes the input, it introduces a small error. ADC performance is based on its bandwidth (sampling rate) and signal-to-noise ratio (SNR). The SNR is affected by resolution, linearity, accuracy, aliasing, and jitter (timing errors).

The new scope-in-a-box kit represents the latest effort to bring a part of radio astronomy to the masses. It is affordable, easy to assemble, and will offer hours enjoyment and a launch pad for other radio astronomy activities.

“Scope in a Box” First Experience and Some Enhancements.

Alberto Sagüés*, KA4MTO, Lutz, Florida

Contact: sagmatcons@earthlink.net

Sharing the Experience

I wrote this to share some of my first, getting-acquainted steps in amateur radio astronomy, which is being revolutionized by the availability of powerful affordable instrumentation and software. Last December Dennis Farr, to whom we owe so much in the Tampa area for promoting astronomy both optical and radio, alerted me that the Society of Amateur Radio Astronomers (SARA) had facilitated things by putting together a “Scope in a box” radio telescope kit for beginners. It did not take much to persuade me to try it, and I ordered one. Here I describe my experience with putting the Scope together, the “first light” try, an enhancement to motorize the antenna, and my first (I think quite lucky) attempt at using the Scope to map the sky on the hydrogen 1.4 GHz line. I hope that this narrative will get others equally animated to try the Scope, and variations like illustrated here.

The Kit

The site <https://www.rtl-sdr.com/cheap-and-easy-hydrogen-line-radio-astronomy-with-a-rtl-sdr-wifi-parabolic-grid-dish-lna-and-sdrsharp/> describes in detail what the Scope is based on, what it does, and how to download and install the (free) software for it. The version sold at the time included the following (I understand that now they supply with the kit a thumb drive with software/instructions):

- RTL-SDR V3 (a Software Defined Radio (SDR) USB dongle made by RTL)
- Type N to SMA adapters (coaxial cable adapters; one large-to-small and one small-to-small)
- 50 ohm termination loads SMA connectors (50 ohm resistors that screw in at the coaxial cable connector)
- Nooelec SAWbird LNA with filter for H1. This is a Low Noise Amplifier (LNA) module with a bandpass filter around the 1420 MHz frequency of the H1 signal, terminated by coax connectors.
- 10ft USB Extension cable (low loss USB-3 cable that connects between the SDR and the computer)
- Tripod for antenna (a sturdy steel/plastic tripod)
- 2.4GHz Directional High-Gain Antenna (about 1m wide parabolic antenna with output via a short Type N coax cable).

The items arrived after just a few days, well packed with no shortages or damage.

Assembly

I assembled the antenna first; it was straightforward. The dish hardware includes metric stainless steel fasteners that will not rust. The dish weighs about 5 lb. Next I assembled the tripod. It has a ~ 2-inch diameter plain steel pipe that fits inside a plastic base that in turn has three plain steel legs. In my unit the plastic base hole was too tight to fit the pipe all the way in, so I used a rasp to enlarge the hole. It goes in further now, allowing for adequate tightening with a provided set screw lever. The antenna is attached to the pipe with provided U-braces; I enlarged a couple of brace holes a bit with a small file for easier fit but overall, mechanical complication in assembly was minimal. The tripod legs open or close with no effort; if you want them not to fold back in you can add in jamming screws, which I did later.

Electrical assembly was straightforward too. The large-to-small coax adapter is connected between the thick antenna coax and the LNA input. The small-to-small coax adapter goes between the LNA output and the SDR, and the USB-3 cable goes between the SDR and the computer. Be prepared to periodically undo the connection between the LNA and the antenna-side adapter to screw in the LNA input one of the 50 ohm termination loads for calibration.

Next, I did software download and installation following the instructions in the website. Remarkably, all installations worked on the first try. Do patiently follow the instructions including those in the Quickstart Guide for the SDR; it is easy to inadvertently skip over some of the steps. The computer I used first was a Microsoft Surface Pro 2 with Windows 10.

First Light

For my first “light” test I took the antenna outdoors and pointed it to the zenith as indicated in the Scope description website. I temporarily disconnected the antenna from the LNA and connected the 50 ohm terminator to the LNA input. I followed then the website instructions under “Receiving and Averaging the Hydrogen line FFT”.

During the first steps, don’t forget to click in the “Offset Tuning” box in the screen, which according to the instructions will “enable the bias tee via the V3 driver hack”. Translation for non-geeks: The USB3 cable powers the SDR dongle, and the SDR dongle passes some of the USB power up to the LNA with a circuit called the “bias tee”, so the LNA can run too. That function is software-controlled by a plug-in called “V3” that you download during installation and is activated by clicking in “Offset Tuning”. When you do that, you will see a white LED turn on in the LNA, indicating that it is getting power. If the LED is dark, the LNA is not getting power; check to make sure you followed correctly the turn-on steps.

After I tuned the SDR to 1,420.000 MHz and got to the IF Average part of the procedure, I departed from their recommended setting (which would average the signal over seven long minutes) to something that renewed screens much faster so you can see results from changes you made after a few seconds: FFT Resolution=1024, Intermediate average=10, Gain = 274, Level=973, and Dynamic Averaging = 27040. Then, I clicked in Window, pressed Background and waited a couple renewal cycles. First times the resulting IF average window tended to be either all blue or all black. I needed then to change the Gain setting up or down until the line graph showed within the screen range. The correct graph looked like a horizontal or moderately sloping line usually with small twists near the left and right ends.

Now it was time to unscrew the 50 ohm terminator and reconnect the antenna coax. The result after a couple screen renewals is shown in Figure1. The H1 line was clearly visible as the blip a bit to the right of the 1420 MHz marker. The display was a bit noisy due to the short time averaging, and the spike near 1421 MHz was an artifact, but otherwise functionality looked good. Checking Stellarium (open source software recommended in the instructions) I found that at the time of the test the Galaxy’s bright “band” was a bit off the zenith, being brighter some 30-40 degrees to the west. Thus I tilted the antenna against a stool a bit in that direction, with the result shown in Figure 2. The line was a bit more substantial, as expected. The results were promising so I moved on the next stage: motorized scanning of the sky.

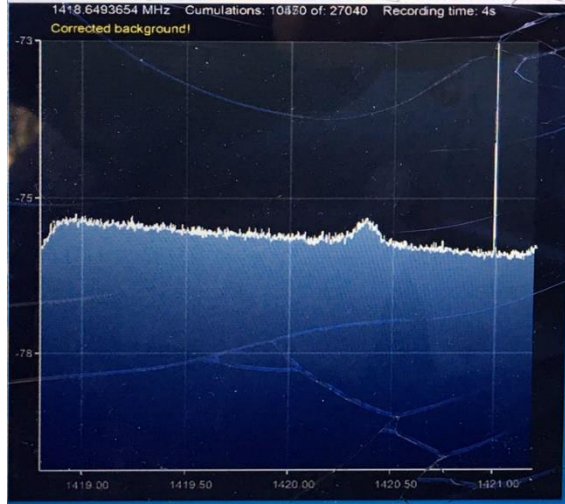
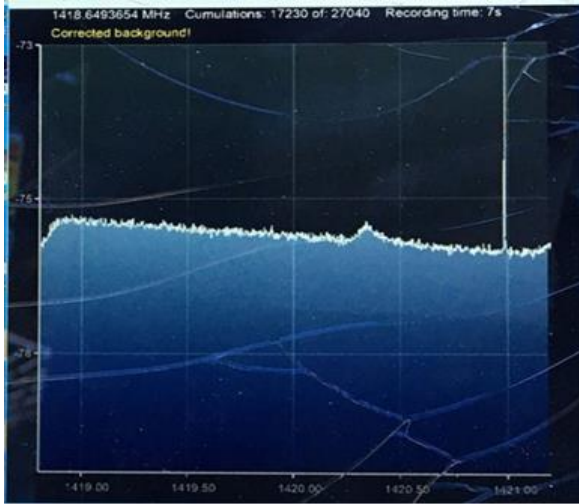


Figure 1 – Antenna to Zenith.



Figure 2 – Antenna tilted to a brighter zone of the Galaxy.

Motorized Altitude Scanning

Having established that the system was operational, the next idea was to motorize the antenna so it would rapidly scan in the N-S direction, and to repeat that at intervals during the day so as to record the scans at various right ascensions, thus getting a 2D H1 map of the sky from which a grayscale image of the galaxy could be constructed.

Note: DO NOT attempt anything hardware-related like this unless you are thoroughly familiar and proficient with mechanical and electric safety practice. That includes, but is not limited to, implementing grounding/isolation of motor, antenna and cables as appropriate; avoiding accidental contact of the antenna with power lines; and adequate lightning protection. Otherwise there is risk of deadly electric shock, and serious computer and other property damage.

To achieve the N-S rotation I revived a 50-year old TV antenna rotor that I had kept in the attic for the last few decades, waiting for just this occasion. It is a genuine Alliance Tenna-Rotor (R) Model U-100 complete with its 1960's style control box. The motor is actually a 1 RPM servo with position encoded at 10 degree intervals by a cam and spring contacts. Control logic is fully electromechanical via a clunky solenoid and lots of cleverness. The motor is synchronous and operated at about 30 V, 60 Hz, powered by the wall socket via a transformer. The control box back-to-back electrolytic capacitors used to get the right phase shift in the motor coils were dead, so I had to replace those. Once that was done and the motor gears and bushings were properly cleaned and re-lubricated, the system worked beautifully.

The rotor was designed to operate in azimuth, so for altitude I turned it on its side and made a bracket to hold it that way on top of the tripod pipe. Then I slipped inside the shaft opening an approximately 1x1 inch square steel channel. The channel protruded on two sides; on one side I attached the antenna bracket and on the other a 6 lb counterweight made of a surplus motor flywheel, positioned to balance by adjusting radial distance on a threaded rod. The arrangement is shown in Figure 3. The adjusted system was in good static balance so on rotation the motor did not need to overcome any large torque on top of friction, which was not much. Center of gravity was on the vertical pipe. I attached the tripod to a board with wheel casters for easy rolling in and out the garage.

At first, I did not know how to prevent the thick coax from twisting back and forth (and eventually failing by fatigue) as the motor rotated. On correspondence with the very helpful SARA team, I followed the great idea from Pablo Lewin, WA6RSV to make a one-time bend of the coax so it met the LNA-SDR dongle tandem near the axis of rotation. Thus, the small residual motion is handled by the much thinner and more flexible USB cable, loosely wrapped $\frac{1}{2}$ turn around the axis. This is shown in Figure 4.



Figure 3 – Motor with antenna on one side and counterweight on the other. Tripod is braced on board with wheel casters.



Figure 4 – Coax twisted once to meet LNA- SDR tandem, attached with zip ties near to rotation axis so USB cable gets minimal torsion when motor rotates.

I have not yet weatherized the system. That will be necessary if exposed permanently, as the motor was intended for vertical axis placement with rain guard placed accordingly and casing was designed for natural drainage. When placed horizontally all kinds of water entry and accumulation are possible. Moreover, the coax, LNA-SDR contacts and USB cable will not like water exposure. To control all that will be another project so for now the antenna is rolled outdoors and operated only when it does not rain.

2D Scanning test procedure

After a preliminary 1D scanning trial to verify combined motor operation and radio acquisition, I conducted my first 2D test on February 5, 2021. The antenna was placed outdoors, oriented so that its axis stayed on a plane that contained the meridian, and in a front yard location that was obscured by trees on N side up to an altitude of about 50 degrees, and on the S side by the garage roofline up to an altitude of about 60 degrees. Thus, there was clear sky view over a 70 degrees interval. The data discussed here were acquired at 8 angular positions 10 degrees apart, starting 40 degrees N of the zenith (position #1), continuing through other points to the zenith (#5), and ending 30 degrees S of the Zenith (#8). Since in Lutz the zenith is at altitude about 62 degrees, the acquisition range matched closely the clear sky range. The test plan consisted of scanning the 8 angular positions (which took about 10 minutes) starting at about 1 pm and repeating the scan at roughly 3/4 hour intervals over the next 10 hours. The result was a grid of 8 x 15 spectra around 1420 MHz, covering a grid of sky positions that contained a portion of the galaxy.

To work from indoors I purchased an extra 10 ft USB3 extension cable identical to the one provided in the kit, and used it in series as an extension. I noticed no problems with operation with the extended cable. Figure 5 shows the antenna ready to start a scan, controlled from inside the garage. The lighter cable is the motor control. The jug on the board is for added stability as it was windy.



Figure 5 – Antenna outdoors operated via two 10 ft USB3 cables in series.

Before starting I calibrated the LNA-SDR by surrounding the sensor at the focus of the antenna with aluminum foil and running the background correction procedure. While this deviates from the recommended procedure of using the 50 ohm terminator, it was less cumbersome than physically disconnecting and reconnecting the stiff and twisted antenna coax, and still produced reasonable results as shown later. The averaging settings I used were FFT resolution=256, Intermediate average=100, Gain =310, Level= 1000, Dynamic averaging = 180300. Those settings resulted in a refresh cycle of about 18 seconds with moderate noise level, and allowed for completion of the 8-point altitude sequence in about 10 minutes.

To acquire a data sequence I first stopped the SDR acquisition (press ■). Then I slewed the antenna to 40 degrees N of zenith. After it stopped I started acquisition by pressing run (▶), then waited for at least one refresh cycle (~20 seconds) until the averaging pattern stabilized. At that moment I pressed “Export single AV” to save the pattern in a .txt file. So as not to spend time choosing folders and naming files anew each time, I had prepared beforehand a folder named by the starting acquisition time, and containing 8 blank .txt files named from 01 to 08. That way I did each save quickly and with only a few clicks. Getting organized is important as otherwise mistakes are made and it is easy to miss or mislabel data. After saving the file I pressed Stop again, slewed to the 30 degrees N from zenith position, and did acquisition and save again. This continued to the other angles until I completed all 8 positions. It was time then to wait until the next scan some 45 minutes later, when the procedure was repeated, and so on until the end of the chosen test period.

I found that if I placed the computer in hibernation between scans the software correctly remembered the previous settings and the calibration. The reason I stopped acquisition while slewing to each next position and stopping there, was that the electric transients of motor start/stop created enough of a local radiation jolt to crash the sensitive signal receiving and processing software if acquisition was turned on. To restore function in those cases I needed to stop the program, unplug and re-plug the USB cable, and restart, with uncertain settings and calibration retention. However, if the SDR acquisition was stopped during motor on-off there was no crash, so I have carefully followed the above procedure for now. As an added safety step, to avoid possible ground loop power supply bad surprises, I did all the entire operation with the computer only on battery power and with the power “brick” completely pulled away from the wall socket. I plan to examine shielding and transient avoidance solutions in future development.

2D Scanning first test results

Each N-S scan produced 8 files, each with a spectrum of 256 frequency values and corresponding signal strength values. Others have developed software to process this type of result into a graphic map of intensities in the sky (see for example Job Geheniau’s work in <https://www.rtl-sdr.com/tag/hydrogen-line/>). As a learning experience, I did a simplified spreadsheet approach of my own, as follows. I started by loading the data files into a Microsoft® Excel spreadsheet. An example a combined x-y chart of the data in the files for one of the scans is shown in Figure 6.

In this example the H1 “line” is clearly visible at most of the directions. At the most Northern directions the line was stronger and broadened toward the high frequency side. More to the S the line was less strong, and it appeared to be narrower. Disregarding the small “blips” at the very ends of the frequency interval sampled, the residual background is clearly apparent on the low frequency side, where it approximates a straight line.

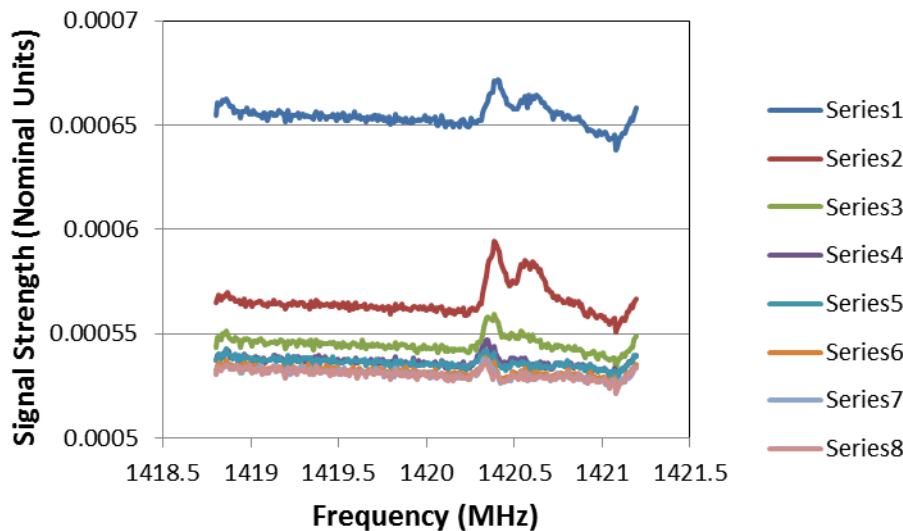


Figure 6 – Example of N-S scan unprocessed results. Acquisition of this set started 03:13 pm. Series 1: Direction is 40 degrees N of Zenith. Series 2-8: Incrementally southward directions at 10 degree intervals (so for Series 5 the antenna aimed at Zenith).

These features, along with others apparent in closer analysis, allowed for the data to be numerically processed in an Excel spreadsheet to approximately subtract the residual background from each series (or to “de-trend” the data, in spectral analysis terms). The result is the H1 peak for each case, more or less clean of extraneous information other than random noise. I leave the detailed description and added working assumptions of the de-trending math for another occasion, and directly show in Figure 7 the result of de-trending the data in Figure 7.

The variation in the line with sky orientation is quite apparent. It was now time to obtain a corresponding value of the intensity of the H1 signal for each antenna orientation. To do that one could take the maximum value of the strength in each case, but given the variety of peak shapes a better indicator is the integrated intensity, or area under the curve.

I did that in Excel simply by summation of the de-trended values in each series for the listed frequencies from 1419.8 MHz to 1421.0 MHz. That range roughly bounded the peak on each side. The result was only a nominal integrated intensity, without normalization or physical units. However, as it was calculated the same way for all series and scan times, it was good enough for creating a relative radiation brightness map. By having the spreadsheet repeat the procedure for each one of the scan times, I ended up with an array of 8 X 12 integrated

H1 intensity values. I further processed the data to interpolate it for precise 40 minute intervals, which correspond to 10 degrees of right ascension rotation.

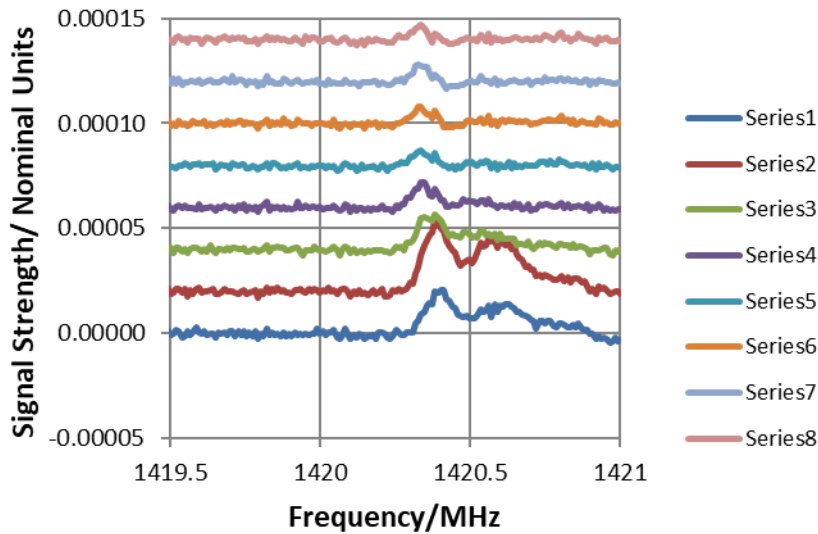


Figure 7 – De-trended version of the data in Figure 6. Series 1 is presented as obtained. The other series have been added incremental 0.00002 unit steps for display clarity only.

That matched the 10 degree altitude spacing used in each scan, thus yielding a “square” angular grid 10 degrees on center, ending up after trimming as an intensity data field on an 80 X 140 degree region of the sky. With those data I prepared a custom Excel grayscale graph where the whitest shade corresponded to the highest signal strength in the array and black to the lowest. The result is shown in Figure 8.

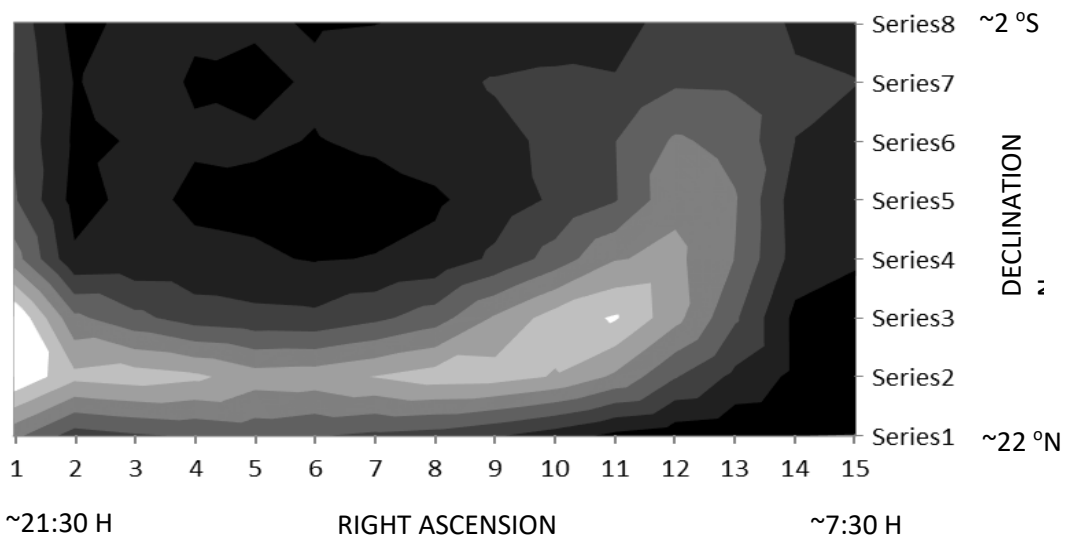


Figure 8 – Relative signal intensity as function of sky position in a 10-degree on-center grid. The roughly approximate right ascension and declination (S is up) values were gleaned from Stellarium for the times/date of observation and are based on local latitude and the altitude antenna orientations.

Clearly the result shows a band of brightness over a generally dark background, with a couple of brighter regions. To see if that made sense, I ran Stellarium for the time corresponding to the middle of the operation (Right ascension #8 on the local meridian). Rather than doing some complicated map projection conversion, I used a cylindrical projection and simply marked in red the (curved) lines roughly corresponding to the edges of the angular square grid in Figure 8. The result is shown in Figure 9, where I matched the S-up orientation of Figure 8. I used the cylindrical projection option to minimize the graphic contraction near the pole. Amazingly, despite all the crude approximations used in processing the data, the noise and the low antenna angular resolution, it looks like the radio map captured the broad features of the galaxy portion sampled. Those include a band of brightness close to the N side of the field, and the bending next up toward the S on the right side. There seems to be also some degree of capturing the relative brightness distribution.

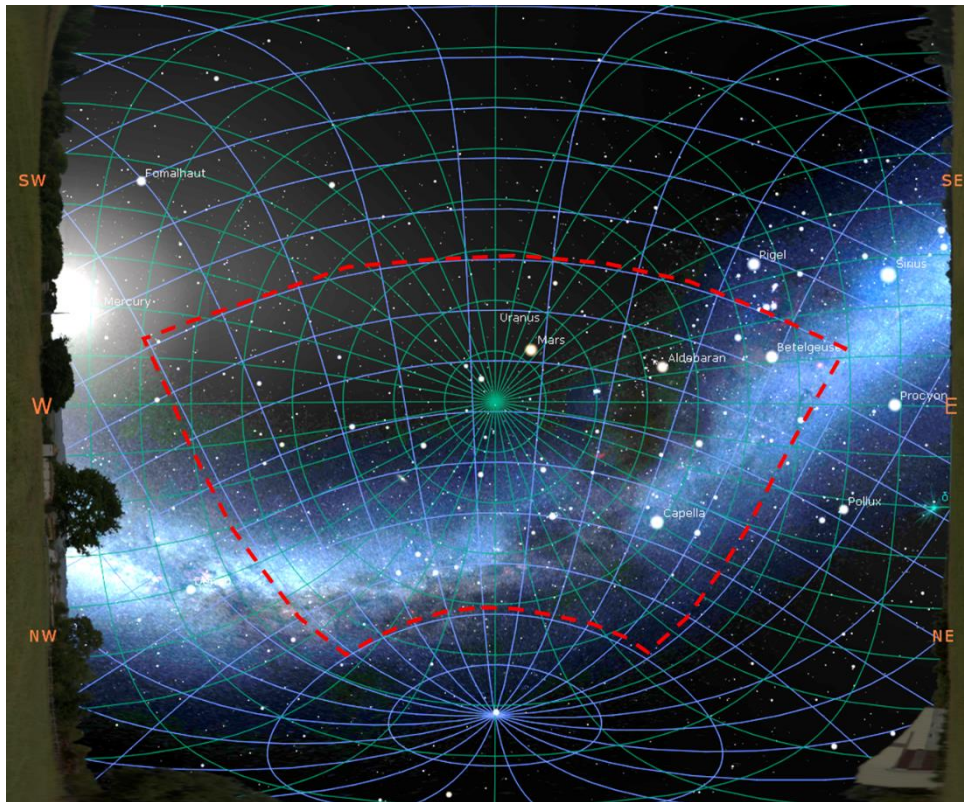


Figure 9 – Stellarium cylindrical projection set to match the orientation (S is up) in Figure 8 for the meridian crossing corresponding to Right Ascension # 8. The square angular interval boundaries in Figure 8 roughly correspond to the curved red lines here.

It should be noted that these results are mostly anecdotic, since I am yet to replicate the observations and go through a more critical evaluation of the data. Analysis was rough and preliminary, subject to correction and update. Nevertheless, considering this was a first try the performance has been very encouraging. I look forward to honing the technique and attempting a more practical antenna steering and data acquisition approach, as well as streamlining data processing.

Summary and What Next

The Scope in a Box experience for me included a greatly facilitated learning curve and the satisfaction of getting encouraging results right away. The SARA team is to be commended for putting together this approach, supplemented with good instructions. I appreciated their helpful attitude and valuable assistance when I got stuck now and then. I hope that other beginners will enjoy similar experiences. I look forward to attempting some follow up steps; my current wish list includes:

- Replacing the manual antenna steering (as well as on-off SDR cycles) with an Arduino (or similar) -based control and power source, so as to have automatic scans performed at regular intervals. Hourly in-person operation is ok for first tests but not practical otherwise.
- Weatherizing the antenna motor and LNA-SDR train. That is a must for round the clock operation. This being Florida, there is also need for robust outdoor mounting against wind, and appropriate lightning protection of the indoor equipment (sadly, the LNA and SDR better be considered as disposable).
- Optimizing data acquisition interval for reduced noise. Enhance evaluation and expand analysis /display to include features such as color coding for Doppler information. Learn more about bias-tee management, toward possibly automating background correction.

Sample of HF Radio Reflections from Aurora Observed at Anchorage, Alaska USA

Whitham D. Reeve

At almost exactly 0600 UTC on 20 February 2021 (9:00 pm local on 19 February), I noticed a bright wavering trace in the Argo plot running on one of my observatory PCs (figure 1). The associated receiver is tuned to 15 000 995 Hz LSB and the demodulated carrier is indicated at 995 Hz on the Argo plot. The trace had not been there for at least 15 min before. Coincidentally, I had my SAM-III magnetogram webpage displayed on the same PC, and it simultaneously showed a very rapid increase in the magnetic induction of all magnetic field components (figure 2).

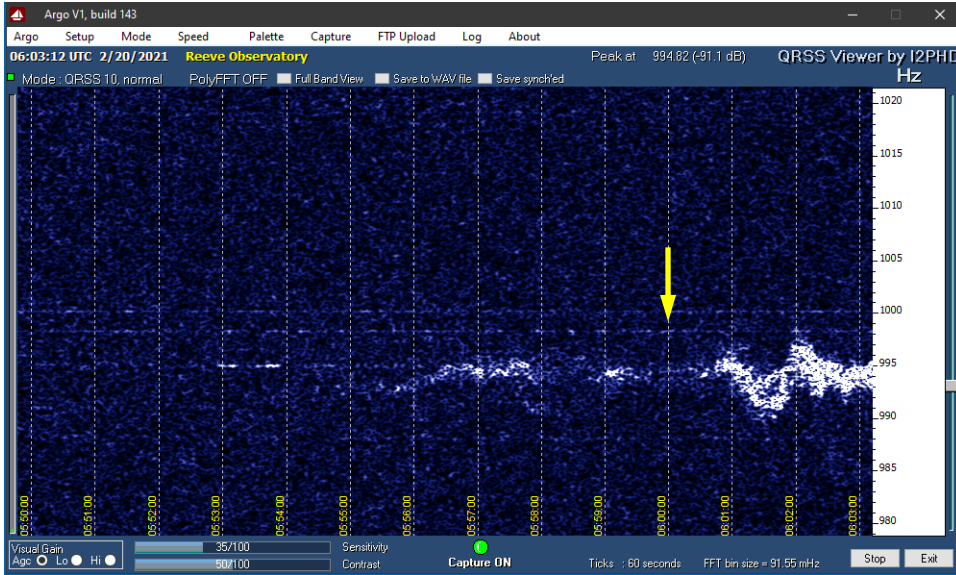


Figure 1 ~ 12-min Argo horizontal waterfall record from 20 February 2021 starting at 0538 and ending at 0603 UTC. The demodulated frequency is shown on the right vertical scale and time-stamps are shown along the bottom in yellow. In this case, the 15 MHz carrier is demodulated to 995 Hz. The yellow arrow marks the nominal start of the aurora reflections at 0600. The traces of aurora reflections exhibit a thick structure and rapid frequency shifts. The trace during *normal* propagation is thin and straight.

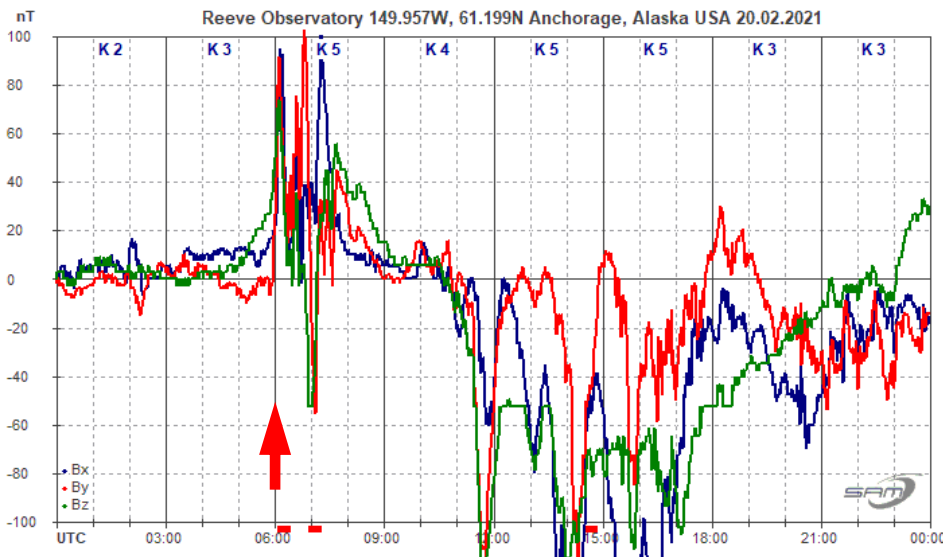


Figure 2 ~ 24-h SAM-III magnetogram for 20 February 2021. The vertical axis has been scaled to match the values for the time period 0600 to 0800; later activity is off-scale. Note the near-step-change in the red trace (By) at 0600 marked by the red arrow. Also, note that Earth's magnetic field almost returned to pre-storm levels by 0900, but then experienced a bay (decrease) lasting the rest of the day.

It is well-known that rapid field changes measured by ground magnetometers indicate the high probability of aurora, which, in turn, indicates the possibility of radio reflections from the aurora (see sidebar at end). I have seen simultaneous magnetic activity and HF radio reflections in my SAM-III and Argo data many times but never before watched them in real-time. I usually see aurora radio reflections in data that are produced near local solar midnight (around 1000 UTC \pm 3 h), but the event described here occurred a little earlier. The event was not unique.

The next night (21 February) the magnetic field By component rapidly increased at 0830 to K5 K-index resulting in 15 MHz enhancements and rapid frequency shifts similar to the night before. These events involved either the time-frequency station WWV or WWVH; however, because the propagation path between WWVH and Anchorage is oriented north-south, it is believed that WWVH is the one being reflected by the aurora (aurora reflections are most often received along north-south paths).

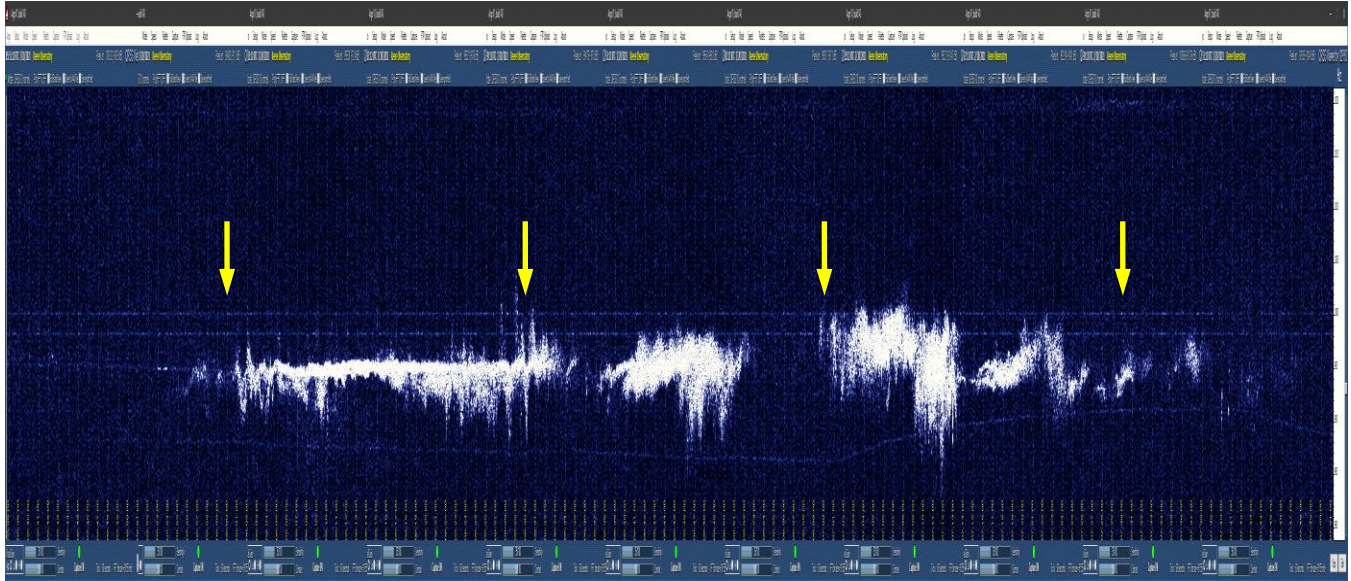


Figure 3 ~ Eleven Argo images spliced together for the time span 0538 to 0751 to cover the 2-h event. The spliced images have been stretched vertically to better show the Doppler frequency shifts of -11 to $+7$ Hz. Yellow arrows are time markers for (left-to-right) 0600, 0630, 0700 and 0730 UTC.

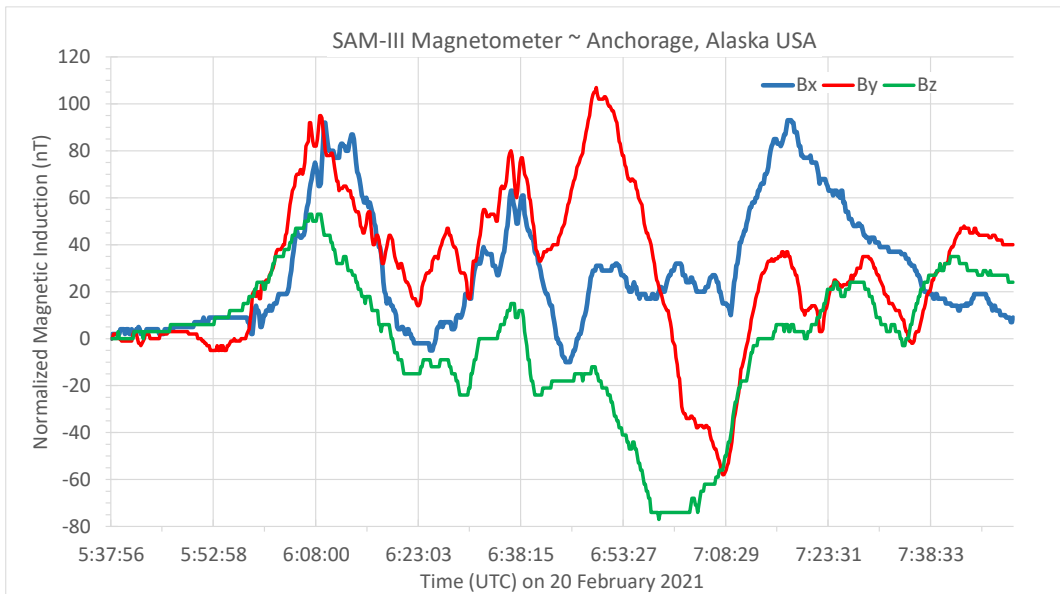


Figure 4 ~ Normalized magnetic data Bx, By and Bz from the Anchorage SAM-III magnetometer covering the same time period as the spliced Argo images shown in the previous figure. The perturbations shown here were followed by a K-index = K5 for the 3-h synoptic period 0600 to 0900 UTC.

This aurora reflection and magnetic event on 20 February lasted about 2 h. Each Argo horizontal waterfall image is 12 min long, so to show the entire event, I spliced 11 images starting at 0538 and ending 0751 UTC (figure 3). A characteristic of aurora radio reflections is their wild frequency changes from Doppler shifts caused by rapid changes in the electron cloud columns associated with the aurora – these changes could be in electron density or drift movement, or both. The frequency shifts are clearly evident in the spliced images but the Doppler frequency range of -11 to $+7$ Hz is low compared to many reflection events I have observed.

The SAM-III magnetic data is replotted for the 2-h period (figure 4). The data have been normalized to the value of each component at the beginning of the period so that only the positive and negative deflections through the period are shown. Aurora forecasts for 20 February showed the likely outcome of the geomagnetic activity (figure 5), but I could not verify them because aurora was not visible at my observatory due to light pollution.

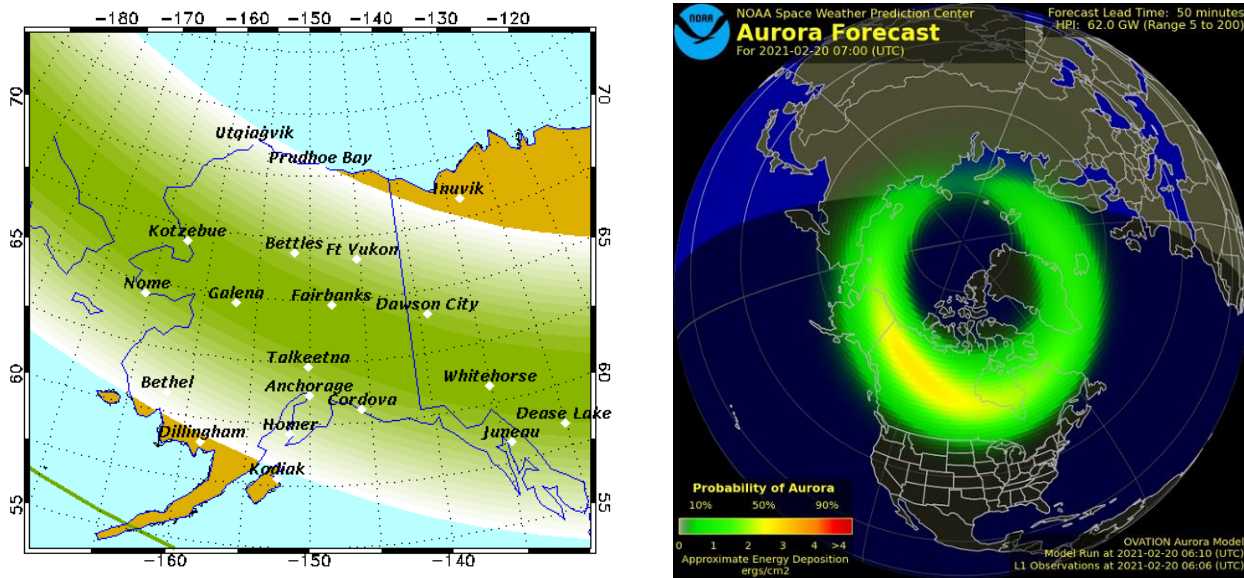


Figure 5 ~ Left: Aurora forecast for 20 February 2021 showing the maximum expansion of the auroral oval above Alaska. Anchorage normally is on the southern edge of the auroral oval but, as can be seen in this prediction, it is well embedded. Image source: University of Alaska Geophysical Institute {[UAF-G](#)}. Right: Northern hemisphere aurora forecast for 0600 UTC 20 February based on the OVATION Aurora Model shows similar predictions. Image source: Space Weather Prediction Center ([SWPC](#)).

According to Space Weather Prediction Center (SWPC), Earth’s magnetic field was under the influence of a coronal hole high-speed stream (CHSS) during the period in question. Along with a solar wind velocity increase to 605 km s^{-1} , the B_z vector component of the interplanetary magnetic field (IMF) pointed southward several times to as much as -11 nT . A southward B_z can cause magnetic disturbances through magnetic reconnection with Earth’s magnetosphere. (Note: The B_z component of the IMF is defined differently than the B_z component of Earth’s magnetic field, see {[Reeve15](#)}). As seen in the 24-h SAM-III magnetogram above, magnetic storm conditions (K -index = $K5$) reappeared at 1100 and lasted until about 1800; however, these did not produce aurora radio reflections on 15, 20 or 25 MHz at Anchorage.

The WWV and WWVH transmitters are about 4000 km from Anchorage (figure 6) and involve multi-hop propagation. The reflections were observed with an Icom R-8600 general coverage receiver. The receiver AGC was turned off, and the receiver was connected to a rotatable 8-element log periodic dipole array through a multicoupler. Another R-8600 was monitoring WWV at 25 MHz but there were no reflections at that frequency. A

block diagram shows the general configuration (figure 7). The Argo software is setup for QRSS10 mode with a waterfall length of 720 s (12 min). Argo is adjusted to show a frequency span from 980 to 1020 Hz, which encompasses the receiver settings mentioned above.

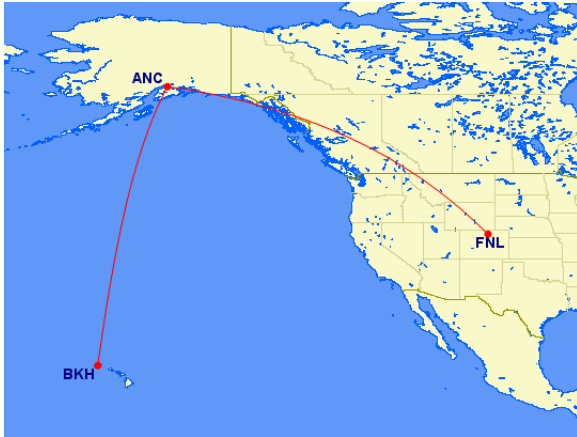


Figure 6 ~ Great circle paths shown in red between WWV near Fort Collins, Colorado (FNL) and Anchorage (ANC) and between WWVH near Kekaha on Kauai, Hawaii (BKH) and Anchorage. The WWVH path is 4414 km and almost entirely over water and encounters different propagation conditions than the WWV path, which is 3801 km and entirely over land. The paths are long enough to require multi-hop propagation. Anchorage is at the southern edge of the auroral oval, which introduces additional complicating factors in propagation toward Anchorage. It is believed that the aurora reflections involve WWVH because of its near-north-south alignment with Anchorage. Image from {GCMaP}.

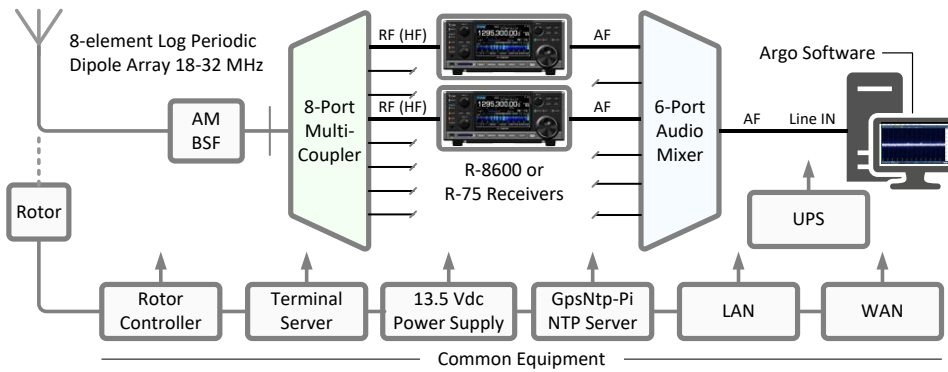


Figure 7 ~ Receiver and antenna system block diagram. PC timing is controlled by two GPS receiver-based network time servers. Common equipment includes infrastructure shared with other observatory equipment. The antenna usually was rotated to point at WWV on a true azimuth of 107°. Image ©2020 W. Reeve

Radio Aurora: Radio reflections from aurora involve solar wind coupling to the magnetosphere during magnetic reconnection (southward B_z in the IMF). The reconnection energizes magnetospheric electrons in the magnetotail, which move back toward Earth where they precipitate into the upper atmosphere along magnetic field lines marked by the *auroral oval*. The electrons collide with atomic and molecular gases in the atmosphere and increase the ionization and electron density, particularly at altitudes of around 100 km (ionosphere E-region). Some of the energy is converted to light and seen as sheets, rays and waves of visible aurora. Since the free electrons follow the magnetic field lines, they form tilted columns of relatively high-density clouds that are able to reflect radio waves. These reflected waves are received when the transmitter, reflective columns and receiver lie in a plane such that the incident and reflection angle are about the same. Rapid fading (also called *flutter* or *sputter*) is a characteristic of radio aurora due to changes in the electron density or drift or movement of the columnar field-aligned electron clouds.

Weblinks and references:

- {GCMaP} <http://www.gcmmap.com/mapui?P=FNL-anc-bkh>
- {Reeve15} <http://www.reeve.com/Documents/SAM/GeomagnetismTutorial.pdf>
- {SWPC} <https://www.swpc.noaa.gov/communities/space-weather-enthusiasts>
- {UAF-GI} <https://www.gi.alaska.edu/monitors/aurora-forecast>

Getting the Best out of PRESTO⁽¹⁾ - Part 2 The PRESTO Period/P-Dot Search Graphic

Peter East

Abstract

This article investigates applying the peak SNR (signal-to-noise ratio) statistic to the PRESTO *prepfold*, Period/P-dot (period search / period-rate search) graphic. Not only does this appear to improve discrimination for low SNR pulsar intercepts but with a simple twist, it can provide some extra recognition confidence.

Introduction

The PRESTO *prepfold* pulsar analysis plot includes a visual sub-plot with orthogonal Period/P-dot axes. Example sub-plots are shown in Figure 1. Confidence in period accuracy and period stability is assured if both period and period rate show peaks at zero error, producing an apparent peak indication in the center of the two-dimensional color graphics.

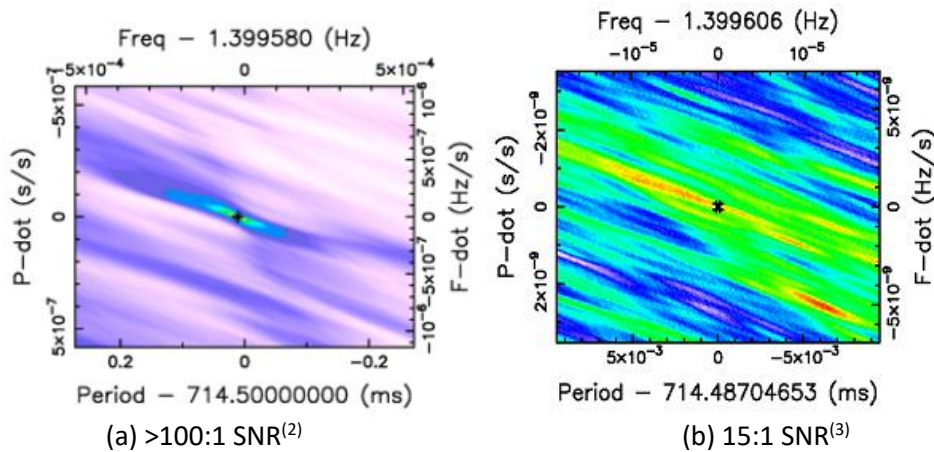


Figure 1. Example Period/P-dot plots using the Chi-square amplitude statistic.

Figure 1a indicates a strong central peak for a very large pulsar SNR whereas the center data peak (red) is stretched out and not quite so central in the lower SNR (= 15:1) example in Figure 1b. The statistic *prepfold* uses to recognize data peaks is Chi-square and for pulsar data SNRs less than 10:1, especially for low duty cycle pulsars such as B0329+54, the plot information is often inconclusive. Two other obvious properties visible in the two plots are the negative slope apparent in the data body and also the extent of central data peaks. In summary, for strong pulsars, this *prepfold* graphic appears present to just confirm the simultaneous peaking of both zero period error and near-zero period spin-down rate.

In the following sections, the basic theory and correlation of period search and period-rate search of pulsar data is examined and applied to real low SNR data using the SNR amplitude statistic. The aim is to show that much more pulsar specific information is available to improve confidence in recognizing pulsar signals in weak data.

Background Theory - Combined Period and P-dot Search Characteristics⁽⁴⁾

Figure 2 illustrates how the detected data is divided into blocks that are summed in the folding process. Due to the period-rate term, the block time lengths change, but in the folding process the blocks are folded into the same number of processing bins.

The upper terms in Figure 2 indicate how the block lengths change, where, P is the pulsar period, p is the search period change (usually in parts per million - ppm) and p^d is the period rate change in s/s, typically of the order 10^{-10} . The lower Figure 2 terms indicate how the pulsar pulse timing position (initially t_0) changes in sympathy with the search parameters and block number.

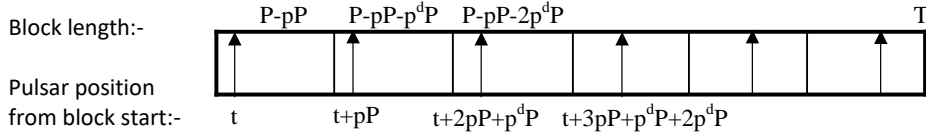


Figure 2. Combined Period and P-dot Search Parameters

It can be deduced from this description that the duration of the n^{th} block is $\{P - pP - (n-1)p^d P\}$ and the corresponding (maximum) pulse position shift is, $nP + \sum np^d P$, or,

$$ps_{max} = +\{(N-1)pP + (N-1)(N-2)p^d P/2\} \quad (1)$$

Equation 1 can be simplified by noting that the data record total duration, $T = NP$, then $ps_{max} = pT + p^d T^2/2P$; where, T is the record duration. It shows that for a small period change, the folded pulse is spread out linearly over a range equivalent to pT and amplitude reduced by the factor, pT/W (W is the pulse half-height duration). The summed peak is shifted by an equivalent amount in fold bins of $-pT/2$.

The explanation is a somewhat more complicated for period-rate change, as the summation is cumulative giving a triangular rather than even summation with the triangle peak closer to t_0 . As a result, the peak shift is closer to the normal fold position and the extent is not so prominent as shown later in Figure 3.

Assuming the pulsar is similar to a Gaussian shaped pulse of half-width W and the pulse train is continuous throughout the data record, the fold algorithm can be expressed as,

$$Fold(t) = \frac{1}{N} \sum_{n=1}^N A(n) \exp\left(-4 \ln(2) \left[\frac{(t - t_0 + (n-1)P(p + (n-2)p^d/2))}{W}\right]^2\right) \quad (2)$$

where,

t is the time variable (bin) in a period

t_0 is the pulse position in a matched period

N is the total number of periods in the record

n is the folded period number

P is the pulsar period

p is the period search factor

p^d is the period rate of change factor

W is the pulsar pulse width

$A(n)$ is the pulse amplitude in each period.

Application of Equation 2 on ideal data is illustrated in Figure 3 to indicate some of the search parameter effects on the pulse position and folded shape.

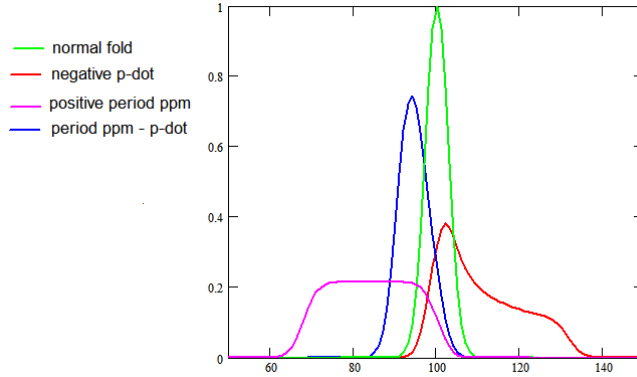


Figure 3. Effect of Period and P-dot Search Parameters on the Final Folded Pulse Shape (green - matched; red - negative p^d ; magenta - positive period shift; blue - both together)

Increasing the fold period away from the matched value alone, reduces the peak amplitude by spreading out the power (magenta curve). With a negative P-dot value alone (red curve), again the pulse broadens but due to the triangular distribution, the peak lies closer to the standard folding position (green curve). Finally combining both the positive and negative period and P-dot values (blue curve), there is some power compensation and much less loss of peak power is evident.

This compensation effect is predicted by Equation 2 and observed in the *prepfold* graphic of Figure 1 as the slope and extent of the central red/green strong amplitude response.

Ideally for a continuous intercept pulsar record, the near-central colored section should appear central and angled such that,

$$\left. \frac{p^d}{p} \right|_{slope} \approx -\frac{2}{N} \quad (3)$$

where, N = number of periods in the data sample
and, p is the period search factor in parts per million

This is derived from Equation 2 by noting that the data peak occurs when,

$$p + (n-1)p^d / 2 = 0 \quad (4)$$

It is possible using Equation 2 to indicate the extent of the pulsar response in the period/P-dot graphic by solving for p , p^d , and joint p , p^d to reduce the peaks by about half the average matched maximum. For just period search, it is predicted that the folded amplitude drops to about one half when the period offset is approximately given by $p = \pm 2W/T$, but for compensating period and P-dot search the slope power drops to one half at approximately $p = \pm 8W/T$ when $p^d = -2p/N$.

Test Data

The data used in this section was collected in August 2017 over a 2 hour period using a 3-channel RTL SDR receiver fed from a pair of 22 element Yagi antennas tuned to 611MHz. The RF IQ data was detected, the bands de-dispersed and combined. There was no data modification to remove RFI. The final folded result is shown in Figure 4a producing a SNR of 4.5:1 for a B0329+54 pulsar intercept.

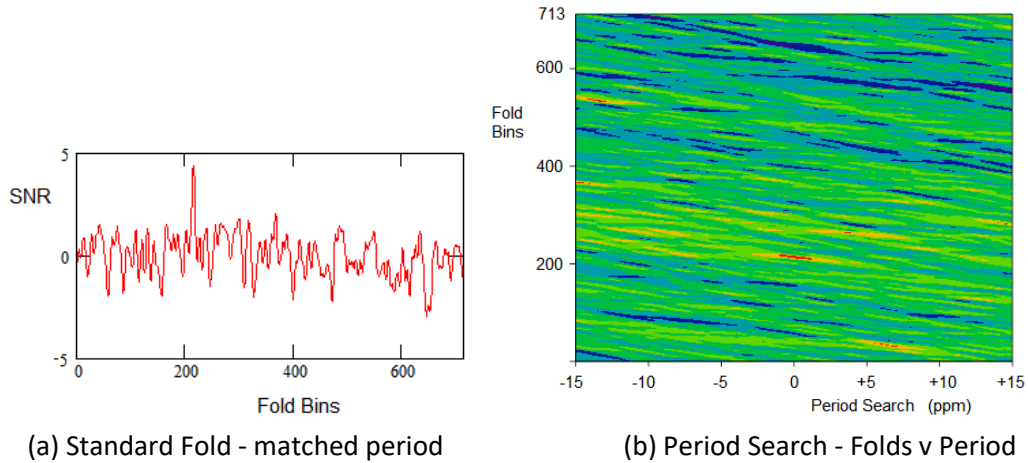


Figure 4. 4.5:1 SNR Fold Results

Figure 4b illustrates how pulsar and noise peaks (red, orange) vary over the folding period range ± 15 ppm. Note that the pulsar zero ppm response peaks around bin number 200 and is significant over a range of about, 0 ± 2 ppm. The slight inclination is as predicted by Equation 3. The other responses are typical of random noise peaks in the apparent SNR range 2:1 to 3:1 as the pulsar signal gets washed out with larger period excursions away from optimum. The general data slope across the period search range implies that there is significant noise data correlation with period value throughout the data record. This might be expected due to the intense filtering of the folding algorithm, with the consequence that the final noise pattern in Figure 4a could have a consistent component base across almost every period block.

Practical Results using the SNR Statistic

A C-program was written⁽⁵⁾ to duplicate the plot data for the *prefold* Period/P-dot graphic, recording the folded peak SNR for each p and p^d combination. This cycled through period values around the pulsar topocentric period of -15 ppm to $+15$ ppm and P-dot values -30×10^{-10} s/s to $+30 \times 10^{-10}$ s/s in ppm increments of 0.5 ppm and P-dot increments of 1×10^{-10} s/s. For each of the 3600 fold runs the folded data peak SNR (PSNR) was recorded and used to plot a simulant of the *prefold* plot considered. The result together with a 3-D version and amplitude code is shown in Figure 5.

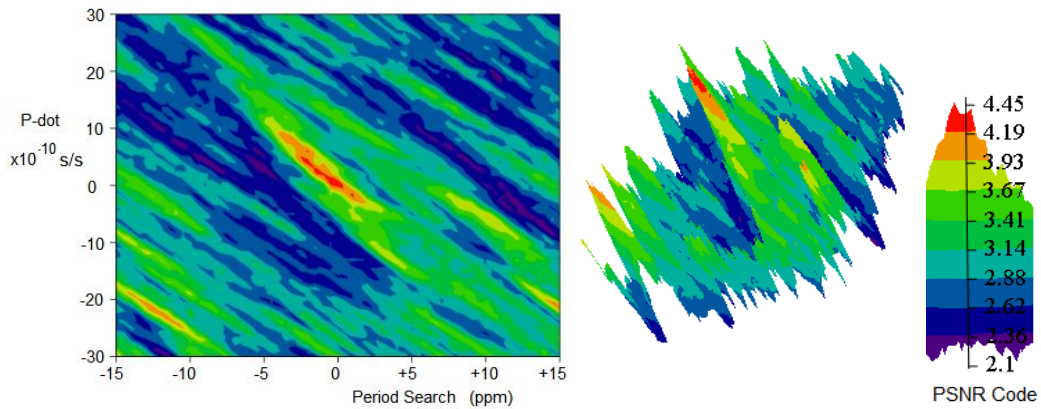


Figure 5 4.5:1 SNR 'prefold' graphic and 3-D Version based on the PSNR amplitude value.

A number of conclusions can be drawn from the Figure 5 presentation,

1. A clear central peak at coordinates 0,0 is evident confirming period match and nominally zero spin-down.
 2. A continuous pulse train matching the pulsar properties occurs throughout the data sample.
 3. The peak signal slope matches the prediction from Equation 3. $N = 10100$, $p = -15\text{ppm}$, and, $p^d/p = -2/N = 28 \times 10^{-10}/-15 \times 10^{-6} = -1.8 \times 10^{-4}$.
 4. Significant strong response occurs over a period variation exceeding 8ppm (compared to less than 4ppm for $p^d = 0$).
 5. There appears a slight offset from symmetry about coordinate (0,0). Possibly due to distortion caused by the underlying noise at this modest SNR level.
 6. Observing the 3-D version, it appears that there is a continued amplitude response along the diagonal including the peak response (examined later in Figure 9).
- This point is interesting as it implies that a vestigial response is possible for any period value over the whole period and P-dot range investigated. This is possible if for any period ppm search value there is a negative p^d value that satisfies Equation 4 as illustrated in Figure 6.
7. Another peak is evident at $p = -12$, $p^d = -22$ but can be discounted as a pulsar candidate due to its significant offset P-dot drift value.

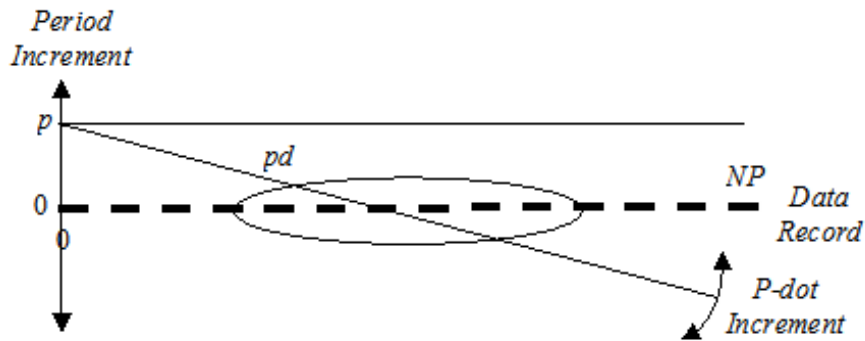


Figure 6. Fold Period and P-dot Timing offset Diagram

Figure 6 depicts folding with an offset period value and partially compensating negative P-dot value. Normally the optimum fold strategy is to have zero period and P-dot offsets and folding all data record N periods. In the case illustrated, the period value is offset by p ppm and compensated by a negative P-dot value of p^d crossing the zero line at $N/2$ periods. The ellipse identifies the data region offering the best periods to produce a positive folded result. The optimum p^d slope is such that $p/(N/2) = p^d$; confirming the result noted in Equation 3. It can also be inferred that partial compensation for increased period offsets is available for all values of opposite polarity p^d providing the P-dot increment slope crosses the zero line within the N data record periods.

Reverse Folding.

It can be inferred from Figure 6 that for a fixed period offset, over the possible values of P-dot offset crossing the data timeline, that the active range moves along the data record. This indicates a certain asymmetry implying a different result would occur if the data record was reversed. For a matched zero p^d fold, the fold response would appear identical to a normal forward fold but be reversed in time. But for a *prepfold* period/P-dot graphic, results could be different and can be compared (Figure 7) with the result given in Figure 5.

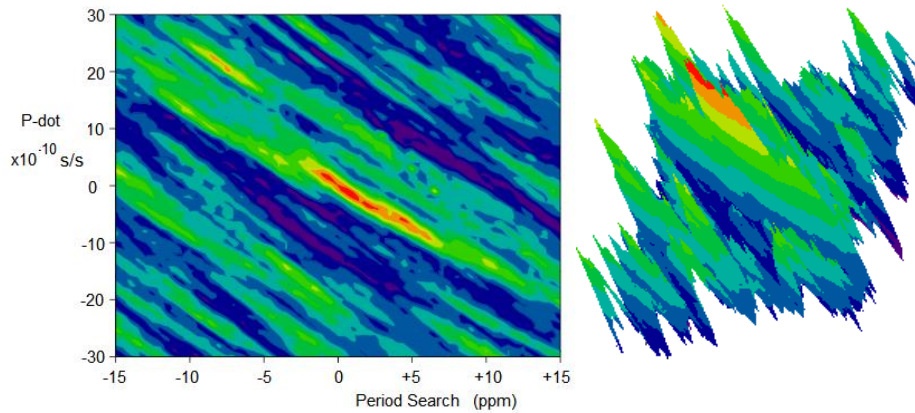


Figure 7 4:5:1 SNR '*prefold*' graphic and 3-D Version - Reverse Folded

Figure 8 shows the result of sum-combining the forward and reverse folded data, which appears to have tended to increase the discrimination, better-centralized the peak response and reduced the amplitude of random noise peaks, the main peak remaining consistently at SNR - 4.5:1. Note the suppression of these outlying noise peaks.

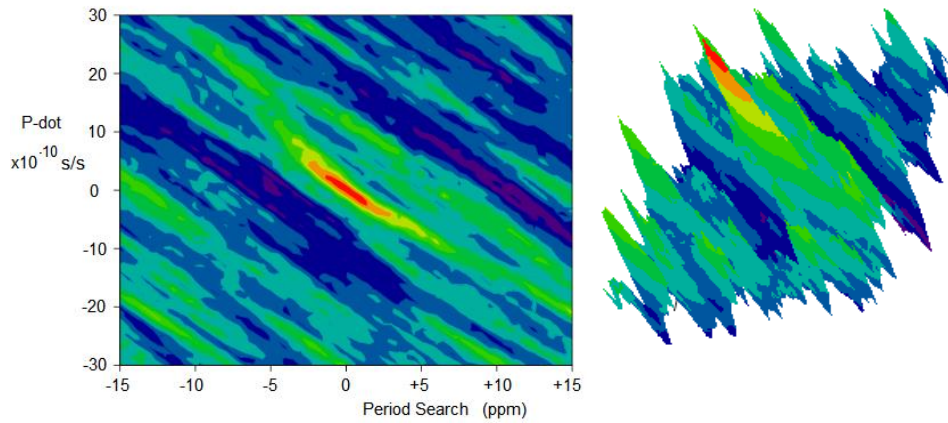


Figure 8 4:5:1 SNR '*prefold*' graphic and 3-D Version - Combined Forward and Reverse Folding

As a calibrating measure, a pulsar simulation embedded in Gaussian noise, matching the characteristics of the data used above with a folded SNR of 4.2:1 has been processed as described and the results submitted in the Appendix.

Figure 9 plots the PSNR response along the Figure 8 diagonal, encompassing the Period/P-dot peak showing no nulls but tending to a constant level. Also shown is the cut along the normal across coordinate (0,0) showing more variability. The random noise peaks are as expected around equivalent SNR of just below 3:1.

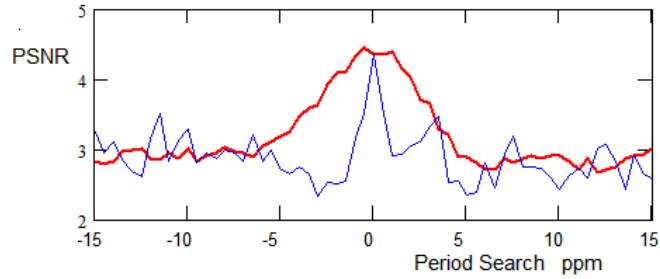


Figure 9 PSNR Across the Figure 8 Peak Signal Diagonal (red), along normal (blue)

Figure 10 below plots the result of performing a standard period search over ± 20 ppm in 0.1 ppm increments, recording the data peaks for zero P-dot and compares the result (red) with the theoretical result (blue) from applying Equation 2 with $p^d = 0$.

The theoretical half-height prediction is, $4W/T = 3.4$ ppm.

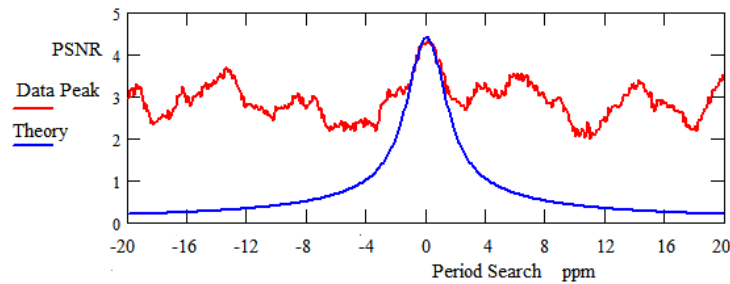


Figure 10 PSNR Period Search at zero P-dot, red - data; blue - theory

Scintillation

Differences between the forward and reverse fold Period/P-dot graphics can be assured by asymmetry of the underlying noise and scintillation effects which can also affect the perceived slope. Scintillation affects the pulse-by-pulse amplitude in a random manner, so for example there may be ranges of strong or weak pulse levels throughout a long data record. Long ranges of below average pulses towards the beginning or end of the record could be responsible for slope differences in the forward and reverse folds, but when combined may still satisfy Equation 3. This can be understood by referring to the fold algorithm Equation 2.

For example, if pulses were only present in the first half of the data record, periods 0 to $N/2$, Equation 4 slope becomes,

$$\left. \frac{p^{dot}}{p} \right|_{slope} \approx -\frac{4}{N}$$

Again, alternatively, if pulses were only present in the second half of the data record, periods, $N/2$ to N , the slope becomes,

$$\left. \frac{p^{dot}}{p} \right|_{slope} \approx -\frac{4}{3N}$$

These results can be deduced by reference to Figure 6. Note that the final slope depends upon both the position and duration of the data.

Data Quality Evaluation

Figures 10 and 11 explore the data to check on evidence of RFI. Figure 10 is an extended range (± 100 ppm in 1 ppm steps) version of the graphic derived in Figure 8. The 4.5:1 SNR pulsar response remains clear at coordinate (0,0) in Figure 10. Only candidates within the narrow band $p^d = 0 \pm 10 \times 10^{-10}$ s/s can be potential pulsars and so other responses outside this range must be noise or RFI. Outside the central region, noise should appear as random peaks but due to the folding algorithm properties may be extended, as for a true pulsar but may exhibit slightly different slopes and offset shapes. These can be extracted and observed in detail if required. RFI modulations if present would be observed as denser patterns in this presentation. The upper right quadrant appears one such.

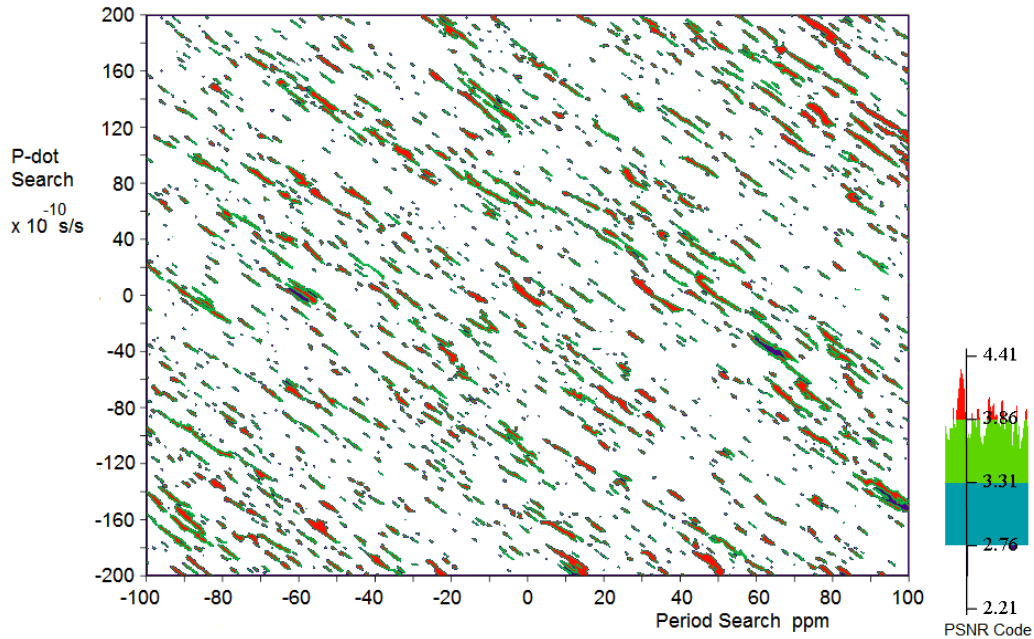


Figure 10 Extended P-dot/Period Search Graphic

Figure 11 extracts all the peaks from the Figure 10 plot folds and plots a histogram providing the peak noise distribution. This appears a typical noise-like (closely Gaussian-Normal) result with only slight asymmetry possibly due to the small RFI influence identified above. The pulsar presence is just observable in the last histogram block. The average peak appears equivalent to a PSNR approximately equal to 2.9:1.

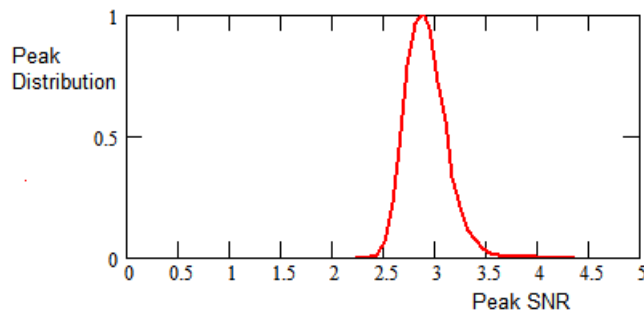


Figure 11 Period/P-dot Search Peak amplitude Distribution

Discussion

The graphic period/P-dot presentation is an important aid to identifying pulsar candidates as, given an accurate knowledge of the target topocentric period, the data peak must lie on the (0,0) coordinate. It provides much more information than just the single period standard fold as discussed. Standard matched folds can be compromised by electrical transients and RFI which can, not only reduce folding efficiency but long term wide band modulation can effectively be fold-filtered to produce false pulse trains. The graphic offers the opportunity to recognize them as such. In itself, it is not sufficient to guarantee a pulsar acquisition.

Conclusions

This article has shown that replacing the Chi-square statistic with peak SNR in the PRESTO *prepfold* Period/Period rate graphic that much more useful information can be inferred at much lower data SNRs than normally expected. A B0329+54 pulsar validated data example with a best-folded SNR of 4.5:1 has been tested. The results, exploring a wide range of Period and Period-rate parameters show excellent suppression of random noise peaks and highlights the presence of a continuous pulse train with properties closely matching that expected of the B0329 pulsar. False candidates can be rejected if lying away from the zero P-dot coordinate. Similar results were observed with a similar level, simulated pulsar embedded in Gaussian-Normal noise as reported in the Appendix. The results are also supported by a theoretical analysis and it is shown that improved discrimination is possible by exploiting the asymmetry in reverse folding the data. Extended range plots are useful for evaluating data quality and checking the presence of disturbing RFI modulations. With base random noise peaks evident in the plots around a mean equivalent SNR of 3:1; depending on the data quality, the lower SNR limit of this technique is expected to be somewhat above this. Whilst not a candidate recognition tool on its own it does add confidence when coupled with other recommended tests such as dispersion search and profile matching.

References

1. PW. East, Getting the Best out of the PRESTO Pulsar Search & Analysis Tools., Journal of the Society of Amateur Radio Astronomers. January-February 2021.
2. RA. Russel, R.Uberecken, RA. Haggart., First Deep Space Exploration Society (DSES) Pulsar Captured on the 60-ft Dish, 2020 SARA Eastern Proceedings.
3. A Dell'Immagine, Private Communication.
4. PW East. An Analytical Method of Recognizing Pulsars at Moderate SNR., Journal of the Society of Amateur Radio Astronomers. November-December 2018.
5. PW East, C-Program, searchpdplotfold.exe, contact author.

Appendix - Simulated Pulsar with SNR = 4.2:1

The plots below are the program results for comparison with the B0329+54 pulsar recorded data used in the main text. The data was generated by simulating a Gaussian shaped pulse of 6.5ms half height and period 701.1ms, sitting on Gaussian-Normal distributed noise base. The data duration was equivalent to a 2 hour recording. The folded SNR was measured at 4.23:1.

These simulation results compare favorably and support the real data results presented in the main article (Figures 4a, 8 and 9). A two-stage method of obtaining a good accuracy SNR was used. It involves first calculating the folded data mean and rms, setting thresholds at $\pm 3 \times \text{rms}$ level, inserting Gaussian random noise at the measured rms level within the range of the thresholded regions, and finally recalculating mean and rms values for SNR or PSNR calculation.

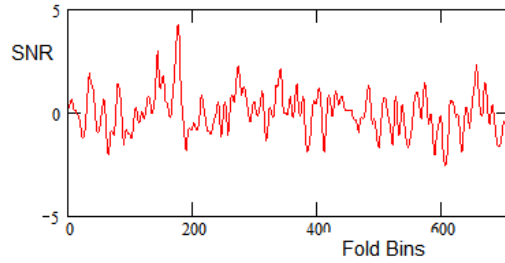


Figure A1. 4.2:1 SNR Simulation in Gaussian Noise Standard Fold Results

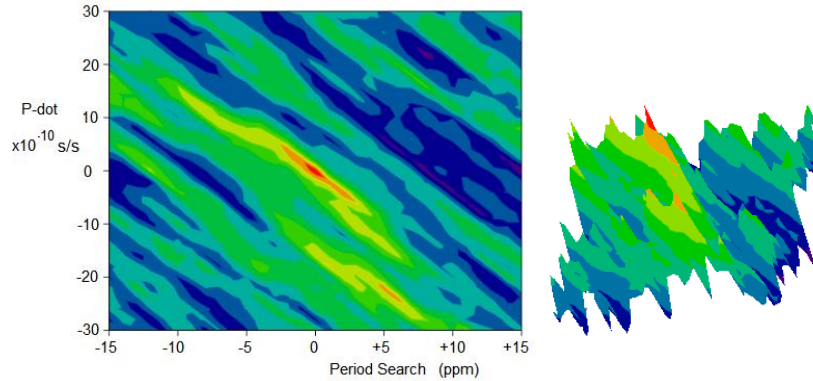


Figure A2 4:2:1 SNR Simulation 'prepfold' graphic and 3-D Version

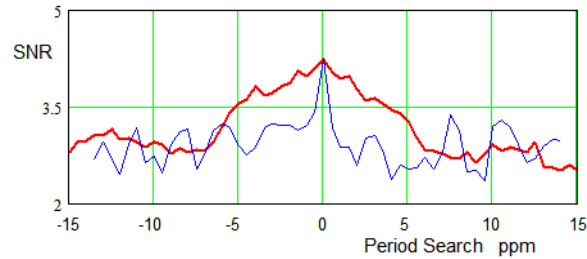


Figure A3 PSNR Across the Figure A2 Peak Signal Diagonal (red), along the normal (blue)



Peter East, pe@y1pwe.co.uk is retired from a career in radar and electronic warfare system design. He has authored a book on Microwave System Design Tools, is a member of the British Astronomical Association since the early '70s and joined SARA in 2013. He has had a lifelong interest in radio astronomy; presently active in amateur detection of pulsars using SDRs, and researching low SNR pulsar recognition. He encourages free information exchange in the amateur community and is keen to widen interest in radio astronomy generally. He maintains an active RA website at <http://www.y1pwe.co.uk>

Mapping Extent of Neutral Hydrogen Clouds near Sagittarius A* at 1420 MHz

E. Sundheim¹, T. Bullett^{2,*}, and T. Cline³

¹Berthoud High School, Berthoud, CO

²University of Colorado, Boulder, CO

^{1,2,3}Little Thompson Observatory, Berthoud, CO, USA

*Corresponding author: Terry Bullett : Terence.Bullett@colorado.edu

1. Abstract

Neutral hydrogen is abundant in the Milky Way Galaxy, making hydrogen radio emissions at 1420 MHz (21 cm) a key tool for mapping the distribution of matter within the Galaxy. Neutral hydrogen can be either emissive or absorptive, depending on its relative temperature and density. The brightness of the Galactic disk at 21cm was used as a background source to detect intervening regions of hydrogen absorption in the Galaxy. It was hypothesized that a uniform region of cool neutral hydrogen exists in the neighborhood of Sagittarius A*. Using a 16-foot diameter parabolic antenna, drift scans of the sky centered around Sagittarius A* were completed, and Doppler spectra revealed an absorption line in the measurements. Using a Python program, an estimate of the background Galactic signal strength and the absorption intensity were generated. The difference between these two values was reduced to a one-dimensional characteristic of absorption depth, which was plotted to generate an image showing the cloud of neutral hydrogen is slightly offset from the Galactic center.

2. Introduction

The interstellar medium (ISM), consisting of dust, neutral hydrogen (HI), and ionized hydrogen (HII), occupies the space between stars. In a disk galaxy such as our own, a large percentage of the interstellar medium is HI [1]. Categories of the ISM relevant to this experiment are the Cold Neutral Medium (CNM), which is cooler (below 300 K) and denser ($n = 20 - 60 \text{ cm}^{-3}$) than the Warm Neutral Medium (WNM), which has typical temperatures of approximately 10^4 K [1]. A cloud is any region where density exceeds $n = 10 \text{ cm}^{-3}$ [2]. At visible wavelengths, the center of the Galaxy is obscured by interstellar dust, but radio waves can provide a much clearer image due to quantum emissions from HI. Radio waves penetrate the dust.

When the proton and electron in a hydrogen atom have the same quantum spins, the atom is in a higher energy state than when the spins are opposed. This transition is highly forbidden as its transition rate is $2.9 \times 10^{-15} \text{ s}^{-1}$, meaning a single atom will flip its electron's spin approximately once every 10 million years. The released photon of radio energy has a rest frequency of 1,420,405,751.768 Hz [3]. Motion of the emitting atom relative to the receiver, such as random thermal motions, are observed as a change in the rest frequency. While this phenomenon would be virtually undetectable at the level of a single atom, when enormous clouds of hydrogen are together the combined radiation is easily detected with a modest radio telescope. Previous studies have established that the Milky Way Galaxy is awash in this kind of radiation and have created detailed maps [4].

Hydrogen is both absorptive and emissive at the 21 cm wavelength. HI emission occurs when higher energy state atoms emit radio photons, and absorption happens when an atom is in its lower state and absorbs energy from a background 21 cm radiation source [5]. Warm, sparse hydrogen tends towards emission, and cooler, denser hydrogen favors absorption. This can be roughly determined using the width of spectral features due to random thermal motion [6]. Therefore, the decrease in signal strength observed in this experiment was assumed to have been caused by absorption from a cooler, denser cloud between the source and the observer. Although the cloud also radiates energy, it disperses the absorbed energy in all directions, resulting in a net decrease along the line of sight [7].

Previous experiments at the Little Thompson Observatory have studied HI emissions around Sagittarius A*, the black hole at the center of the Milky Way and noticed a decrease in the strength of signal when observing some regions. These reductions were narrow in spectral bandwidth compared to the Galactic emissions and irregularly shaped on the sides in a manner inconsistent with a sum of multiple sources and are postulated to be due to absorption. This experiment was designed to further examine this observation near the center of the Milky Way in order to create a map of the cold neutral hydrogen in that area.

3 Methods

3.1 Data Collection



Figure 1: The 16-foot dish at Little Thompson Observatory

Using the 16-foot (4.88 m) diameter parabolic antenna shown in Figure 1 at Little Thompson Observatory (LTO), 29 drift scans were completed over the months of August to October 2020 at 1420 MHz, covering an area of the sky approximately 35° centered at Sagittarius A* (RA: 17:45:40, DEC: $29^\circ 00' 28''$). Each day, the antenna elevation was changed while keeping the azimuth at 180° . The drift scan was obtained by keeping the antenna position constant and letting Earth's rotation scan the antenna beam across the sky [8]. To cover the entire region, elevations were increased and decreased starting with wide steps of six degrees elevation until edge scans showed no absorption line signature. This was verified by using a secondary data collection system using the open-source MIT Haystack logging program [9]. Because the Haystack system had lower spectral resolution and required less processing than the primary system, rough results were available in near real time to determine when no absorption feature was present during the transit of the Galactic plane, which was the maximum signal intensity of each drift scan. Knowing where no absorption was visible allowed those elevations to serve as the outer boundaries of the scanned region. The space between these edge elevations was gradually filled in, first with 3° steps of elevation change, and then with 1.5° steps as seen in Figure 2. The antenna beamwidth is approximately 3° .

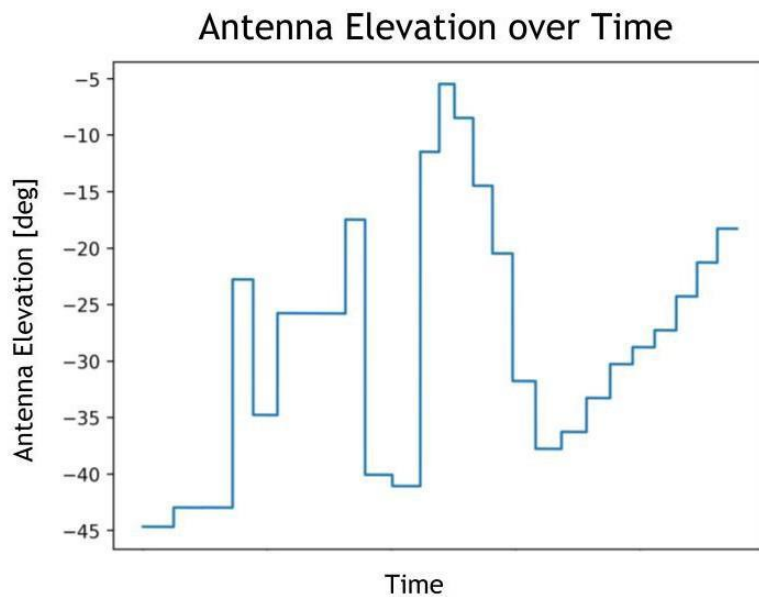


Figure 2: Antenna Elevation over Time, showing the decreasing size of steps

Averaged spectra, as shown in Figure 3 were taken approximately once per minute for a 6-hour scan daily, with the transit of Sagittarius A* or the inner Galactic plane roughly in the center of observation interval. Calibrations had been made so that the incoming radio waves could be measured as equivalent noise temperature of the observed volume (T_{sky}) plus the noise temperature of the receiver (nominally 100 K), the sum of which we call Antenna Temperature T_{ant} . A custom FORTRAN 95 program created by the authors reduced the raw 10 MHz In-phase and Quadrature time domain samples into power spectra, eliminated interference, flattened the frequency domain data, produced 1- minute averages and provided some initial data analysis. The most important of this was identifying HI data by examining the standard deviation of the entire spectra, then flagging any data above a threshold and recalculating standard deviation to isolate spectral lines with a high confidence of being dominated by HI emissions and calculating baseline value for continuum radiation temperature levels.

3.2 Data Analysis

Figure 3 depicts a typical one minute observation for this experiment. The signal is noticeably weaker around 925 kHz spectral frequency, forming a valley in the plot. This plot's center frequency is not 1420 MHz as the actual receiver was set slightly off-frequency to avoid noise sources, but rather 1,419,398 kHz. By connecting the two peaks with a line as seen in Figure 4, a reasonable estimate of the strength of un-absorbed signal between the frequencies of the two peaks can be obtained. The absorption depth value is the difference between the predicted value at the valley frequency minus the actual measured value. This one-dimensional characteristic of the absorption depth can then be plotted as color intensity on either a Galactic coordinate (l vs b) plot or a RaDec (RA vs DEC) plot.

Each drift scan generated approximately 3600 spectra. To measure the absorption depth value for each spectrum, a Python program was written to:

1. Identify plots containing an absorption valley
2. Verify the existence of absorption by cross-comparing with the Doppler-adjusted frequency
3. Calculate the aforementioned characteristic

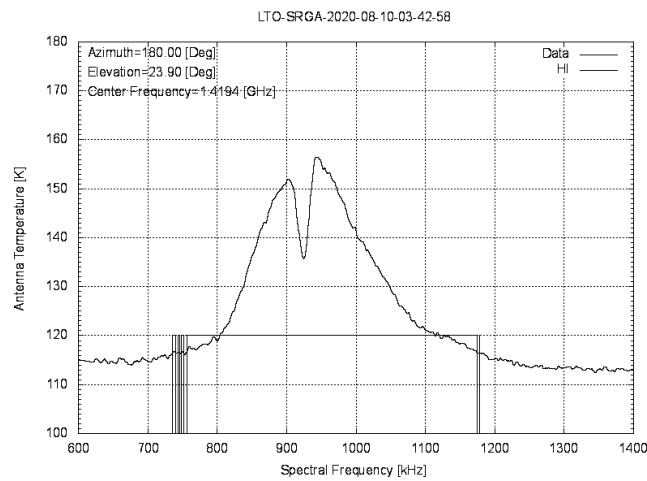


Figure 3: A representative spectra of Antenna temperature vs spectral frequency with a clear absorption valley at 925 kHz. The green line indicates spectral lines detected as containing HI power.

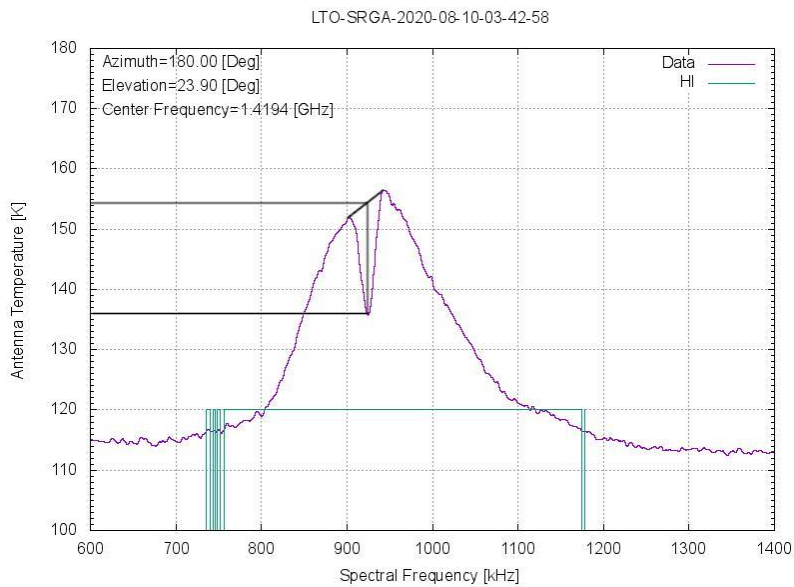


Figure 4: The same spectra, labeled to show how absorption depth was calculated

The first task of the program, to identify plots where absorption was occurring, proved challenging. While a human eye can clearly determine existence of a valley surrounded by two peaks, a program requires numerical criteria for this task. Originally, this was done by calculating the slope for each spectral point, and checking to see where slope was zero, indicating a peak or valley. However, due to noise in the data even after a binomial expansion smoothing algorithm had been applied, this method was insufficiently accurate, forcing the use of another technique.

The method eventually used relied on a brute force approach and therefore was less computationally efficient but more accurate than the original one, as determined by manual identifications of maxima/minima. Using a shifting frame of 20 data values, the center value was compared to the maximum and minimum within that range. If the given point equaled either of these values, its index was stored in the corresponding list. Finally, sets of 2 peaks were tested using different combinations of valleys that retained ascending numerical order of the indices.

For each combination, an absorption depth value was generated. If there was more than one depth, the largest value was kept. This was necessary to avoid counting non-absorption valleys that resulted either from non-smooth data or other, non-absorption sources. Each absorption valley was recorded in a text file (.ltoe file) along with the RaDec and Galactic coordinates, maximum T_{ant} for the spectra, and the valley frequency.

To verify the existence of a true valley, the frequency domain was restricted to a 100 kHz bandwidth between 900 and 1000 kHz spectral frequency. This bandwidth was determined by performing a probability distribution analysis on an earlier data reduction to identify where most absorption valleys occurred, as shown in Figure 5. This was used to impose a continuity constraint in the spectral frequency domain. Reducing the number of detected valleys generated a clearer image of the main cloud.

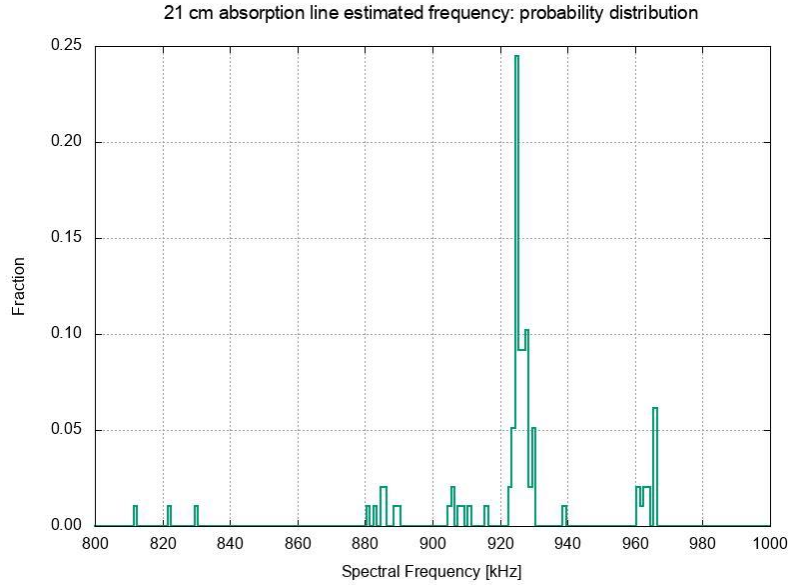


Figure 5: Probability distribution of the spectral frequency of absorption valleys prior to applying a frequency domain constraint

To create the displays, another Python program previously created by the authors was modified. Using matplotlib, the data from each .ltoe file was plotted in a variety of ways to show the absorption depth compared to the maximum T_{ant} . Plots were interpolated using the Python matplotlib contourf function to provide a smoother image. The comparison of absorption depth and maximum T_{ant} (in white) was provided to show that the areas of lower absorption depths may be caused by either a lack of intervening interstellar hydrogen or a lower intensity of the background source.

4. Results

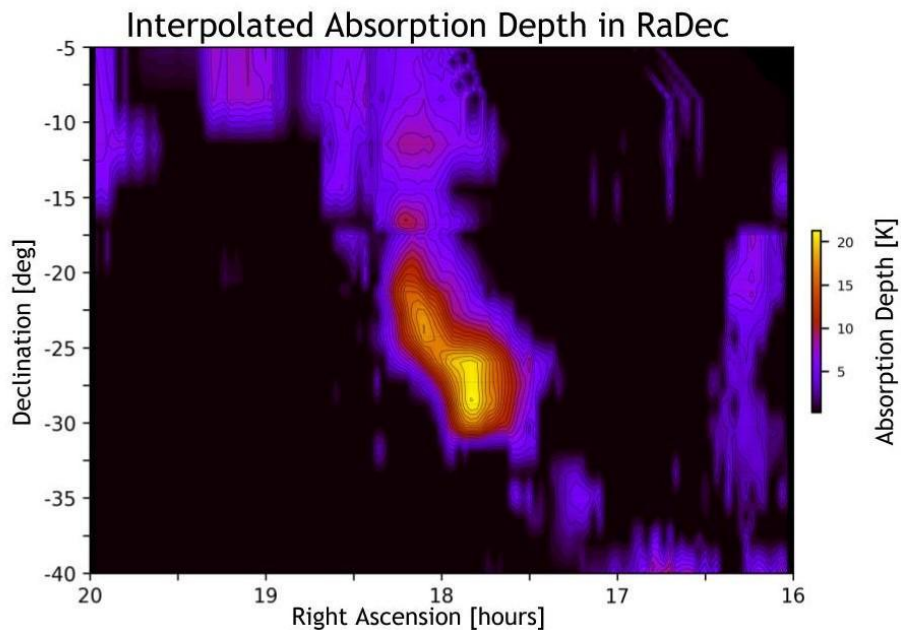


Figure 6: Interpolated Absorption Depth displayed in RaDec

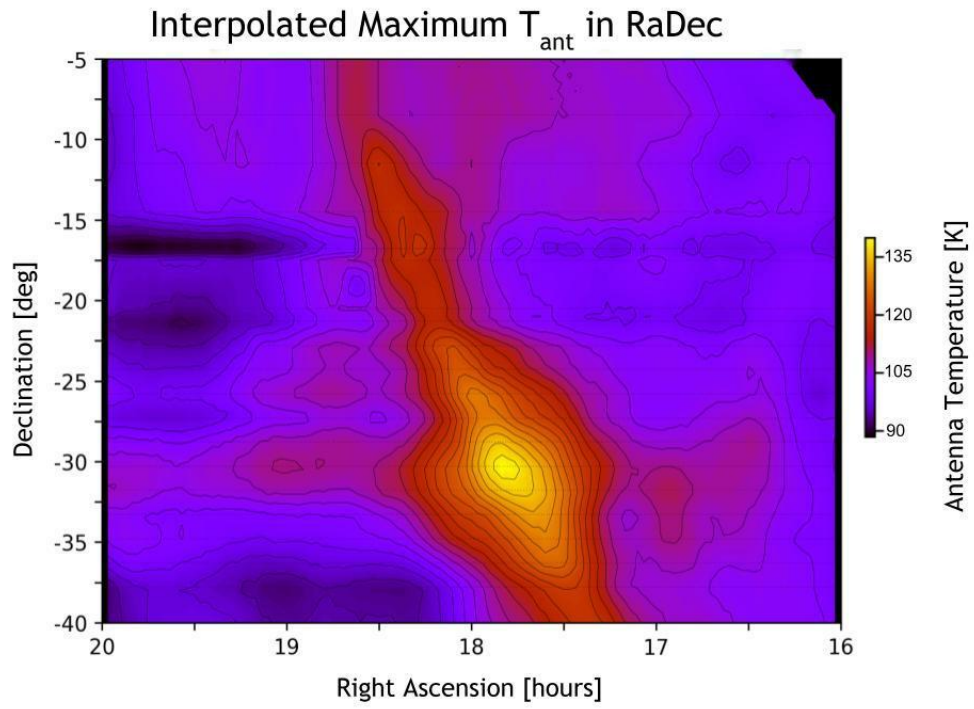


Figure 7: Interpolated Maximum T_{ant} displayed in RaDec

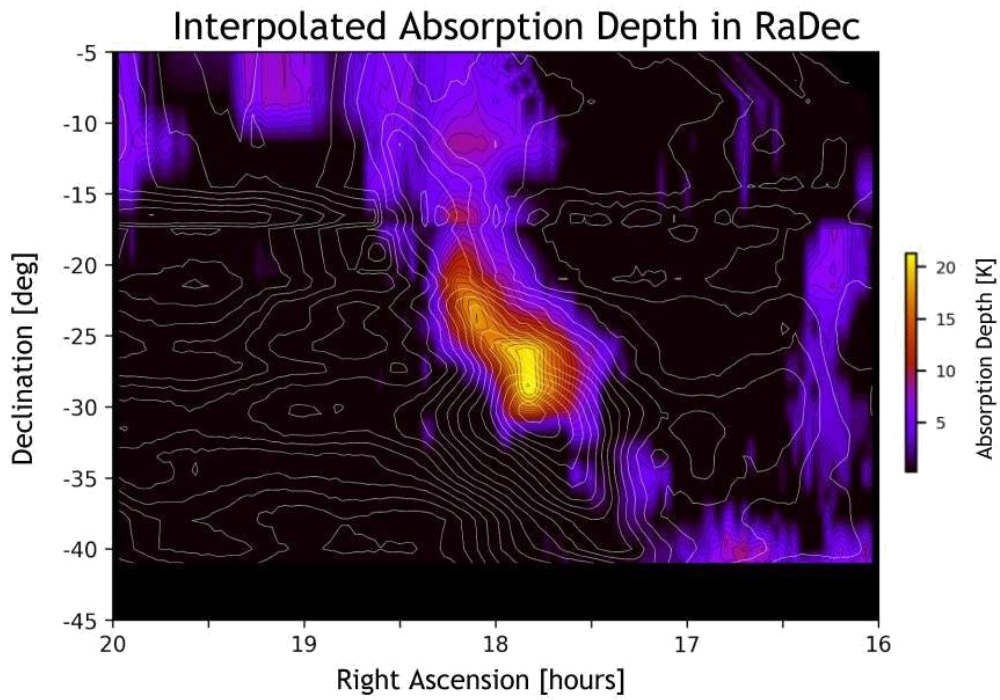


Figure 8: Interpolated Absorption Depth with white contours of Maximum T_{ant} for comparison in RaDec

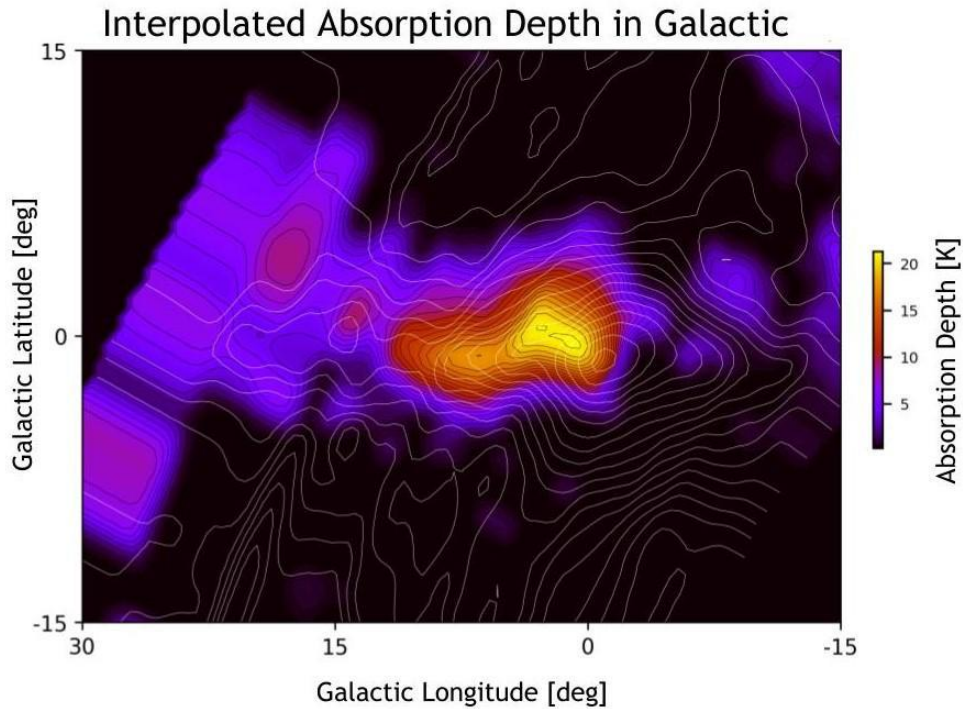


Figure 9: Interpolated Absorption Depth with white contours of Maximum T_{ant} for comparison in Galactic coordinates

6 Discussion

Figures 6 - 9 demonstrate this absorption is not located precisely towards the center of the Galaxy, but rather is offset slightly in the positive Galactic longitude direction. Two coordinate systems were used to provide a clearer picture of the relative position of the differences between the two plots. The narrow spectral width of the valley suggests this feature is caused by something with low temperature, which we suggest is cold hydrogen cloud absorption. This spatial offset confirms that the dip in signal strength was not a side effect of the background source because if it was, it would vary with the source. The maximum absorption depth and maximum T_{ant} do not occur at the same point in the sky. This means that the location of the densest part of the cloud is unrelated to the variation in the background source and therefore occupies its own location near the center of the Milky Way.

Another finding of note is that this cloud is not uniform, but rather denser towards the Galactic center; this is surmised because more absorption implies a greater amount of neutral hydrogen between the observer and the source. As seen in Figure 9, the denser areas (colored yellow and orange) are on the side of the cloud closest to 0 degrees Galactic longitude. Other smaller patches located a greater distance away from the center are also likely smaller clouds of neutral hydrogen; however, due to this study's focus on the Galactic center their true shape may be distorted by the interpolation due to a lack of data in those areas.

7 Conclusions

A neutral hydrogen cloud near Sagittarius A* was mapped and found to have an irregular shape. The working hypothesis of a uniform sphere of gas was rejected in favor of the discovered oblong shape. The main finding of note is that the cloud is offset from the Galactic center. This project was successful in its purpose to investigate the weakening signal strength observed in previous explorations at Little Thompson Observatory and map the cloud of neutral hydrogen.

Additional research on this topic is suggested. Future investigations could determine the respective temperatures of the background source and absorption cloud by examining the spectral widths. To confirm the location of this cloud and determine the distance to the cloud, and potentially pinpoint a specific Galactic arm, parallax could be used with a 6-month spacing of observations. Parallax is the apparent shift in position of a celestial object compared to the relatively stationary background. By determining the parallax angle using the spaced observations, only trigonometry is needed to solve for the distance to the celestial object. However, the telescope used for this project does not have sufficient spatial resolution to determine this. Alternatively, a synthetic aperture technique using Doppler shifts created by the Earth's orbital motion could be used. Similar to parallax, different Doppler shifts would give radial velocities based on the change of Earth's line of sight orbital velocity in the direction of the cloud. In theory the cloud parallax could be measured based on changing Doppler shifts over time. To achieve a higher map resolution, more observation days would be required with a tighter beamwidth, which could be achieved by using a larger dish at another observatory.

8 Acknowledgments

In addition to my co-authors, I would like to thank Kevin McManus, Ivy Knudsen, Meinte Veldhuis, Jay Wilson, Dave Eckhart and the other volunteers at Little Thompson Observatory for their support and advice.

References

- [1] Mark G Wolfire, Christopher F McKee, David Hollenbach, and AGGM Tielens. Neutral atomic phases of the interstellar medium in the galaxy. *The Astrophysical Journal*, 587(1):278, 2003.
- [2] Laura A Whitlock and Kiley Pulliam. *Listen Up! Laboratory Exercises for Introductory Radio Astronomy with a Small Radio Telescope*. iUniverse, 2008.
- [3] Helmut Hellwig, Robert FC Vessot, Martin W Levine, Paul W Zitzewitz, David W Allan, and David J Glaze. Measurement of the unperturbed hydrogen hyperfine transition frequency. *IEEE Transactions on Instrumentation and Measurement*, 19(4):200-209, 1970.
- [4] RX McGee and JD Murray. A sky survey of neutral hydrogen at λ 21 cm. i. the general distribution and motions of the local gas. *Australian Journal of Physics*, 14(2):260-278, 1961.
- [5] John Edward Dyson and David Arnold Williams. *The physics of the interstellar medium*. CRC Press, 2020.
- [6] V Radhakrishnan, WM Goss, JD Murray, and JW Brooks. The parkes survey of 21-centimeter absorption in discrete-source spectra. ii. galactic 21-centimeter observations in the direction of 35 extragalactic sources. *The Astrophysical Journal Supplement Series*, 24:15, 1972.
- [7] Michael Paul Hughes, Anthony Richard Thompson, and Roger Sidney Colvin. An absorption-line study of the galactic neutral hydrogen at 21 centimeters wavelength. *The Astrophysical Journal Supplement Series*, 23:323, 1971.
- [8] Richard Barvainis. Multiple drift scans: a method for radio continuum observations in a radome. *Publications of the Astronomical Society of the Pacific*, 109(740):1167, 1997.
- [9] Dustin Johnson and AE Rogers. Developing a new generation small radio telescope. In *American Astronomical Society Meeting Abstracts# 221*, volume 221, pages 255-10, 2013.

RF Choke for VLF and LF Applications

Whitham D. Reeve

1. Introduction

Very few places on Earth are not plagued by radio frequency interference (RFI) in the very low frequency (VLF, 3 to 30 kHz) and low frequency (LF, 30 to 300 kHz) bands. The RFI may be produced by switchmode power supplies, poor quality LED lights and light dimmers, motors, powerline network adapters, so-called smart home controls, a multitude of electronic devices and their chargers, and nearby powerlines. The RFI may be coupled to a coaxial cable transmission line as *common-mode* (longitudinal) currents and then appear at the input to a receiver where it can easily override weak signals.

An *RF choke* may reduce the interfering RF currents flowing on the cable. The chokes described in this article are lossy inductors made by winding small diameter coaxial cables through ferrite cores. The chokes are inserted in series with the coaxial feedline between the antenna and receiver, usually one at each end (figure 1). The inductors present a high impedance to the longitudinal currents. These currents are absorbed by the choke and dissipated as heat. The chokes have no effect on the desired signals (*differential mode* currents) between the center conductor and shield.

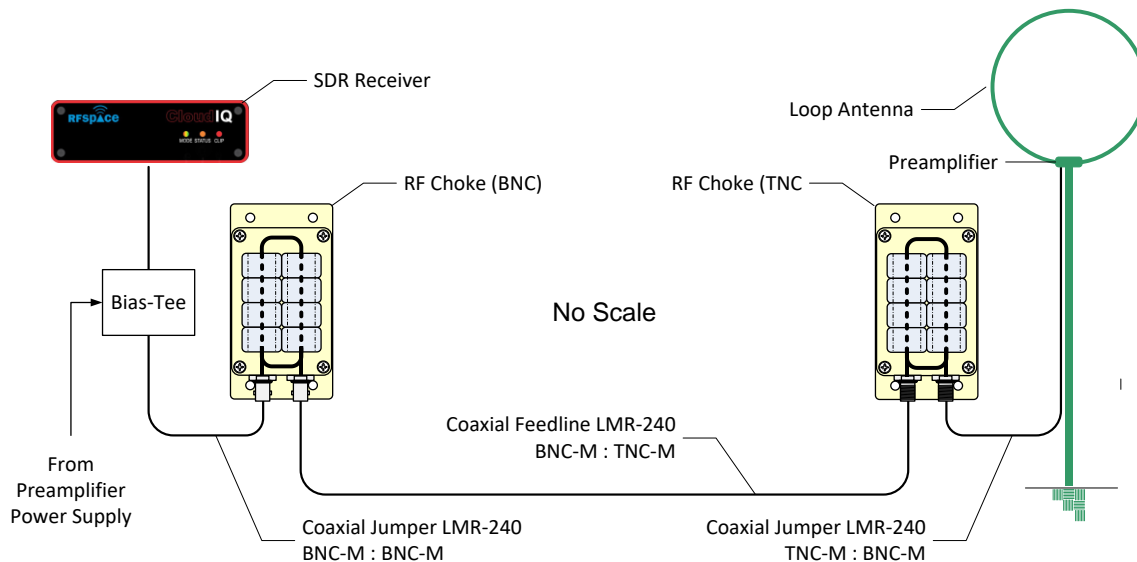


Figure 1 ~ Working diagram of choke application to reduce interference coupled to the transmission line. Sometimes only one choke is needed and its location is determined experimentally. ©2020 W. Reeve

If the antenna has a preamplifier that is powered through a bias-tee on the coaxial feedline, the dc flows in opposite directions on the center and shield conductors. Direct current flowing through ferrite core windings could generate a magnetic field that saturates the core and reduces the choke inductance; however, in this case, the magnetic fields are generated in opposite directions and cancel each other, thus having no effect on the choke inductance. For this to work as intended, it is important that the powering currents are confined to the coaxial cable and there are no stray paths.

The remainder of this article describes chokes that I built specifically for use with an HP 10509A loop antenna that originally was designed for reception of the time-frequency station WWVB at 60 kHz. The chokes are not limited to this specific application and may be usable with any antenna and receiver that uses a coaxial feedline and operates in the VLF and LF bands. The chokes also may be suitable for higher frequencies such as the MF and HF bands (300 kHz to 3 MHz and 3 MHz to 30 MHz, respectively) (see section 4 for measurements). At some locations only one choke may be needed to adequately suppress interference. The chokes described here are intended only for receiver circuits.

2. Choke Types

Electrically, the choke is a lossy (low Q) inductor. At lower frequencies, its reactive impedance is proportional to the inductance and frequency, but the choke may be self-resonant and show capacitive reactance at frequencies above resonance (see [Reeve13](#)). To be effective at low frequencies, the inductance must be high to achieve a high impedance.

I initially considered three basic choke constructions (table 1). From a practical standpoint, only one type provides high impedance at low frequencies and that is the type made with multiple toroid cores and multiple coaxial cable turns on those cores. This construction is described in the next section.

Table 1 ~ Comparison of basic choke constructions

Description	Construction	Impedance dependencies	Low frequency applications
Air core coil	Multiple windings of coaxial cable formed into an air core coil	Cable and core diameters and number of turns; has resonant effects	Requires extreme number of turns; not practical
1-turn series string of toroid cores	Coaxial cable inserted through multiple toroid cores	Number of cores and core material	Requires extreme number of toroid cores; not practical
Toroid core coil	Multiple windings of cable through one or more toroid cores; requires small coax and large cores	Number of cores, core material and number of turns	Requires moderate number of turns and toroid cores

3. Choke Construction

My construction plan was simple: Pack as many toroid cores and as many windings as possible into the small weatherproof plastic enclosures I had on-hand. I did not target a specific choke impedance but hoped to achieve at least 1 kohm in the operating frequency range 10 to 100 kHz. My expectation was that the chokes would have no effect on normal signal transmission. There is nothing unique or original about the construction techniques described in the following paragraphs. I built two chokes, one with TNC connectors for outdoor use and the other with BNC connectors for indoor use.

I found that 8 pcs of Fair-Rite mix 75, p/n 2675821502, EMI suppression toroid cores would fit in the enclosures. I purchased the cores from Mouser Electronics for a little more than 1 USD apiece. The dimensions of each toroid are 31 OD x 19 ID x 15 T mm (1.22 x 0.748 x 0.591 in). These manganese-zinc (MnZn) toroids have high relative permeability μ , which is given as 5000 in the manufacturer's datasheet. Permeability indicates the ability of a

material to become magnetized when placed in a magnetic field; a high permeability is necessary for attaining high inductance at low frequencies.

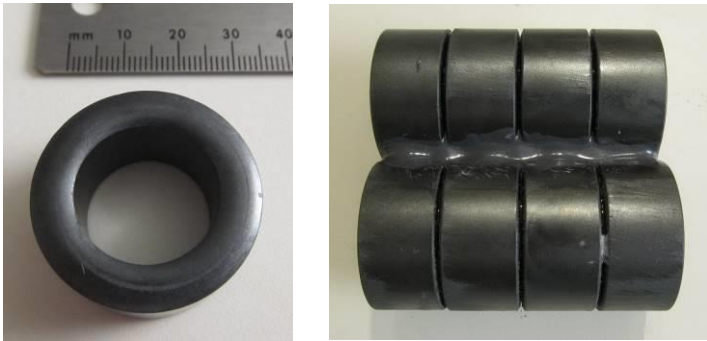


Figure 2 ~ Left: Fair-Rite toroid core, p/n 2675821502; Right: Binocular core formed from eight toroids in two rows. The cores in each row are first glued with superglue and after curing the two assemblies are then glued together with epoxy. ©2020 W. Reeve



Figure 3 ~ Alignment and clamping of each half of the binocular core. Two 1/2 x 2-3/4 in aluminum angles were clamped laterally in a vice and then the two blocks of four toroid cores each were placed on the angles for alignment. One of the angles is visible at the left-middle. Each block was held together with a non-metallic hobby clamp that uses a rubber band as seen with four toroids at the right-middle. The clamp was left in-place while the glue cured for 24 h. ©2020 W. Reeve

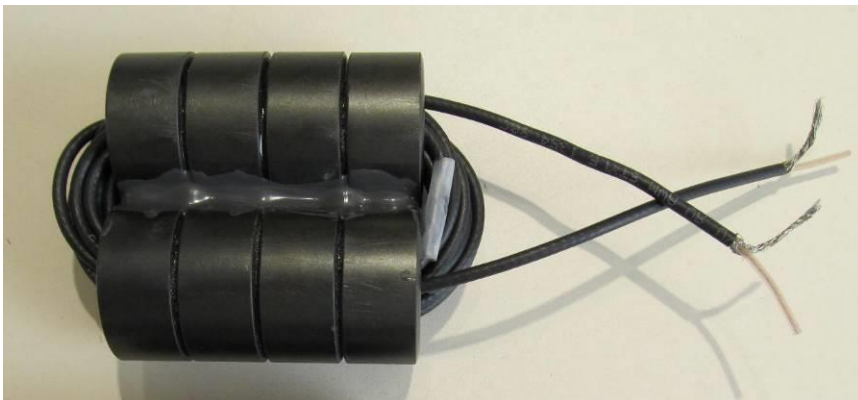


Figure 4 ~ Completed binocular core with windings ready for installation in the plastic enclosure. A piece of tape is seen at the center of the image. It was used to mark the center of the length of cable so that the core could be wound evenly from both ends. ©2020 W. Reeve

I glued the individual toroids into the form of a binocular core (figure 2). I used a small bead of Loctite SuperGlue Gel on the individual toroids to hold them in two blocks of four toroids per block. The toroids were first aligned on a piece of aluminum angle held in a bench vice (figure 3). A non-metallic hobby clamp held the toroids together while the glue cured. After 24 h two block assemblies were clamped together with non-metallic hobby clamps through their apertures while a mixture of 2-part epoxy was applied at the junction between the two assemblies. The epoxy was allowed to cure overnight. I built two complete binocular cores using this procedure. After the epoxy had cured, the binocular core assemblies were cleaned with a cloth wetted with paint thinner. The finished binocular cores measure 60 L x 62 W x 31 H mm (2.364 x 2.440 x 1.22 in).

I wound the chokes with RG-174/U coaxial cable, which has 2.79 mm (0.11 in) outside diameter. I estimated that the average turn on the binocular core would require 7.25 in of cable (2x length of core block + 2x center-to-center spacing) and that 20 turns may be possible (each loop through both eyes of the binocular core is counted as 1 turn). This resulted in a total cable length of 145 in (just over 12 ft, or 3.7 m) for each choke. A 145 in piece of RG-174/U coaxial cable was cut from a spool and spread out on the floor for inductance measurements. The measured shield inductance with a Keysight U1733C LCR meter was 4.37 μH at 10 kHz and 4.33 μH at 100 kHz. This inductance may be compared to the later measurements of the completed chokes in section 4. The coax was then wound through each eye of the binocular assembly, resulting in 20 turns (as predicted) with approximately 100 mm long pigtails at each end (figure 4).

The measured dimensions of the weatherproof ABS plastic enclosures are 131 L x 69 W x 49 H mm (5.2 x 2.7 x 1.9 in) including the mounting flanges (figure 5). I acquired them through eBay for 3 USD each, and the listing showed the dimensions as 100 x 68 x 50 mm, not including the flanges. The enclosure is barely wide enough for the eight cores; in fact, the enclosure inside width is about 0.5 mm undersized, which required the binocular core to be tilted at a slight angle so as to not bend or stress the enclosure sides.

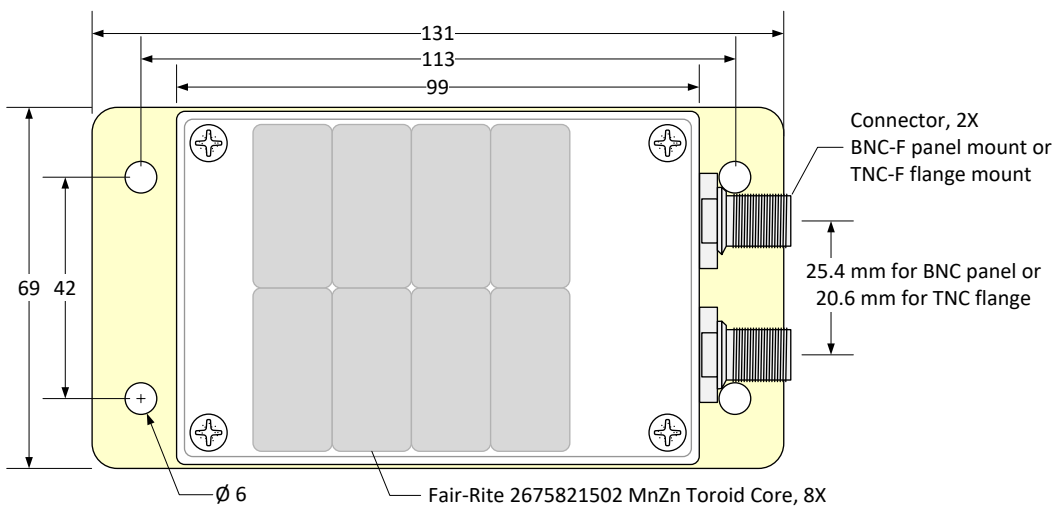


Figure 5 ~ 75% scale drawing showing basic enclosure dimensions (mm) as measured. The binocular core is not centered. Both connectors were placed at one end to ensure enough space for internally connecting the coax to the connectors and to allow the enclosure to shield the connections from rain. ©2020 W. Reeve

The enclosures were first prepared by cutting holes with brad-point drill bits on one end for the connectors. The holes for the BNC panel-mount connectors were cut with an undersized drill bit and then reamed so the connectors could be self-threaded into the plastic. The washer, ground lug and nut were then placed on the connector, tightened and secured with a small drop of superglue. The openings for the TNC flange-mount connectors were cut with a 1/8 in drill bit for the mounting holes and a 19/64 in drill bit for the center (figure 6). I used 3 mm fasteners (machine screw, internal star ground lug and nut) for the TNC flanges.

The binocular cores with windings were then placed in the enclosures. Before using hot glue to anchor the cores, I soldered the center and shield conductors to the connectors (figure 7). I originally hoped to use crimp connectors, but the crimp sleeves were too long for the limited space between the connectors and the cores. The final task was to install the supplied rubber seal in each top cover and fasten the cover to the units (figure 8).

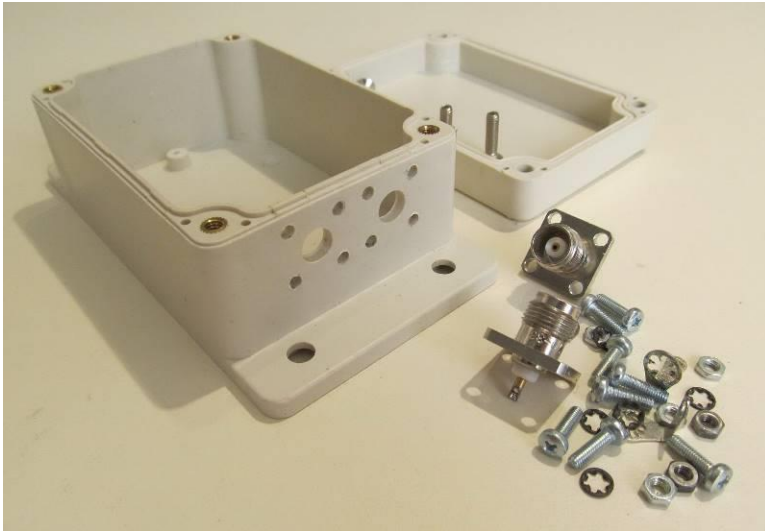


Figure 6 ~ Choke enclosure ready for installation of TNC flange-mount connectors. All connector holes were cut with brad-point drill bits and deburred. ©2020 W. Reeve



Figure 7 ~ Interior view of the choke with TNC connectors. Hot glue holds the binocular core in place. The coax shield is soldered to a ground lug on each connector flange. ©2020 W. Reeve



Figure 8 ~ Completed units ready for final testing, BNC on the left and TNC on the right. ©2020 W. Reeve

4. Measurements

The shield inductance, Q and impedance of each completed choke was measured with the Keysight LCR meter at 10 and 100 kHz (table 2). The dc resistance was measured with the Keithley 2110 DMM setup for 4-terminal (Kelvin) resistance measurements. I also measured the same parameters for the center conductor and all measurements were very similar to the shield except the center conductor dc resistance was higher (about 1 ohm, as expected). The impedance measurements were in line with my expectations based on the core permeability. At the low end (10 kHz) the shield impedance is approximately 1 kohm and at the high end (100 kHz) is 15 kohm.

Only slight measurement differences are seen between the TNC and BNC chokes. For example, the difference between the impedances of the two chokes at 100 kHz amounts to only about 4.5%. The slight differences can be ascribed to the manufacturing variations in the toroid cores as well as the non-precision construction of the windings. Even variations in the coaxial cable construction contribute to the difference, although these are expected to be small for the high-quality cable used here (Coleman RG-174/U). For my application, the slight differences between the two chokes are not important.

Ideally, the choke impedance is proportional to frequency; for example, if the impedance at f_1 is $Z(f_1)$, then the impedance at $10 \times f_1$ will be $10 \times Z(f_1)$. However, it is seen from the tabulated data that the impedance $Z(100 \text{ kHz})$ actually is $13.5 \times Z(10 \text{ kHz})$. This probably is due to the higher resistance at 100 kHz caused by skin and proximity effects (these also affect the inductance to some degree).

Table 2 ~ Shield conductor inductance, Q, impedance and dc resistance
Note the much lower Q at 100 kHz compared to 10 kHz due to higher losses

Frequency	TNC Choke	BNC Choke	Instrument
Inductance, 10 kHz	18.084 mH	17.797 mH	U1733C
Inductance, 100 kHz	24.17 mH	23.10 mH	U1733C
Q, 10 kHz	200	211	U1733C
Q, 100 kHz	27.4	29.0	U1733C
Impedance, 10 kHz	1.130 kohms	1.113 kohms	U1733C
Impedance, 100 kHz	15.201 kohms	14.523 kohms	U1733C
Resistance, dc (20 °C)	0.143 ohms	0.142 ohms	2110, 4-terminal measurement

In addition to the basic measurements described above, I measured the reflection coefficients (S11 and S22) and transmission coefficients (S12 and S21) of each choke with a VNWA-3E vector network analyzer and S-Parameter Test Set (see {Reeve17} for a description of this instrument combination). I made two sets of calibrations and measurements, one from 5 kHz to 105 kHz and another from 100 kHz to 10 MHz. The purpose of these measurements was to confirm good transmission properties of the chokes (figure 9).

The measurements from 5 kHz to 105 kHz required special CoDec settings in the VNWA-3E (900 Hz sample rate and 1 x4 samples per IF period for a 225 Hz IF). For the measurements from 100 kHz to 10 MHz, I used default settings (48 kHz sample rate and 1 x4 samples per IF period for a 12 000 Hz IF).

My S-Parameter Test Set has SMA connectors so I used short (150 mm) jumper cables with SMA-M connectors on one end for connection to the test set and BNC-M on the other for connection to the chokes. I set the software for 1001 sweep frequency points and calibrated the VNA at the end of these cables with an SDR-Kits BNC

Calibration Kit. For the TNC choke I used BNC-F to TNC-M adapters and assumed the adapters have negligible effect at the low frequencies used in the measurements.

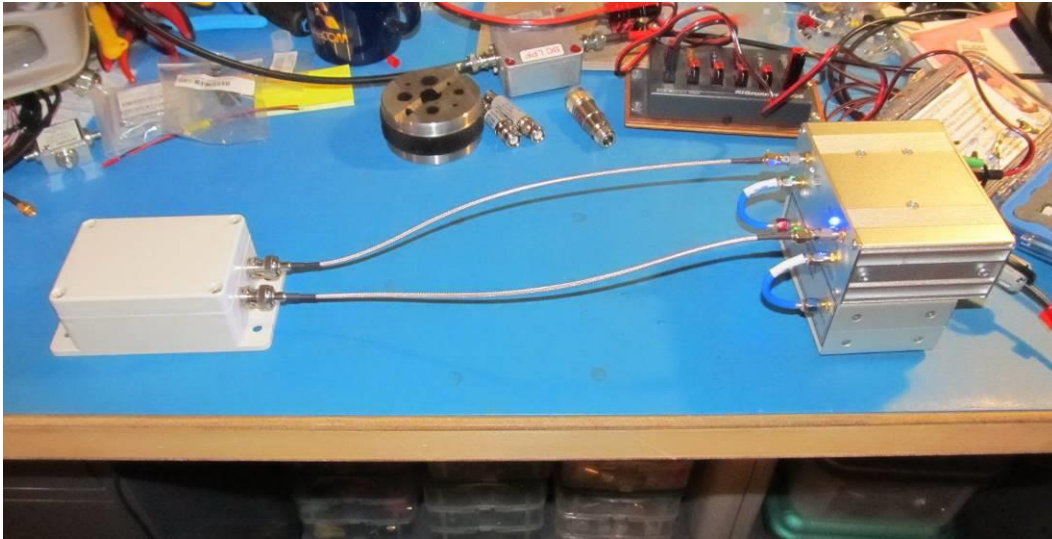


Figure 9 ~ BNC choke on the bench (left) connected to the VNWA-3E vector network analyzer with shop-built S-Parameter Test Set (right). The two jumper cables on the S-Parameter Test Set are made from RG-316 coaxial cable and are 150 mm long. ©2020 W. Reeve

The reflection and transmission coefficient measurements held no surprises and all plots are smooth with no resonant effects up to 10 MHz (figures 10 and 11). The S21 and S12 transmission coefficients in dB are equivalent to *insertion loss* in dB ($IL = |S_{21}|$ or $|S_{12}|$) and negligible up to 100 kHz and < 0.4 dB up to 10 MHz. Similarly, the S11 and S22 reflection coefficients in dB are equivalent to *return loss* in dB ($RL = |S_{11}|$ or $|S_{22}|$) and almost 40 dB at 100 kHz and still quite good at 25 dB up to 10 MHz. The forward (S11, S21) and reverse (S12, S22) measurements for both chokes were identical.

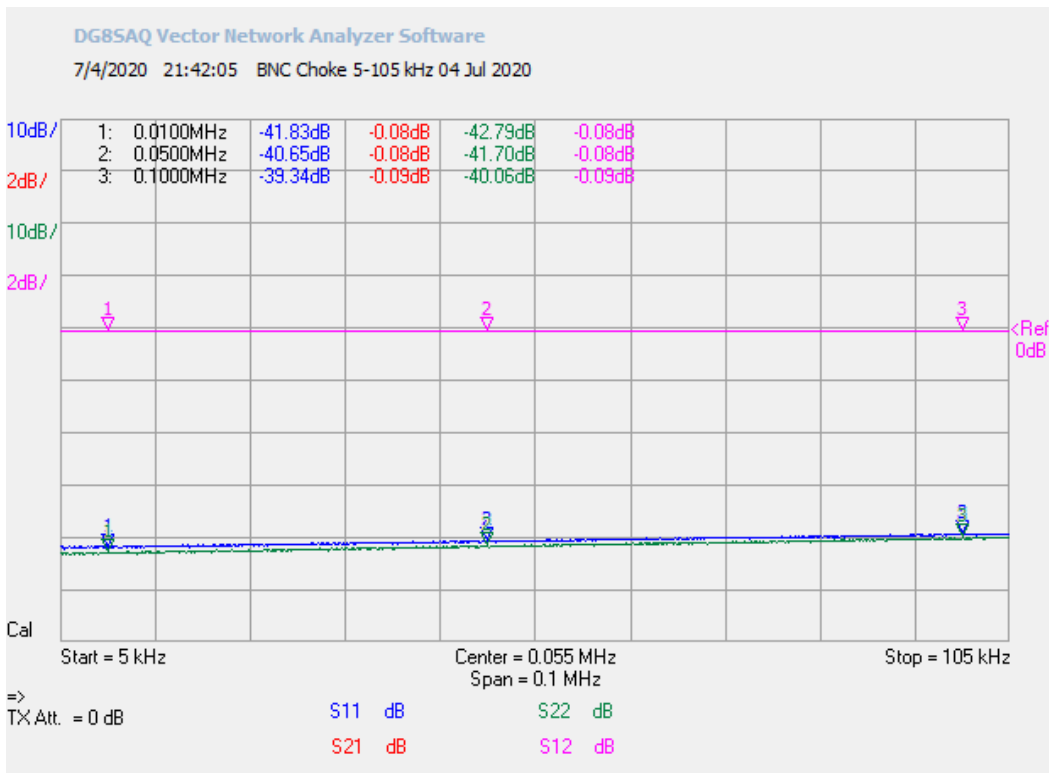


Figure 10 ~ S-parameter measurements for the BNC choke from 5 to 105 kHz. The scales for the reflection coefficients, S11 and S22, are 10 dB/div and for the transmission coefficients, S21 and S12, are 2 dB/div. The reference for all coefficients is the 6th division from the bottom. The marker table at the top-left shows the values for 10, 50 and 100 kHz.

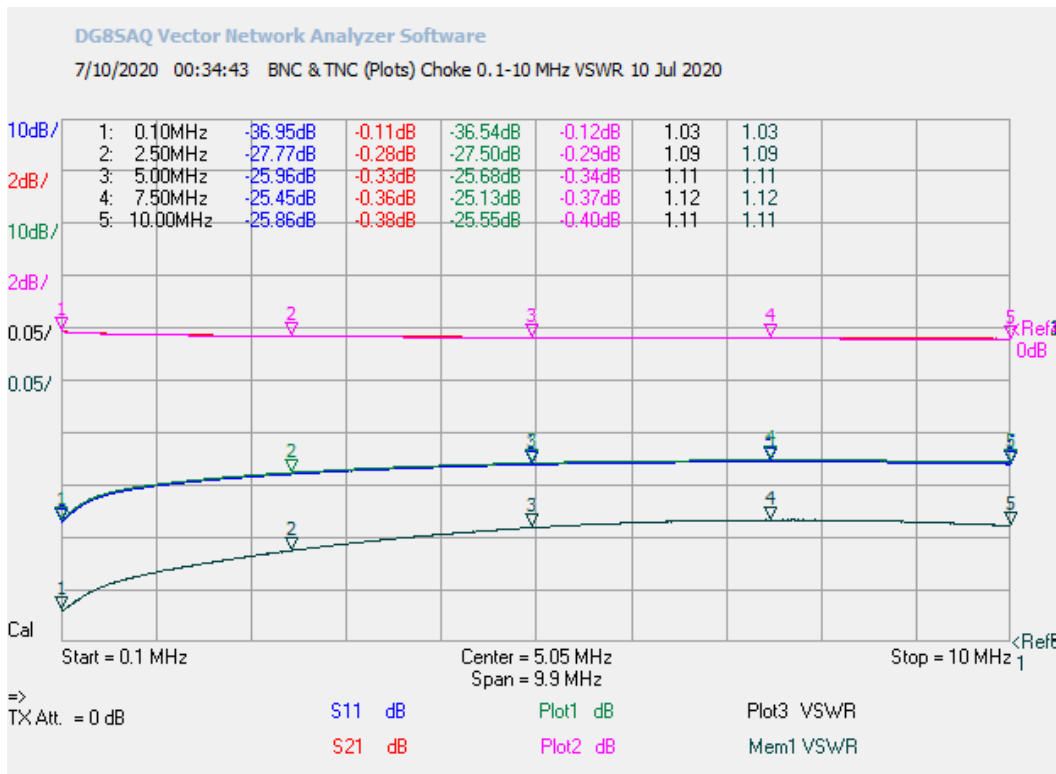


Figure 11 ~ S-parameter measurements for the BNC and TNC chokes from 0.1 to 10 MHz overlaid on the same plot. The traces marked S11, S21 and Mem1 VSWR are for the BNC choke. The traces marked Plot1, Plot2 and Plot3 VSWR are the same parameters for the TNC choke. The scales and references for S11 and S21 are the same as the previous figure. The scales for VSWR are 0.05/div with the 1.00:1 VSWR reference at 0 division.

The reflection coefficients (S11, S22) and the equivalent return losses represent the degree of impedance matching at the choke input and output. Impedance matching also can be represented by voltage standing wave ratio, VSWR, so I also plotted VSWR on the 100 kHz to 10 MHz plot. The VSWR never exceeded 1.12:1 throughout the frequency range 5 kHz to 10 MHz.

5. Conclusions

Two RF chokes were made from high-permeability ferrite round cable cores glued into the form of a binocular core. A 3.7 m length of RG-174/U coaxial cable was wound on each binocular core, which yielded an inductance of about 18 mH at 10 kHz and 24 mH at 100 kHz. Measurements with an LCR meter showed a shield impedance of about 1 kohm at 10 kHz and 15 kohm at 100 kHz, and measurements with a vector network analyzer up to 10 MHz showed no transmission degradation.

6. Weblinks and References

- {Reeve13} Reeve, W. and Hagen, T., Applying and Measuring Ferrite Beads: Part I ~ Ferrite Bead Properties and Test Fixtures, 2013, available at: http://www.reeve.com/Documents/Articles%20Papers/Ferrite%20Beads/Reeve-Hagen_FerriteBeads_P1.pdf
- {Reeve17} Reeve, W., Building Version 2 of an S-Parameter Test Set for the VNA-3E, 2017, available at: http://www.reeve.com/Documents/Articles%20Papers/Reeve_S-ParamTestSet_V2.pdf



Author: Whitham Reeve obtained B.S. and M.S. degrees in Electrical Engineering at University of Alaska Fairbanks, USA. He worked as a professional engineer and engineering firm owner/operator in the airline and telecommunications industries for more than 40 years and now manufactures electronic equipment used in radio astronomy. He also is a part-time space weather advisor for the High-frequency Active Auroral Research Program (HAARP) and a member of the HAARP Advisory Committee. He has lived in Anchorage, Alaska his entire

life. Email contact: whitreeve@gmail.com

Superlatives in Science Journalism and other Science Junk compiled for April 1, 2021

Julian Jove

Here are actual headlines from actual online science publications including ScienceNews and AGU's own EoS, among many others. They are listed here to show that some science writers know just about as much about science journalism as a Mynah Bird. No fake news here, that's for sure...!

- German firm introducing game-changing solar-wind-wave energy platform (I was right all along, it is a game)
- Presence of airborne dust could signify increased habitability of distant planets (But then again, it could not)
- An unexpected result from a dark matter experiment may signal new particles (And then, again, it may not)
- Physical activity prevents almost four million early deaths worldwide each year (Give or take a few million)
- This Cosmologist Knows How It's All Going to End (Thank you, Mrs. Bellane, for reading my palms and predicting my future)
- Experiment confirms 50-year-old theory describing how an alien civilization could exploit a black hole (Wow, that's great. Knowing this, I'll now be able to sleep at night)
- Geochemists solve mystery of Earth's vanishing crust (Oh, did they really make measurements at the site or is this just another wild guess?)
- The Arctic is on fire: Siberian heat wave alarms scientists (Are those the same scientists we see on the *UFOs*, *The Truth* channel?)
- Hubble finds that Betelgeuse's mysterious dimming is due to a traumatic outburst (Now they are using medical terms to describe stellar outbursts)
- Energy firm says its nuclear-waste fueled diamond batteries could last thousands of years (Yes, just like alkaline batteries)
- Could *Planet 9* be a primordial black hole? (Or, could Planet 9 be a flying pig?)
- In July 2012, NASA and European spacecraft watched an extreme solar storm erupt from the sun and narrowly miss Earth. "If it had hit, we would still be picking up the pieces," announced Daniel Baker of the University of Colorado at a NOAA Space Weather Workshop 2 years later. "It might have been stronger than the Carrington Event itself." (If my aunt had a beard, she'd be my uncle)
- Geoengineering Might Not Save Us From a Cloud Apocalypse (Oh? Who said it might?)
- Simulations suggest geoengineering would not stop global warming if greenhouse gasses continue to increase (There are those simulations again)
- Solar eclipse plunges southern Chile, Argentina into darkness (This headline plunges into hyperbole)
- Could we harness energy from black holes? (Could we harness White Fang?)
- Earth's oceans are storing record-breaking amounts of heat. (Please tell us who or what held the previous record)
- FM Radio on Jupiter, Brought to You by Ganymede. (The last time we checked, the radio emissions from Jupiter in question here are not "FM" [frequency modulations] and are not by Ganymede. The only new thing is that the emissions in the article are associated with Ganymede instead of Io. Next time, do a little thinking. Oh yeah, and do a little research, too). NOTE: Ganymede has long been associated with emission in the HOM

range, but not in the DAM range. That's the new part here. DAM isn't FM, nor is it even near the FM band. The AGU pulled the original article and replaced it with this one, which no longer mentions FM <https://eos.org/editor-highlights/radio-on-jupiter-brought-to-you-by-ganymede>

- A Robot Made of Ice Could Adapt and Repair Itself on Other Worlds (A Robot Made of Reese's Buttercups Could Eat Itself and Not Be Sorry)
- Reindeer lichens are having more sex than expected (Dr. Ruth, Dr. Ruth, come quick, we need you!)
- Use of pronouns may show signs of an impeding breakup (Doesn't anyone use spell-check anymore or is that just too complicated?)
- These distant 'baby' black holes seem to be misbehaving—and experts are perplexed (Quick, call a child psychiatrist so we can help this bad baby find her *happy place*)
- Asteroid dust found in crater closes case of dinosaur extinction (Does anyone really believe that this case is closed? How many times have we been beat over the head with “Immutable, inarguable evidence” on this subject?)
- Were it not for humans, woolly mammoths would have lived for 4,000 more years, simulation shows (This obviously is a case of mammoth in, mammoth out. We all know that computer simulations of the past to predict the past-future always are right-on the tusk)

Membership

New Members

Please welcome our new or returning SARA members who have joined since the last journal. If your name is missing or misspelled, please send an email to treas@radio-astronomy.org. We will make sure it appears correctly in the next Journal issue.

First name	Last name	City	State	Country	Call Sign
David	Galloway	Victoria	BC	Canada	
Alberto	Sagues	Lutz	FL	USA	KA4MTO
Gary	Friedlander	Buffalo Grove	IL	USA	WD9HDM
Dylan	Moore	Santa Monica	CA	USA	
John Zum	Brunnen	Tucson	AZ	USA	
Dustin	Brace	Waynesboro	PA	USA	W3III
Martin	Smith	Sharon	VT	USA	AC1FT
Richard	Carrigan, Jr.	Naperville	IL	USA	
Henry	Knoepfle	Tucson	AZ	USA	KB7NIE
Michael	McCormick	Edmond	OK	USA	
Martin	Richmond-Hardy	Ipswich	Suffolk	UK	
Jeffrey	DeVries	Sherwood Park	Alberta	Canada	

Membership dues are \$20.00 US per year and all dues expire in June. Student memberships are \$5.00 US per year. Memberships must be renewed on June of each year. Or pay once and never worry about missing your dues again with the SARA Life Membership. SARA Life Memberships are now offered for a one-time payment of twenty times the basic annual membership fee (currently \$400 US).

Journal Archives & Other Promotions

The rich and diverse legacy of member contributed content is available in the SARA Journal Archives. Table of contents for journals is available online at <http://www.radio-astronomy.org/content-journal>

The entire set of The Journal of The Society of Amateur Radio Astronomers is available on USB drive. It goes from the beginning of 1981 to the end of 2017 (over 6000 pages of SARA history!) Or you can choose one of the following USB drive's or DVD:* (Prices are US dollars and include postage.)

† SARA Journals from 1981 through 2017

Prices, US dollars, including postage

Members

Each USB drive	\$15.00	
USB drive + 1-year membership extension		\$30.00

Non-members

Each USB drive	\$25.00	
USB drive + 1-year membership	\$30.00	

Non-USA members

Each USB drive	\$20.00 (airmail)	
USB drive+ 1-year members extension	\$35.00	

*Already a member and want any or all these USB drives or DVD's? Buy any one for \$15.00 or get any three for \$35.00.

SARA Store (radio-astronomy.org/store.)

SARA offers the above USB drives, DVDs, printed Proceedings and Proceedings on USB drive and other items at the SARA Store: <http://www.radio-astronomy.org/e-store>. Proceeds from sales go to support the student grant program. Members receive an additional 10% discount on orders over \$50 US. Payments can be made by sending payment by PayPal to treas@radio-astronomy.org or by mailing a check or money order to SARA, c/o Brian O'Rourke, 337 Meadow Ridge Rd, Troy, VA 22974-3256

SARA Online Discussion Group

SARA members participate in the online forum at <http://groups.google.com/group/sara-list>. This is an invaluable resource for any amateur radio astronomer.

SARA Conferences

SARA organizes multiple conferences each year. Participants give talks, share ideas, attend seminars, and get hands-on experience. For more information, visit <http://www.radio-astronomy.org/meetings>.

Facebook

Like SARA on Facebook

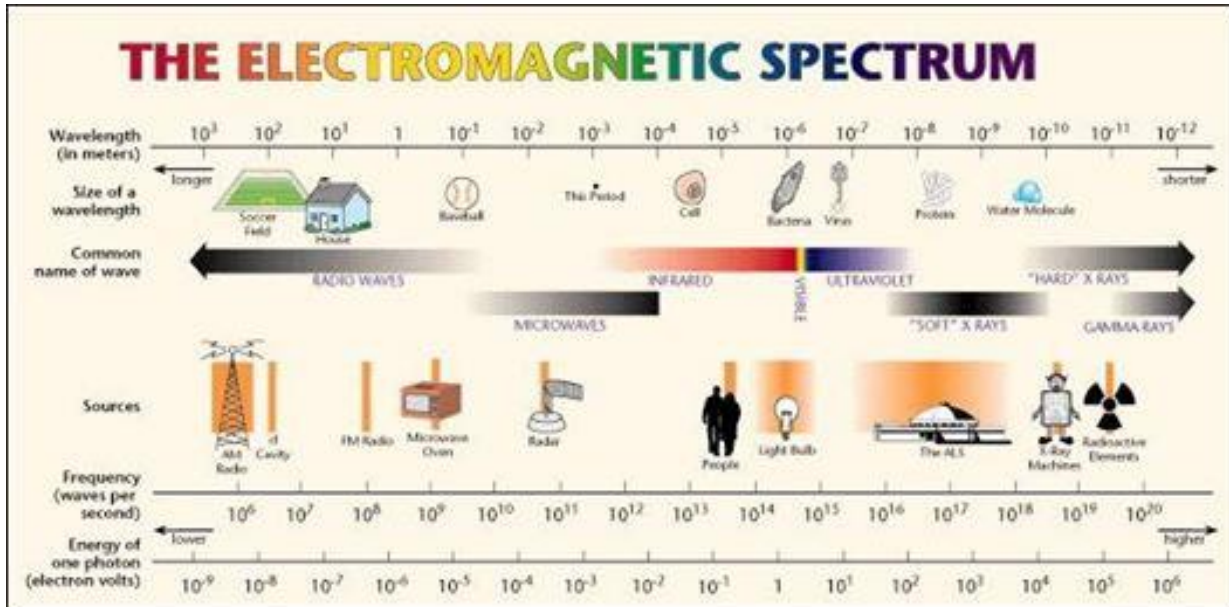
<http://www.facebook.com/pages/Society-of-Amateur-Radio-Astronomers/128085007262843>

Twitter

Follow SARA on Twitter @RadioAstronomy1

What is Radio Astronomy?

This link is for a booklet explaining the basics of radio astronomy.
<http://www.radio-astronomy.org/pdf/sara-beginner-booklet.pdf>



Administrative

Officers, directors, and additional SARA contacts

The Society of Amateur Radio Astronomers is an all-volunteer organization. The best way to reach people on this page is by email with SARA in the subject line SARA Officers.

President: Dennis Farr, WB4RJK, <http://www.radio-astronomy.org/contact/President> +1 813 833-3918

Vice President: Rich Russel, AC0UB <http://www.radio-astronomy.org/contact/Vicepresident>

Secretary: Bruce Randall, NT4RT, <http://www.radio-astronomy.org/contact/Secretary> +1 803-327-3325

Treasurer: Brian O'Rourke, K4UL, <http://www.radio-astronomy.org/contact/Treasurer>

Past President: Ken Redcap, tbd@radio-astronomy.org +1 319-591-1131

Founder Emeritus and Director: Jeffrey M. Lichtman, KI4GIY, jeff@radioastronomysupplies.com +1 954-554-3739

Board of Directors

Name	Term expires	Email
Wayne McCain, KS0S	2021	wayne.mccain@athens.edu
Charles Osborne, K4CSO	2021	k4cso@charter.net
Ed Harfmann	2022	edharfmann@comcast.net
Steve Tzikas	2022	Tzikas@alum.rpi.edu
Keith Payea, AG6CI	2022	kbpayea@bryantlabs.net
David Westman	2022	david.westman@engineeringretirees.org
Jon Wallace	2021	wallacefj@comcast.net
Dr. Wolfgang Herrmann	2021	messbetrieb@astropeiler.de

Other SARA Contacts

All Officers	http://www.radio-astronomy.org/contact-sara	
All Directors and Officers	http://www.radio-astronomy.org/contact/All-Directors-and-Officers	
Eastern Conference Coordinator	http://www.radio-astronomy.org/contact/Annual-Meeting	
All Radio Astronomy Editors	http://www.radio-astronomy.org/contact/Newsletter-Editor	
Radio Astronomy Editors	Richard A. Russel	drrichrussel@netscape.net
	Bogdan Vacaliuc	bvacaliuc@gmail.com
Contributing Editors	Steve Black	edit@radio-astronomy.org
	Whitham D. Reeve	whitreeve@gmail.com
	Mike Stewart	edit@radio-astronomy.org
Educational Outreach	http://www.radio-astronomy.org/contact/Educational-Outreach	
Grant Committee	Tom Crowley	grants@radio-astronomy.org
Membership Chair	http://www.radio-astronomy.org/contact/Membership-Chair	
Technical Queries (David Westman)	http://www.radio-astronomy.org/contact/Technical-Queries	
Webmaster	Ciprian (Chip) Sufitchi, N2YO	webmaster@radio-astronomy.org

Resources

Great Projects to Get Started in Radio Astronomy

Radio Observing Program

The Astronomical League (AL) is starting a radio astronomy observing program. If you observe one category, you get a Bronze certificate. Silver pin is two categories with one being personally built. Gold pin level is at least four categories. (Silver and Gold level require AL membership which many clubs have membership. For the bronze level, you need not be a member of AL.)

Categories include

- 1) SID
- 2) Sun (aka IBT)
- 3) Jupiter (aka Radio Jove)
- 4) Meteor back-scatter
- 5) Galactic radio sources

This program is a collaboration between NRAO and AL. Steve Boerner is the Lead Coordinator and a SARA member.

For more information:

Steve Boerner

2017 Lake Clay Drive

Chesterfield, MO 63017

Email: sboerner@charter.net

Phone: 636-537-2495

<http://www.astroleague.org/programs/radio-astronomy-observing-program>

Radio Jove



The Radio Jove Project monitors the storms of Jupiter, solar activity and the galactic background. The radio telescope can be purchased as a kit or you can order it assembled. They have a terrific user group you can join. <http://radiojove.gsfc.nasa.gov/>

INSPIRE Program



The INSPIRE program uses build-it-yourself radio telescope kits to measure and record VLF emissions such as tweeks, whistlers, sferics, and chorus along with man-made emissions. This is a very portable unit that can be easily transported to remote sites for observations.

<http://theinspireproject.org/default.asp?contentID=27>

SARA/Stanford SuperSID



Stanford Solar Center and the Society of Amateur Radio Astronomers have teamed up to produce and distribute the SuperSID (Sudden Ionospheric Disturbance) monitor. The monitor utilizes a simple pre-amp to magnify the VLF radio signals which are then fed into a high definition sound card. This design allows the user to monitor and record multiple frequencies simultaneously. The unit uses a compact 1-meter loop antenna that can be used indoors or outside. This is an ideal project for the radio astronomer that has limited space. To request a unit, send an e-mail to supersid@radio-astronomy.org

Radio Astronomy Online Resources

<p>A New Radio Telescope for Mexico - ORION 2021 01 20. Dr. Stan Kurtz https://www.youtube.com/watch?v=Q9aBWr1aBVc</p>	<p>National Radio Astronomy Observatory http://www.nrao.edu</p>
<p>AJ4CO Observation of Jovian decametric emission http://www.radiojove.org/SUG/Observation%20Reports/AJ4CO/</p>	<p>NRAO Essential Radio Astronomy Course http://www.cv.nrao.edu/course/ast534/ERA.shtml</p>
<p>British Astronomical Association – Radio Astronomy Group http://www.britastro.org/baa/</p>	<p>Pulsar Sounds: Audio recordings made by professional observatories http://www.typnet.net/AJ4CO/Pulsar_Sounds/</p>
<p>CALLISTO Receiver & e-CALLISTO http://www.reeve.com/Solar/e-CALLISTO/e-callisto.htm CALLISTO data archive: www.e-callisto.org</p>	<p>Radio Astronomy calculators http://www.typnet.net/AJ4CO/Calculators/Calculators.htm</p>
<p>Deep Space Exploration Society http://DSES.science</p>	<p>Radio Astronomy Supplies http://www.radioastronomysupplies.com</p>
<p>Deep Space Object Astrophotography Part 1 -- ORION 2021 02 17. George Sradnov https://www.youtube.com/watch?v=Pm_Rs17KlyQ</p>	<p>Radio Jove Spectrograph Users Group http://www.radiojove.org/SUG/</p>
<p>European Radio Astronomy Club http://www.eraonet.org</p>	<p>Radio Sky Publishing http://radiosky.com</p>
<p>Exotic Ions and Molecules in Interstellar Space -- ORION 2020 10 21. Dr. Bob Compton https://www.youtube.com/watch?v=r6cKhp23SUo&t=5s</p>	<p>RF Associates Richard Flagg, rf@hawaii.rr.com 1721-1 Young Street, Honolulu, HI 96826 RFspace, Inc. http://www.rfspace.com</p>
<p>Forum and Discussion Group http://groups.google.com/group/sara-list</p>	<p>SARA Facebook page https://www.facebook.com/pages/Society-of-Amateur-Radio-Astronomers/128085007262843</p>
<p>GNU Radio http://www.gnu.org/licenses/gpl.html</p>	<p>SARA Twitter feed https://twitter.com/RadioAstronomy1</p>
<p>Graphs, plots, equations, miscellaneous cheat sheets http://www.typnet.net/AJ4CO/index.htm</p>	<p>SARA Web Site http://radio-astronomy.org</p>
<p>Inspire Project http://theinspireproject.org</p>	<p>SETI League http://www.setileague.org</p>

<p>Introduction to Amateur Radio Astronomy (presentation) http://www.typnet.net/AJ4CO/Publications/Intro%20to%20Amateur%20Radio%20Astronomy,%20Typinski%20(AAC,%202016)%20v2.pdf</p>	<p>Shirleys Bay Radio Astronomy Consortium marcus@propulsionpolymers.com</p>
<p>NASA Radio JOVE Project http://radiojove.gsfc.nasa.gov Archive: http://radiojove.org/archive.html</p>	<p>Simple Aurora Monitor Magnetometer http://www.reeve.com/SAMDescription.htm</p>
<p>National Radio Astronomy Observa-tory http://www.nrao.edu</p>	<p>Stanford Solar Center http://solar-center.stanford.edu/SID/</p>
<p>NRAO Essential Radio Astronomy Course http://www.cv.nrao.edu/course/astr534/ERA.shtml</p>	<p>The Arecibo Radio Telescope; It's History, Collapse, and Future - ORION 2020.12.16. Dr. Stan Kurtz, Dr. David Fields https://www.youtube.com/watch?v=rBZIPOLNX9E</p>
<p>Pulsar Sounds: Audio recordings made by professional observatories http://www.typnet.net/AJ4CO/Pulsar_Sounds/</p>	<p>The Radio JOVE Project & NASA Citizen Science – ORION 2020.6.17. Dr. Chuck Higgins https://www.youtube.com/watch?v=s6eWAXjywp8&t=5s</p>
<p>Radio Astronomy calculators http://www.typnet.net/AJ4CO/Calculators/Calculators.htm</p>	<p>UK Radio Astronomy Association http://www.ukraa.com/</p>

For Sale, Trade and Wanted

At the SARA online store: radio-astronomy.org/store.

SARA Polo Shirts

New SARA shirts have arrived.

We now have a good selection of X, XX, and XXX shirts available in all colors including white!

Shirts are \$20 at the conference and \$25 shipped.

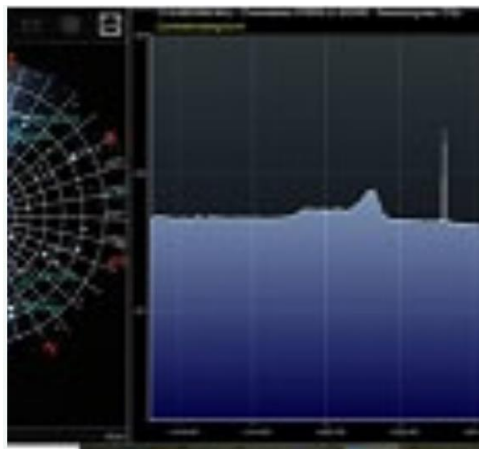
Contact the treasurer at treas@radio-astronomy.org for availability and shipping.



Scope in a Box \$295

radio-astronomy.org/store.

Kit of parts and software to build a working Radio Telescope to detect Hydrogen Line emissions. Available to USA addresses only at this time.



SuperSID Complete Kit (\$112-\$160 depending on options)

radio-astronomy.org/store.



SARA Publication, Journals and Conference Proceedings (various prices)

radio-astronomy.org/store.

SARA Journal USB Drive (\$15-\$35 depending on shipping option)

radio-astronomy.org/store.

The USB drive covers the society journal "Radio Astronomy" from the founding of the organization in 1981 thru 2020. Articles cover a wide range of topics including: cosmic radiation, pulsars, quasars, meteor detection, solar observing, Jupiter, Radio Jove, gamma ray bursts, the Itty Bitty Telescope (IBT), dark matter, black holes, the Jansky antenna, methanol masers, mapping at 408 MHz and more. This CD contains all of the above and more with over 4800 pages of articles on radio astronomy. Also included is a copy of Grote Reber's handwritten, 34 page document "Carriage and Mirror Detail" of his historic antenna now on display at the National Radio Astronomy Observatory (NRAO) in Green bank, WV. You also get an electronic copy of the 109 page "Basics of Radio Astronomy" from JPL Goldstone-Apple Valley Radio Telescope. Also included is the NRAO 40-foot radio telescope "Operators Manual", which by the way, you get to operate if you attend the Eastern SARA conference in July.

SARA Advertisements

There is no charge to place an ad in Radio Astronomy; but you must be a current SARA member. Ads must be pertinent to radio astronomy and are subject to the editor's approval and alteration for brevity. Please send your "For Sale," "Trade," or "Wanted" ads to edit@radio-astronomy.org. Please include email and/or telephone contact information. Please keep your ad text to a reasonable length. Ads run for one bimonthly issue unless you request otherwise.

Typinski Radio Astronomy, Inc., info@typinski.com

Antenna systems and feed line components for HF radio astronomy

Jeff Kruth, WA3ZKR, kmec@aol.com

RF components from HF to MMW, various types including mixers, RF switches, amplifiers, oscillators, coaxial components, waveguide components, etc. I have a very large collection of stuff and the facilities to test and provide data. Please email with your needs and I will see if I have something for you. Have fun!

Stuart and Lorraine Rumley, sales@valontechnology.com

The Valon Technology 2100 Downconverter, when combined with our 5009 frequency synthesizer module, provides a high-performance, compact receiver downconverter system. Applications include hydrogen line studies at 1420MHz and radio astronomy in the protected 30MHz segment of the 21 cm band. For more information visit <http://www.valontechnology.com/2100downconverter.html> or send an email.

Radio2Space, filippo.bradaschia@primalucelab.com

SPIDER radio telescopes and turn-key-systems designed specifically for education.

<https://www.radio2space.com>

We developed our SPIDER radio telescopes as turn-key-system just to avoid the problem you perfectly highlighted in your website: "Purchasing a radio telescope isn't like buying an optical telescope. They are harder to find, and usually require assembly and software troubleshooting. In some cases, a radio telescope must be built from components." Our SPIDER radio telescopes are not designed for amateurs that prefer to build a radio telescope but to schools, universities, museums, and other science institutes that needs for a complete and ready-to-use system, just like the optical telescopes they can normally buy!

Radio Astronomy Supplies

<http://www.radioastronomysupplies.com>

jeff@radioastronomysupplies.com

Research and Educational Radio Telescopes and all associated equipment since 1994

Wombat Mk IV Globe Torus Antenna (advertisement)

The Wombat Mk IV Globe Torus antenna exploits Maxwell's Equations to deliver super performance. This antenna is so advanced that all attempts to electromagnetically model it have failed. In use by discriminating antenna professionals and aficionados around the world. Tested at the Spherical Conversion Antenna Test Site (SCATS).

Specifications: *

- Frequency (10 dB reference), f : 1 Hz to 109.9 THz
- Frequency impedance, Z_0 : 50.0 + j0.0 ohms (1 Hz to 10.9 THz), 0.00 + j50.0 ohms (11.0 to 109.9 THz)
- Radiation resistance, R_{Rad} : 51 ±102 ohms
- VSWR: As close to 1.0:1 over full frequency range, and then some, as the law allows
- Shape, σ_s : Donut (aka torus)
- Volume, Φ_{Eff} : 1 m³
- Effective area, A_{Eff} : 11 km² give or take a few
- Beamwidth (3 dB), BW_{HP} : 0.001 microarc-seconds (steerable)
- Gain, G : Uniformly random in all directions and frequencies within ±0.005 dB
- Antenna temperature, T_{ant} : immeasurably close to 0.0 K
- G/T : ∞/0 K
- Modulus of elasticity, E_0 : 2021 GPa
- Mass, m : 3 kg give or take a few
- Wind resistance, R_{wind} : 0.5 m² at 20 °C
- Altitude, H : As high as you can go
- Operating environment: 20 ±0.001 °C and 99.999% relative humidity (non-condensing)
- Bonding and grounding: Self-grounding through electrostatic discharge-free convection from any direction



Attestations:

- ✓ "I detected 34 FRBs and discovered 200 exoplanets within 24 hours of hooking up the Wombat Mk IV." Dr. Cal Meacham of the California Radiation and Antenna Palace (CRAP)
- ✓ "This antenna has worked superbly from the get-go." Joe in Tuskanoma County, Tennessee
- ✓ "I'll never go back to a rubber duck antenna after using the Wombat Mk IV!" Marvin in Hake, Ontario
- ✓ "By golly, the Global Torus is one heck-uv-a deal." Geoff of the Gigametre Institute in Bollywood, Indiana

Call today for a quote: +69 WOMBATMRKIV or visit our website www.wombatmarkiv.com (report trouble reaching this site to goaheadandcomplain@wombatmarkiv.com). Place your order before April 1st and receive a free Wombat Mark IV cooky-cutter keychain.

* Measurements by Phenomenological Calibration Labs, Bruno, California and independently verified by Best Psychics & Mediums, Farfletch, California

Membership Information

Annual SARA dues: Individual \$20, Classroom \$20, Student \$5 (US funds) anywhere in the world. Membership includes a subscription to Radio Astronomy, the bimonthly Journal of The Society of Amateur Radio Astronomers, delivered electronically (via a secure web link, emailed to you as each new issue is posted). We regret that printing and postage costs prevent SARA from providing hardcopy subscriptions to our Journal.

We would appreciate the following information included with your check or money order, made payable to SARA:

Name: _____
 Email Address : _____
(required for electronic Journal delivery)
 Ham call sign: _____ (if applicable)
 Address: _____
 City: _____
 State: _____
 Zip: _____
 Country: _____
 Phone: _____

Please include a note of your interests. Send your application for membership, along with your remittance, to our Treasurer.

For further information, see our website at:
<http://radio-astronomy.org/membership>

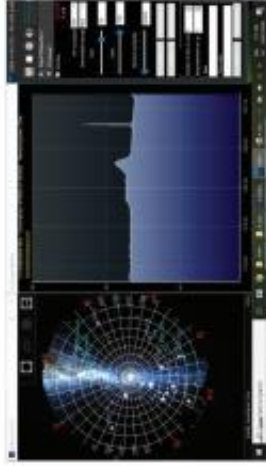


Society of Amateur Radio Astronomers, Inc.
 Founded 1981

Membership supported, nonprofit [501(c) (3)]
 Educational and Radio Astronomy Organization
**Knowledge through Common Research,
 Education and Mentoring**

How to get started?

SARA has a made a kit of software and parts to detect the Hydrogen line signal from space. This is an excellent method to get started in radio astronomy. It teaches the principles of antenna design, signal detection, and signal processing. Read more about this and other projects on our web site.



SARA members have been privileged to use this forty foot diameter drift-scan hydrogen line radio telescope every year at their annual meeting in Green Bank.

Why Radio Astronomy?

Because about sixty five percent of our current knowledge of the universe has stemmed from radio astronomy alone. The discovery of quasars, pulsars, black holes, the 3K background from the "Big Bang" and the discovery of biochemical hydrogen/carbon molecules are all the result of professional radio astronomy.

 <http://radio-astronomy.org>



The Society of Amateur Radio Astronomers

SARA was founded in 1981, with the purpose of educating those interested in pursuing amateur radio astronomy.

The society is open to all, wishing to participate with others, worldwide.

SARA members have many interests, some are as follows:

SARA Areas of Study and Research:

- ✔ Solar Radio Astronomy
- ✔ Galactic Radio Astronomy
- ✔ Meteor Detection
- ✔ Jupiter
- ✔ SETI
- ✔ Gamma Ray/High Energy Pulse
- ✔ Detection
- ✔ Antennas
- ✔ Design of Hardware / Software

The members of the society offer a friendly mentor atmosphere. All questions and inquiries are answered in a constructive manner. No question is silly!

SARA offers its members an electronic bi-monthly journal entitled Radio Astronomy. Within the journal, members report on their research and observations. In addition, members receive updates on the professional radio astronomy community and, society news.



The Reber Telescope at NRAO. Constructed by Grote Reber in 1937 in his back yard in Wheaton, Illinois

Once a year SARA meets for a three-day conference at the Green Bank Observatory in Green Bank West Va.

There is also a spring conference held at various cities in the Western USA. Previous meetings have been at the VLA in Socorro, NM and at Stanford University.



How do I get started?

Just as a long journey begins with the first step, the project you elect must start with a clear idea of your objectives. Do you wish to study the sun? Jupiter? Make meteor counts? Do you wish to engage in imaging radio astronomy? What you decide will not only determine the type of equipment you will need, but also the local radio spectrum.



SARA Members discussing the IBT (itty Bitty Telescope)

How do amateurs do radio astronomy?

Radio astronomy by amateurs is conducted using antennas of various shapes and sizes, from smaller parabolic dishes to simple wire antennas. These antennas are connected to receivers and most of these receivers are software defined radios these days. Data from the receivers are collected by computers, and the received signals will be displayed as charts, graphs or maybe even sky maps. As diverse as the observed objects, so is are the instruments and tools used. SARA members will always be supportive to find good solutions for what one wishes to observe.

Is amateur radio astronomy instrumentation expensive?

Technical information freely circulated in our monthly journal helps amateurs to obtain good low noise equipment from off the shelf assemblies, or to build their own units. The actual cash investment in radio astronomy equipment need not exceed that of any other hobby.

What are amateurs actually looking for in the received data?

The aim of the radio amateur is to find something new and unusual. Just as an amateur optical observer hopes to notice a supernova or a new comet, so does an amateur radio observer hope to notice a new radio source, or one whose radiation has changed appreciably.

